SASR 88-24
DRF B13-01445
Class I
May 1988

PEACH BOTTOM ATOMIC POWER STATION
UNIT 2 VESSEL SURVEILLANCE MATERIALS
TESTING AND FRACTURE TOUGHNESS ANALYSIS

Prepared by: T. A. Caine

T. A. Caine, Senior Engineer
Structural Analysis Services

Verified by: Gary L. Stevens 5/6/88

G. L. Stevens, Engineer
Structural Analysis Services

Approved by: S Ranganath 5/6/88

S. Ranganath, Manager
Structural Analysis Services

IMPORTANT NOTICE REGARDING
CONTENTS OF THIS REPORT
PLEASE READ CAREFULLY

This report was prepared by General Electric solely for the use of the Philadelphia Electric Company. The information contained in this report is believed by General Electric to be an accurate and true representation of the facts known, obtained or provided to General Electric at the time this report was prepared.

The only undertakings of the General Electric Company respecting information in this document are contained in the contract governing Philadelphia Electric Company Purchase Order No. PB999125-N and nothing contained in this document shall be construed as changing said contract. The use of this information except as defined by said contract, or for any purpose other than that for which it is intended, is not authorized; and with respect to any such unauthorized use, neither General Electric Company nor any of the contributors to this document makes any representation or warranty (express or implied) as to the completeness, accuracy or usefulness of the information contained in this document or that such use of such information may not infringe privately owned rights; nor do they assume any responsibility for liability or damage of any kind which may result from such use of such information.

CONTENTS

CONTENTS

TABLES

ILLUSTRATIONS

ILLUSTRATIONS

ABSTRACT

A surveillance capsule was removed from the Peach Bottom Atomic Power Station, Unit 2 reactor at the end of Fuel Cycle 7. The capsule contained flux wires for neutron fluence measurement and Charpy and tensile test specimens for material property evaluation. A combination of flux wire testing and computer analysis was used to establish the vessel peak flux location and magnitude. Charpy V-Notch impact testing and uniaxial tensile testing were performed to establish the material properties of the irradiated vessel beltline. The irradiation effects were projected, based on Regulatory Guide 1.99, Revision 2, to conditions for 32 EFPY of operation. The 32 EFPY conditions are predicted to be less severe than the limits requiring vessel thermal annealing. Pressure-temperature operating limits curves valid to 32 EFPY were developed to July 1983 requirements of 10CFR50 Appendix G, accounting for irradiation shift per Regulatory Guide 1.99, Revision 2. The non-beltline limits are more severe than the beltline limits, even including predicted 32 EFPY shift.

The irradiated Charpy specimen data for base metal were compared to the best available unirradiated data. The results, which cannot be considered "credible" as defined in Regulatory Guide 1.99, Revision 2, are close to the upper bound predictions of the Regulatory Guide.

ACKNOWLEDGMENTS

Flux wire testing was performed by G. C. Martin. L. S. Burns provided the evaluation of flux distribution. The Charpy V-Notch impact testing was done by G. P. Wozadlo and G. E. Dunning. S. B. Wisner and G. H. Hendersen performed the tensile specimen testing. C. R. Judd performed the chemical composition testing.

1. INTRODUCTION

Part of the effort to assure reactor vessel integrity involves evaluation of the fracture toughness of the vessel ferritic materials. The key values which characterize a material's fracture toughness are the reference temperature of nil-ductility transition (RT_{NDT}) and the upper shelf energy (USE). These are defined in 10CFR50 Appendix G (Reference 1) and in Appendix G of the ASME Boiler and Pressure Vessel Code, Section III (Reference 2). These documents contain requirements used to establish the pressure-temperature operating limits which must be met to avoid brittle fracture.

Appendix H of 10CFR50 (Reference 3) and ASTM E185 (Reference 4) establish the methods to be used for surveillance of the reactor vessel materials. In January, 1988 one of the Peach Bottom 2 vessel surveillance specimen capsules required by Reference 3 was sent to General Electric for testing after exposure to seven fuel cycles of irradiation, or 7.53 effective full power years (EFPY) of operation. The surveillance capsule contained flux wires for neutron flux monitoring and Charpy V-Notch impact test specimens and uniaxial tensile test specimens fabricated from the vessel materials nearest the core (beltline). The impact and tensile specimens were tested to establish material properties for the irradiated vessel materials.

The results of surveillance specimen testing are presented in this report. The irradiated material properties are compared to available unirradiated properties from earlier tests. Predictions of the RT_{NDT} and USE at 32 EFPY are made for comparison with allowable values in Reference 1. Predictions of 32 EFPY properties were made based on Regulatory Guide 1.99, Revision 2 (Reference 5).

Operating limits curves for the Peach Bottom 2 reactor vessel are presented in this report. The curves account for current requirements of References 1 and 2. Geometric discontinuities and highly stressed regions, such as the feedwater nozzles and the closure flanges, are evaluated separately from the core beltline region. The operating limits developed consider the most limiting conditions of the discontinuity regions and the beltline region (including irradiation) to bound all operating conditions. The operating limits developed include irradiation shift in the beltline materials, based on the Reference 5 methods.

2. SUMMARY AND CONCLUSIONS

2.1 SUMMARY OF RESULTS

Surveillance capsule 2 was removed from the Peach Bottom 2 reactor at the end of Fuel Cycle 7 and shipped to the General Electric Vallecitos Nuclear Center. The flux wires, Charpy V-Notch and tensile test specimens removed from the capsule were tested according to ASTM E185-82 (Reference 4). Revised operating limits curves were developed using the test results along with 10CFR50 Appendix G (Reference 1) and Appendix G of the ASME Code (Reference 2). The methods and results of the fracture toughness evaluation are presented in this report as follows:

a. Section 3: Surveillance Program Background

b. Section 4: Peak Vessel Fluence Evaluation

c. Section 5: Charpy V-Notch Impact Testing

d. Section 6: Tensile Testing

e. Section 7: Operating Limits Curve Development

Data used to determine the RT_{NDT} of the electroslag welds in the beltline are documented in Appendix A. Photographs of fractured Charpy specimens are in Appendix B. The significant results of the evaluation are summarized as follows:

a. Capsule 2 was removed from the 120° azimuth position of the reactor. The capsule contained 6 flux wires: 2 each of pure copper (Cu), iron (Fe), and nickel (Ni). There were 24 Charpy V-Notch specimens: 8 each of plate material, weld material and heat affected zone (HAZ) material. The 8 tensile specimens removed consisted of 3 plate, 3 weld and 2 HAZ metal specimens. All specimen materials were positively identified as being from the vessel beltline.

b. The chemical compositions of the beltline materials were identified through a combination of literature research and testing. The copper (Cu) and nickel (Ni) contents were determined for all heats of plate material. The values for the limiting beltline plate are 0.12% Cu and 0.57% Ni. The values for the limiting beltline weld are 0.21% Cu and 0.21% Ni.

c. Results from the fabrication program materials certification testing were located and adjusted to be equivalent to test results done to current standards. The initial RT_{NDT} values for locations of interest in the vessel were determined. They are -6°F for the limiting beltline plate, -45°F for the limiting beltline weld, 10°F for the closure flange region and 52°F for the bottom head torus, which is the component with the highest RT_{NDT} in the non-beltline regions.

d. The flux wires were tested to determine the neutron flux at the surveillance capsule location. The fast flux (>1.0 MeV) measured was 7.5×10^{8} n/cm^2-sec. Based on the flux wire data, the surveillance specimens had received a best estimate fluence of 1.8×10^{17} n/cm^2 at removal.

e. The vessel peak inner surface and 1/4 T lead factors were established using an analysis that combines two-dimensional and one-dimensional finite element computer analysis. The flux peak occurs at an azimuthal location 25.5° past the vessel quadrant references. The lead factors for the surveillance capsule are 0.95 to the peak vessel surface and 1.38 to the peak 1/4 T depth location.

f. The maximum accumulated neutron fluence at 32 EFPY was determined at the peak 1/4 T location. The maximum 1/4 T vessel 32 EFPY fluence is 5.5×10^{17} n/cm^2 (best estimate) and 6.9×10^{17} n/cm^2 (upper bound).

g. The surveillance Charpy V-Notch specimens were impact tested at temperatures selected to define the transition of the fracture toughness curves of the plate, weld, and HAZ materials. Measurements were taken of absorbed energy, lateral expansion and percentage shear. Fracture surface photographs of each specimen are presented in Appendix B. From absorbed energy and lateral expansion results for the plate and weld materials the following values are extracted: index temperatures for 30 ft-lb, 50 ft-lb, and 35-mil lateral expansion (MLE) values and USE.

h. The irradiated plate and weld impact energy curves are compared to very limited unirradiated data from fabrication records to establish the 30 ft-lb index temperature irradiation shifts for the surveillance program. The plate material shows an estimated 30°F shift. The weld material shift and weld and plate decreases in USE could not be determined because the appropriate unirradiated data were not available.

i. The irradiated tensile specimens were tested at room temperature (70°F), reactor operating temperature (550°F), and estimated onset to upper shelf temperature (130°F for plate material and 180°F for weld material). The results tabulated for each specimen include yield and ultimate tensile strength, uniform and total elongation, and reduction of area.

j. The irradiated plate and weld tensile test results are compared to unirradiated data from the vessel fabrication test program. The materials show increased strength and generally decreased ductility, as expected for irradiation embrittlement.

k. As a part of the construction of the updated operating limits curves, the irradiation shift in RT_{NDT} was based on predictions calculated with Regulatory Guide 1.99, Revision 2 (Reference 5). For information purposes, the measured surveillance shift for base material was compared to the shift predicted by Reference 5. The surveillance test shift of 30°F in plate material RT_{NDT} for a fluence of 1.8×10^{17} n/cm^2 (best estimate) is slightly higher than the predicted upper limit on shift of 26°F.

l. The USE at 32 EFPY is predicted using the methods in Reference 5. The longitudinal weld USE is predicted to be 80 ft-lb at 32 EFPY. The surveillance plate USE is 132 ft-lb longitudinal at 32 EFPY. Branch Technical Position MTEB 5-2 (Reference 6) recommends 65% of the longitudinal USE as an estimate of transverse USE, so the 32 EFPY plate transverse USE would be 86 ft-lb. Data needed to predict USE for the other beltline plates and for the circumferential weld are not available.

m. Operating limits curves were constructed for three reactor conditions: hydrostatic pressure tests, non-nuclear heatup and cooldown, and core critical operation. The curves are valid up to 32 EFPY of operation. The limiting regions of the vessel affecting the curves' shapes are typically the core beltline (shifted to account for irradiation), the feedwater nozzle and CRD penetration discontinuities, and the closure flange region. The bolt preload and minimum permissible operating temperatures on the curves of 70°F provide some additional margin in the closure flange region where a detectable flaw size of 0.24 inch is used instead of 1/4 T. The predicted irradiation shift for the beltline is low enough that the beltline is not predicted to be limiting through 32 EFPY of operation. The operating limits curves for Peach Bottom 2 are shown in Figures 2-1 through 2-3.

2.2 CONCLUSIONS

The requirements of Reference 1 deal basically with vessel design life conditions and with limits of operation designed to prevent brittle fracture. Based on the evaluation of surveillance testing, the following conclusions are drawn:

a. The adjusted reference temperature for the plate material of 51°F is the limiting beltline value at 32 EFPY. This is below the Reference 1 allowable limit of 200°F, above which annealing is required.

b. The 32 EFPY values of USE for one beltline plate and the longitudinal weld materials are 86 ft-lb transverse and 80 ft-lb, respectively. These are above the Reference 1 allowable of 50 ft-lb, below which annealing is required. Data are not available for the other beltline plates and the circumferential weld, but based on data for similar materials, and considering the low fluence, it is expected that all beltline materials will have USE above 50 ft-lb through 32 EFPY.

c. Based on (a) and (b) above, provisions for complete volumetric examination or annealing of the reactor vessel before completing 32 EFPY of operation need not be considered.

d. Examination of the normal and upset operating conditions expected for the reactor shows that the worst pressure-temperature conditions expected from unplanned temperature transients are acceptable relative to the limits in Figures 2-1 through 2-3. Therefore, the only operating conditions for which the operating limits are a concern are those involving operator interaction, such as hydrotest and initiation of core criticality.

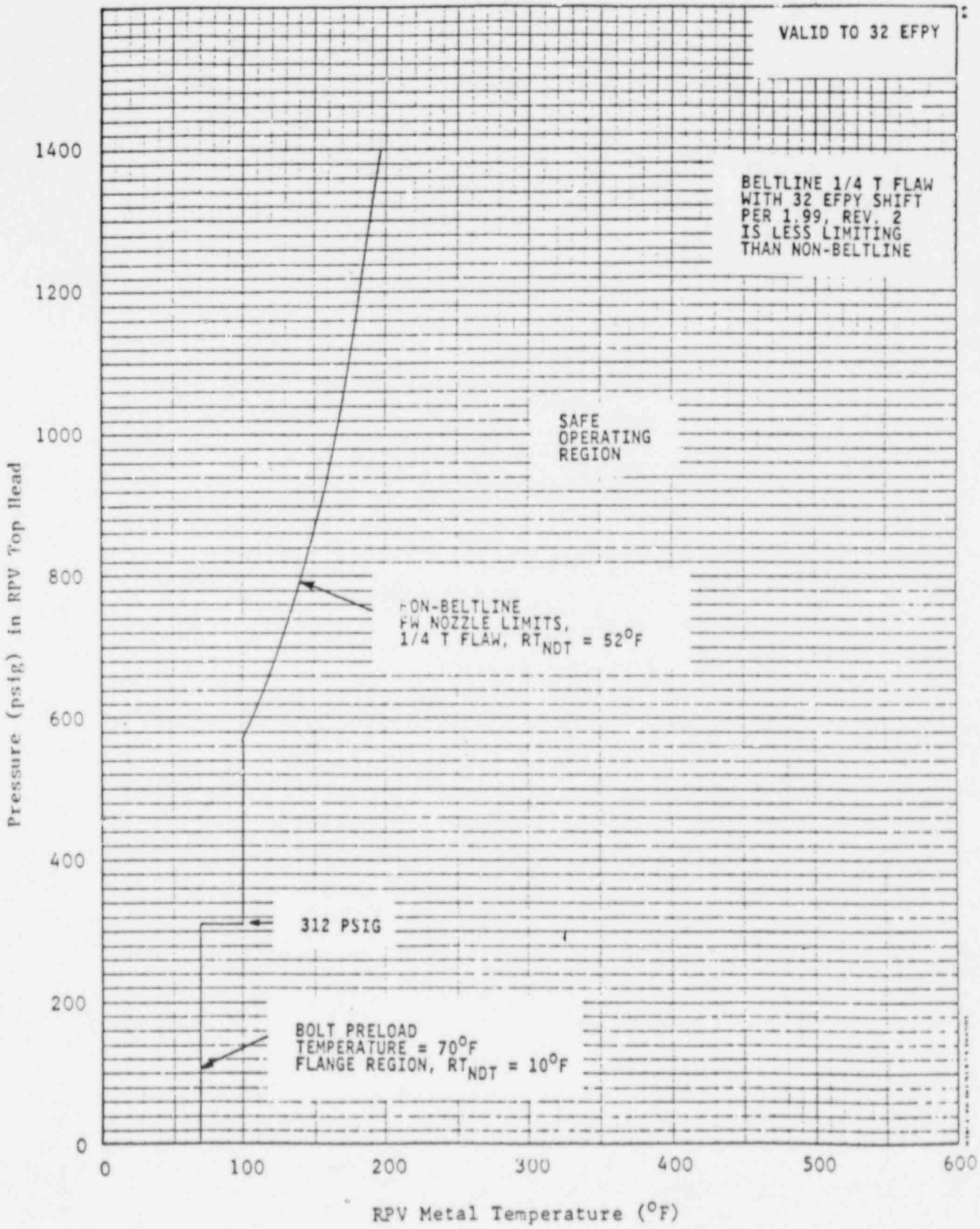

Figure 2-1. Minimum Temperature for Pressure Tests Such as Required by Section XI

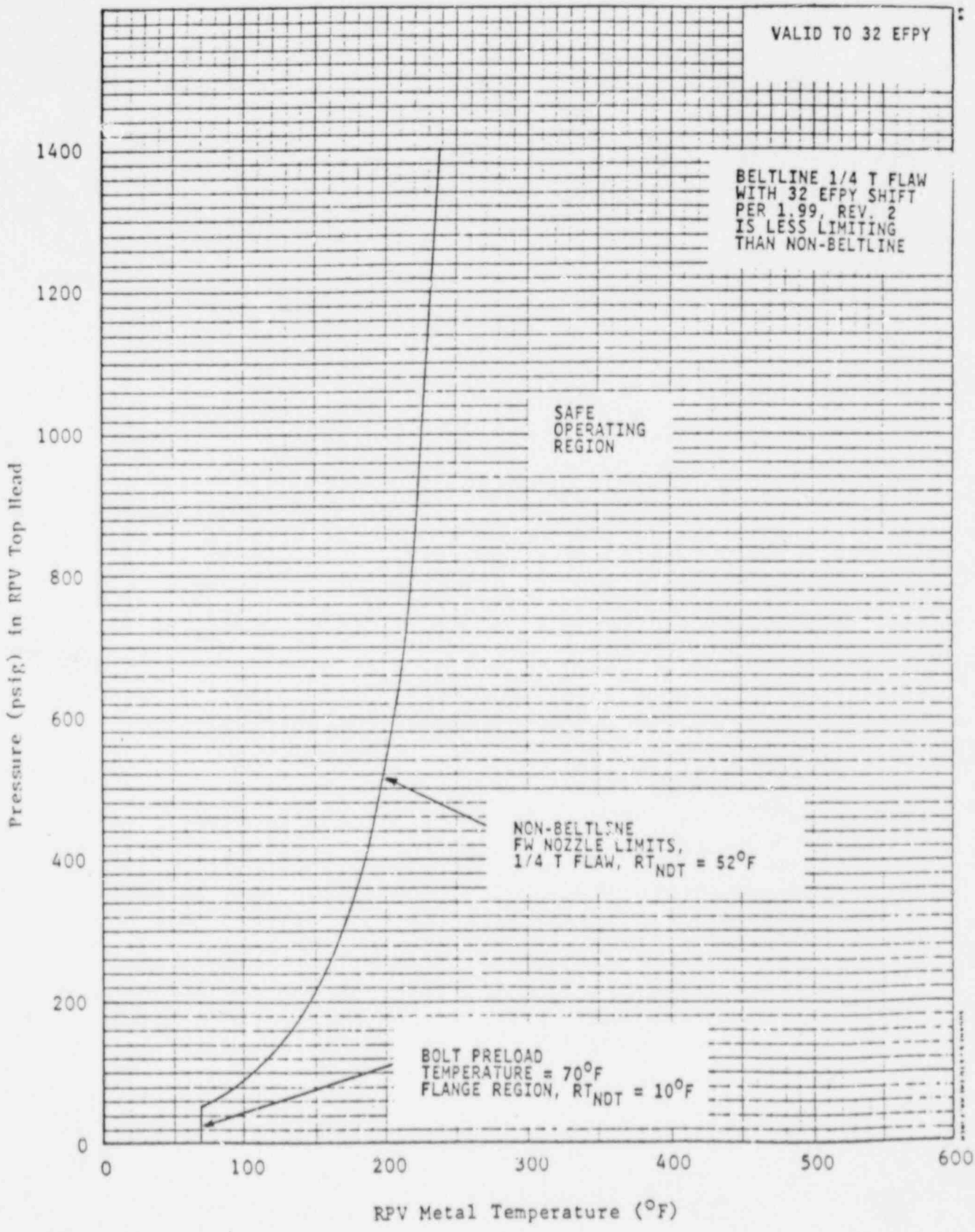

Figure 2-2. Minimum Temperature for Mechanical Heatup or Cooldown Following Nuclear Shutdown

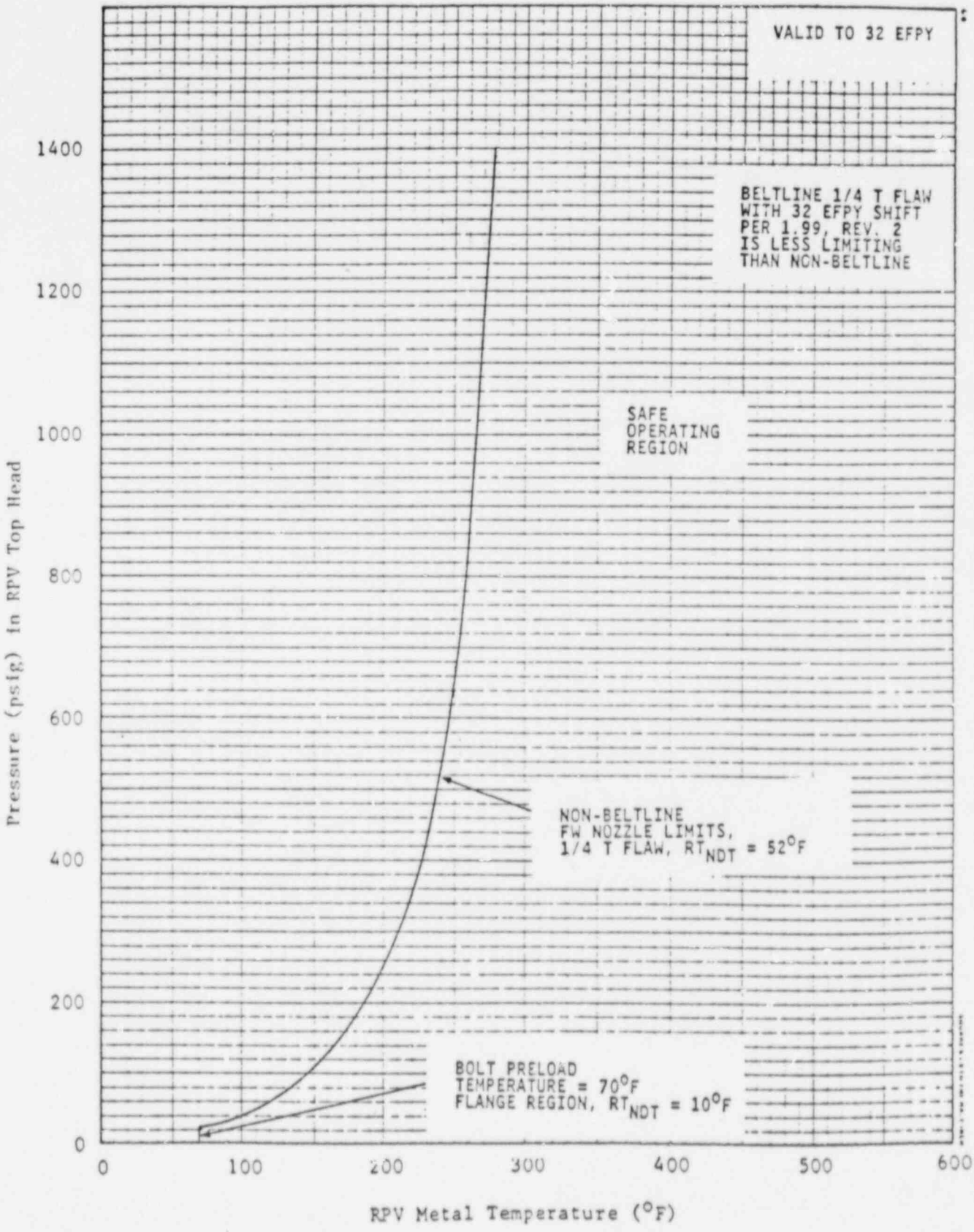

Figure 2-3. Minimum Temperature for Core Operation (Criticality)

3. SURVEILLANCE PROGRAM BACKGROUND

3.1 CAPSULE RECOVERY

The Peach Bottom 2 reactor was shut down in March, 1987 for refueling and maintenance. The accumulated thermal power output was 9.06×10^6 MWd or 7.53 EFPY. The reactor pressure vessel (RPV) originally contained three surveillance capsules, at 30°, 120° and 300° azimuths at the core midplane. The specimen capsules are held against the RPV inside surface by a spring loaded specimen holder. Each capsule receives equal irradiation because of core symmetry. During the outage, Capsule 2 at 120° was removed. The capsule was cut from the holder assembly and shipped by a 200 Series cask to the General Electric Vallecitos Nuclear Center in Pleasanton California.

Upon arrival at Vallecitos, the capsule was examined for identification. The reactor code of 25 and the code for Capsule 2 shown on the GE drawing (Reference 7) were confirmed on the capsule, as shown in Figure 3-1. The capsule contained two Charpy specimen packets and four tensile specimen tubes. Each Charpy packet contained 12 Charpy specimens and 3 flux wires. The four tensile specimen tubes contained eight specimens. The specimen gage sections were covered by aluminum sleeves, and during removal of the sleeves, the gage section of one tensile specimen was nicked. The specimen was tested in spite of this, as discussed in Section 6. All other specimens were removed without incident.

3.2 RPV MATERIALS AND FABRICATION BACKGROUND

3.2.1 Fabrication History

The Peach Bottom 2 RPV is a 251-in. BWR/4. Construction was started by Babcock & Wilcox (B&W) to the Winter 1965 addenda of the 1965 edition of the ASME Code. Chicago Bridge & Iron (CB&I) completed the vessel, generally to the 1968 edition of the ASME Code. The shell and head plates are ASME SA302, Grade B low alloy steel (LAS), modified per Code Case 1339. The nozzles and closure flanges are ASTM A508 Class 2 LAS, modified per

Code Case 1332-2, and the closure flange bolting materials are ASTM A540 Grade B24 LAS, modified by Code Cases 1335-2 and -4. The fabrication process employed double quench and temper heat treatment immediately after hot forming, then electroslag or submerged arc welding and post-weld heat treatment. The post-weld heat treatment was typically 30 hours at 1125°F ± 25°F. The arrangement of plates and welds relative to the core beltline and various nozzles is shown in Figure 3-2.

3.2.2 Material Properties of RPV at Fabrication

A search of General Electric Quality Assurance (QA) records was made to determine the chemical properties of the plates and welds in the RPV beltline. Table 3-1 shows the chemistry data obtained for the beltline materials. All data shown for the beltline plates were taken from QA records, and has been incorporated into DRF B13-01445. Available data for the beltline longitudinal electroslag welds were obtained from B&W (Reference 8), and have been evaluated in Appendix A to determine conservative values representative for the beltline longitudinal welds. The data for the girth weld, made by CB&I, were in QA records.

The surveillance weld was fabricated with the same electroslag weld procedure as was used in the longitudinal seam welds, but records of the actual weld metal used in the surveillance weld were not found. Only one weld wire heat was used for the vessel electroslag welds, and the usual B&W practice was to use the same heat in the surveillance weld. However, the chemical analysis results in Subsection 3.2.3 do not appear to support the assumption that the surveillance and beltline welds are the same weld heat. This is discussed in more detail in Subsection 3.2.3.

A search of QA records was made to collect results of certification mechanical property tests performed during RPV fabrication, specifically tensile test, Charpy V-Notch and dropweight impact test results. Properties of the beltline materials and other locations of interest are presented in Table 3-2. The Charpy data collected were used to establish the RT_{NDT} values for each vessel component, as described in Subsection 3.2.4. Charpy data from Reference 8 for the electroslag welds have been evaluated in Appendix A to determine a mean RT_{NDT} and standard deviation.

3.2.3 Specimen Chemical Composition

Samples were taken from tensile specimens 7K1 and 7JE (base) and from 7KK and 7KL (weld) after they were tested. The tensile specimens were fabricated from the same plates and weld as were the Charpy specimens, as detailed in Subsection 3.3, so the samples chosen are representative of all surveillance specimens. Chemical analyses were performed using a plasma emission spectrometer. Each sample was decomposed and dissolved, and a portion prepared for evaluation by the spectrometer. The spectrometer was calibrated with a standard solution containing 700 ppm Fe, 8 ppm Mn, 5 ppm Cu, 5 ppm Ni, 5 ppm Mo, 5 ppm Cr, and levels of perchloric acid and lithium consistent with the test. The calibration for phosphorus was done by analyzing two National Bureau of Standards steels with known quantities of phosphorus. The chemical composition results are given in Table 3-3.

The results for the plate are consistent with QA record information. However, the B&W suggestion that the surveillance weld wire heat is the same as in the vessel electroslag welds appears to be questionable. The tested Cu content of 0.10% is not within testing uncertainty of the 0.16% to 0.21% range in Appendix A. Similarly for Ni, the test value of 0.32% is not within uncertainty limits of the 0.14% to 0.21% range in Appendix A.

3.2.4 Initial Reference Temperatures

The requirements applicable to establishing the vessel component RT_{NDT} values in the ASME Code prior to 1972 can be summarized as follows:

a. Test specimens shall be longitudinally oriented Charpy V-Notch specimens.

b. At the RT_{NDT}, no impact test result shall be less than 25 ft-lb, and the average of three test results shall be at least 30 ft-lb.

c. Pressure tests shall be conducted at a temperature at least 60°F above the acceptable RT_{NDT} for the vessel.

The current requirements for establishing RT_{NDT} are significantly different. For plants constructed to the ASME Code after Summer 1972, the requirements are as follows:

a. Charpy V-Notch specimens shall be oriented normal to the rolling direction (transverse).

b. RT_{NDT} is defined as the higher of the dropweight NDT or 60°F below the temperature at which Charpy V-Notch 50 ft-lb energy and 35 mils lateral expansion are met.

c. Bolt-up in preparation for a pressure test or normal operation shall be performed at or above the RT_{NDT} or lowest service temperature (LST), whichever is greater.

Reference 1 states that for vessels constructed to a version of the ASME Code prior to the Summer 1972 Addendum, fracture toughness data and data analyses must be supplemented in an approved manner. General Electric has developed methods for analytically converting fracture toughness data for vessels constructed before 1972 to comply with current requirements. GE developed these methods from data in WRC Bulletin 217 (Reference 9) and from data collected to respond to NRC questions on FSAR submittals in the late 1970s. These methods and example RT_{NDT} calculations for vessel plate, weld, weld HAZ, forging, and bolting material are summarized in the remainder of this subsection. Calculated RT_{NDT} values for selected RPV locations are given in Table 3-2.

For vessel plate material, the first step in calculating RT_{NDT} is to establish the 50 ft-lb transverse test temperature given longitudinal test specimen data. There are typically three energy values at a given test temperature. The lowest energy Charpy value is adjusted by adding 2°F per ft-lb energy to 50 ft-lb. For example, for the six beltline plates the limiting combination of test temperature and Charpy energy from Table 3-2 is 43 ft-lb at +10°F for Heat C2873-1. The equivalent 50 ft-lb longitudinal test temperature is:

$$T_{50L} = 10°F + [(50 - 43)\ ft\text{-}lb * 2°F/ft\text{-}lb] = 24°F$$

The transition from longitudinal data to transverse data is made by adding 30°F to the test temperature. In this case, the 50 ft-lb transverse Charpy test temperature is T_{50T} = 54°F. The RT_{NDT} is the greater of NDT or (T_{50T} - 60°F). From Table 3-2, the NDT for Heat C2873-1 is -20°F. Therefore, the RT_{NDT} for the core beltline plate is -6°F.

For vessel weld material, the Charpy V-Notch results are usually limiting in establishing RT_{NDT}. The 50 ft-lb test temperature is established as for the plate material, but the 30°F adjustment to convert longitudinal data to transverse data is not applicable to weld metal. The limiting beltline weld Charpy V-Notch energy for the submerged arc weld in Table 3-2 is 41 ft-lb at +10°, so

$$T_{50T} = 10°F + [(50 - 41)\ ft\text{-}lb * 2°F/ft\text{-}lb] = 28°F.$$

As shown in Table 3-2, there are no NDT data available for the weld metal. The GE procedure requires that, when no NDT is available, the resulting RT_{NDT} be greater than -50°F. In this example, (T_{50T} - 60°F) is greater than -50°F, so the RT_{NDT} is -32°F.

The initial RT_{NDT} for the longitudinal electroslag welds is determined in Appendix A by fitting Charpy curves to nine sets of data for the weld heat used in the vessel electroslag welds. The T_{50T} values were determined by statistical fit for each curve and the T_{50T} values were used to calculate the mean and standard deviation of the electroslag weld RT_{NDT}.

For the vessel weld HAZ material, the RT_{NDT} is assumed the same as for the base material since ASME Code weld procedure qualification test requirements and post-weld heat treatment data indicate this assumption is valid.

For vessel forging material, such as nozzles and closure flanges the method for establishing RT_{NDT} is the same as for vessel plate material. Heat EV9934 in recirculation inlet nozzle N2F, listed in Table 3-2, has a calculated value of T_{50T} = 110°F. The NDT is 40°F. Therefore, with the RT_{NDT} being the greater of NDT or (T_{50T} - 60°F), the RT_{NDT} is 50°F. This is the highest forging RT_{NDT} in the vessel.

For bolting material, the current Code requirements define the LST as the temperature at which transverse Charpy V-Notch energy of 45 ft-lb and 25 mils lateral expansion (MLE) are achieved. If the required Charpy results are not met, or are not reported, but the Charpy V-Notch energy reported is above 30 ft-lb, the requirements of the ASME Code at construction are applied. As shown in Table 3-2, the limiting Charpy V-Notch energy for bolting material is 35 ft-lb at +10°F. The current requirements are not met, so the construction Code requirements are used. The LST is defined as 60°F above the temperature at which 30 ft-lb Charpy V-Notch energy is achieved. Therefore, the LST of the closure bolting material is 70°F.

3.3 SPECIMEN DESCRIPTION

The surveillance capsule contained 24 Charpy specimens: base metal (8), weld metal (8), and HAZ (8). There were 8 tensile specimens: base metal (3), weld metal (3), and HAZ (2). The 6 flux wires recovered were iron (2), nickel (2) and copper (2). The chemistry and fabrication history for the Charpy and tensile specimens are described in this section.

3.3.1 Charpy Specimens

The fabrication of the Charpy specimens is described in the Vessel Purchase Specification (Reference 10). All materials used for specimens were beltline materials from the lower intermediate shell course.

The base metal specimens were cut from Heat C2761-2, a beltline plate. The chemical analysis of this heat is in Table 3-1, and confirmed by the results in Table 3-3. The test plate was double quench and tempered and then given a stress relief heat treatment for 30 hours at 1125°F ± 25°F to simulate the post-weld heat treatment of the vessel. The method used to machine the specimens from the test plate is shown in Figure 3-3. Specimens were machined from the 1/4 T and 3/4 T positions in the plate, in the longitudinal orientation (long axis parallel to the rolling direction). The identifications of the base metal Charpy specimens recovered from the surveillance capsule are shown in Table 3-4.

The weld metal and HAZ Charpy specimens were fabricated from trim-off pieces of Heats C2761-2 and C2761-1 that were welded together by electroslag welding, using the same weld process for the longitudinal seam welds in the RPV beltline. The chemical analyses of the plates are given in Table 3-1. The weld metal chemistry from two specimens is presented in Table 3-3.

As discussed in Subsection 3.2.3, the surveillance weld wire heat and vessel weld wire heat do not appear to be the same. It may be possible for B&W to trace the weld wire heat in the surveillance weld, but this would require a B&W record search beyond the scope of the current effort. In any case, the information on the vessel welds has so much scatter that it could not be credibly compared to the surveillance weld results.

The welded test plate for the weld and HAZ Charpy specimens received a stress relief heat treatment at 1125°F ± 25°F for 30 hours to simulate the fabricated condition of the RPV. The weld specimens and HAZ specimens were fabricated as shown in Figures 3-4 and 3-5, respectively. The base metal orientation in the weld and HAZ specimens were longitudinal. Contained in Table 3-4 are the identifications of the weld metal and HAZ Charpy specimens from the surveillance capsule.

3.3.2 Tensile Specimens

Fabrication of the surveillance tensile specimens is described in Reference 9. The chemical composition and heat treatment for the base, weld and HAZ tensiles are the same as those for the corresponding Charpy specimens. The identifications of the base, weld, and HAZ tensile specimens recovered from the surveillance capsule are given in Table 3-4. A summary of the fabrication methods is presented in the remainder of this subsection.

The base metal specimens were machined from material at the 1/4 T and 3/4 T depth from Heat C2761-2. The specimens, oriented along the plate rolling direction, were machined to the dimensions shown in Figure 3-6. The gage section was tapered to a minimum diameter of 0.250 inch at the center. The weld metal tensile specimen material was cut from the welded test plate, as shown in Figure 3-7. The specimens were machined entirely from weld metal, scrapping material that might include base metal. The fabrication method for the HAZ tensile specimens is illustrated in Figure 3-8. The specimen blanks were cut from the welded test plate such that the gage section minimum diameter was machined at the weld fusion line. The finished HAZ specimens are approximately half weld metal and half base metal oriented along the plate rolling direction.

Table 3-1

CHEMICAL COMPOSITION OF RPV BELTLINE MATERIALS

Identification	Heat/Lot No.	Composition by Weight Percent							
		C	Mn	P	S	Si	Ni	Mo	Cu
Lower Plates:									
Mk-57	C2791-2	0.21	1.39	0.010	0.018	0.22	0.52	0.48	0.12
"	C2761-1	0.22	1.30	0.011	0.015	0.23	0.54	0.47	0.11
"	C2873-2	0.22	1.39	0.010	0.018	0.22	0.57	0.52	0.12
Lower-Intermediate Plates:									
Mk-58	C2894-2	0.22	1.30	0.013	0.018	0.21	0.42	0.46	0.13
"	C2873-1	0.22	1.39	0.010	0.018	0.22	0.57	0.52	0.12
"	C2761-2	0.22	1.30	0.011	0.015	0.23	0.54	0.47	0.11
Longitudinal Welds:									
B1,B2,B3 [a] C1,C2,C3	Heat 37C065	0.17	1.41	0.015	0.013	0.09	0.21	0.53	0.21
Lower to Lower-Int. Girth Weld:									
BC	Adcom INMM Heat S-3986 Linde 124 Flux, Lot 3876	0.09	1.46	0.019	0.015	0.35	0.97	0.53	0.06

[a] The basis for the electroslag weld chemistry determination is in Appendix A.

Table 3-2

RESULTS OF FABRICATION TEST PROGRAM FOR SELECTED RPV LOCATIONS

Location	Ident. Number	Heat Number	Tensile: Yield (ksi)	Tensile: UTS (ksi)	Tensile: Total Elong (%)	Tensile: Area Reduc. (%)	Test Temp. (°F)	Charpy Energy (ft-lb)	NDT (°F)	T_{50T}-60 (°F)	RT_{NDT} (°F)
Beltline:											
Lower Shell Plates	Mk-57	C2791-2	67.6	86.3	28.5	73.6	10	61,55,44	-30	-8	-8
	"	C2761-1	69.4	88.8	28.0	71.5	10	47,59,63	-30	-14	-14
	"	C2873-2	73.8	91.0	28.0	73.1	10	60,69,64	-30	-20	-20
Lower-Intermediate Shell Plates	Mk-58	C2894-2	68.0	85.0	28.0	72.1	10	57,52,54	-30	-20	-20
	"	C2873-1	74.8	91.5	26.6	71.5	10	43,52,48	-20	-6	-6
	"	C2761-2	67.0	91.8	29.3	70.5	10	57,69,58	-20	-20	-20
Longitudinal Welds	B1,B2,B3 C1,C2,C3	37C065	65.5	83.4	26.8	65.4	--see Appendix A---			15 [a]	-45
Girth Weld	BC	Ht. S-3986 Linde 124 Flux Lot 3869	74.7	91.2	25.5	66.0	10	41,45,46	n/a	28	-32
Non-Beltline:											
Upper Shell Plate	Mk-60	C2796-2					10	43,53,49	10	-6	10
Vessel Flange	Mk-48	124V-201					10	111,123,141	10	-20	10
Head Flange	Mk-209	5P2744					10	57,78,96	10	-20	10
Top Head Torus	Mk-202	C3131-3					10	75,46,91	10	-12	10
Bottom Head Torus	Mk-2	A0931-2					40	29,65,50	40	112	52
Recirculation Inlet	N2F	EV9934					40	30,31,31	10	110	50
Closure Bolts	Mk-61	6720443					10	35,36,37	n/a	LST - 70	

[a] As discussed in Appendix A, the RT_{NDT} value has a standard deviation of 16.44°F.

Table 3-3

PLASMA EMISSION SPECTROMETRY CHEMICAL ANALYSIS OF RPV SURVEILLANCE PLATE AND WELD MATERIALS

Element	Base Metal Tensile 7K1	Base Metal Tensile 7JE	Weld Metal Tensile 7KK	Weld Metal Tensile 7KL
Mn	1.24	1.28	1.43	1.46
P	0.009	0.011	0.010	0.012
Cu	0.10	0.10	0.09	0.10
Ni	0.54	0.53	0.32	0.32
Mo	0.48	0.49	0.49	0.49
Cr	0.09	0.09	0.08	0.08

Table 3-4

IDENTIFICATION OF CHARPY AND TENSILE SPECIMENS REMOVED FROM SURVEILLANCE CAPSULE

Charpy Specimens [a]

Base	Weld	HAZ
75M	7AM	7D1
75P	7AT	7D3
765	7B3	7DK
76K	7B4	7DL
772	7BA	7DU
77A	7BL	7J1
77D	7BT	7J3
77K	7C1	7JA

Tensile Specimens [a]

Base	Weld	HAZ
7K1	7KD	7LA
7K3	7KK	7LE
7JE	7KL	

[a] All specimens have two dots over the center identification digit.

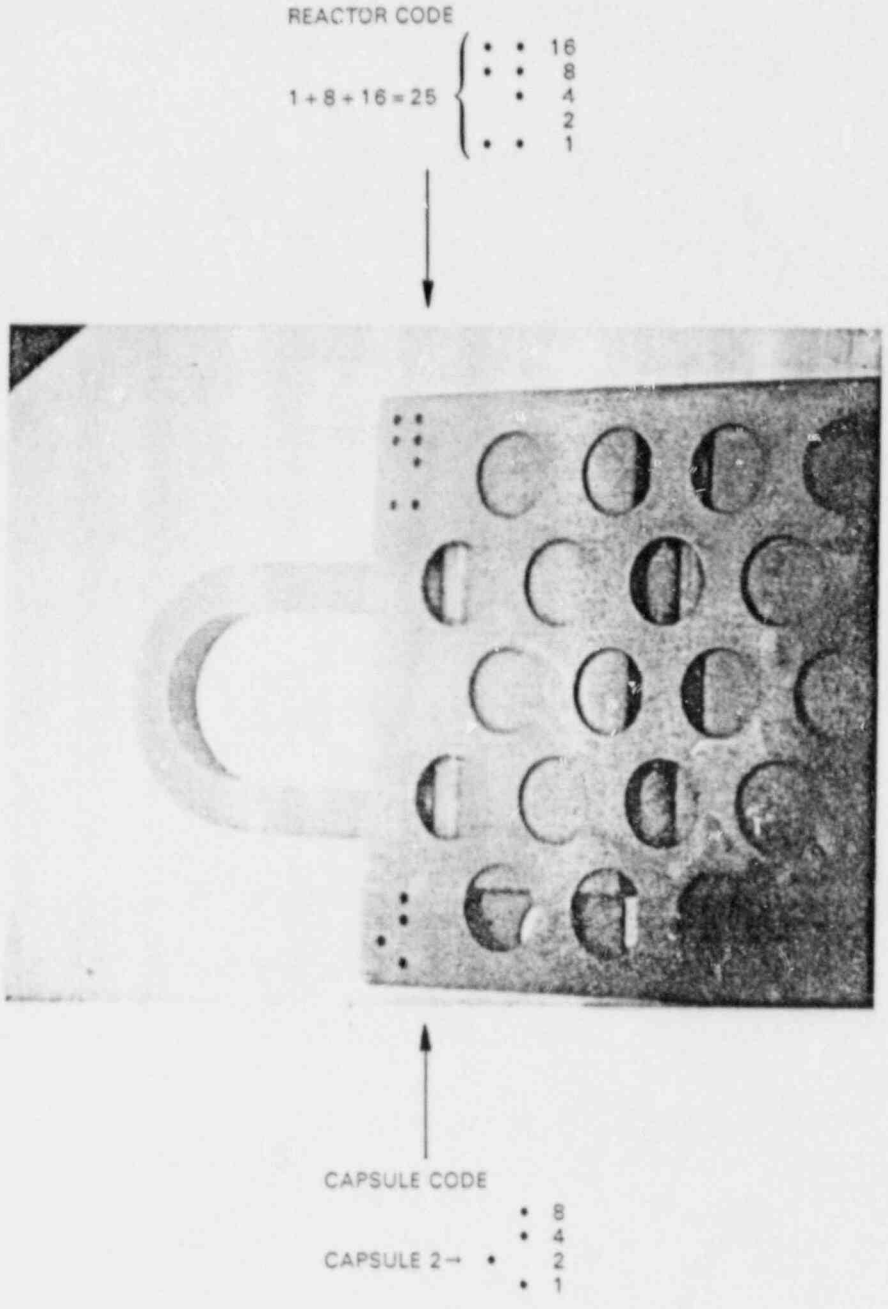

Figure 3-1. Surveillance Capsule Recovered from Peach Bottom 2 Reactor

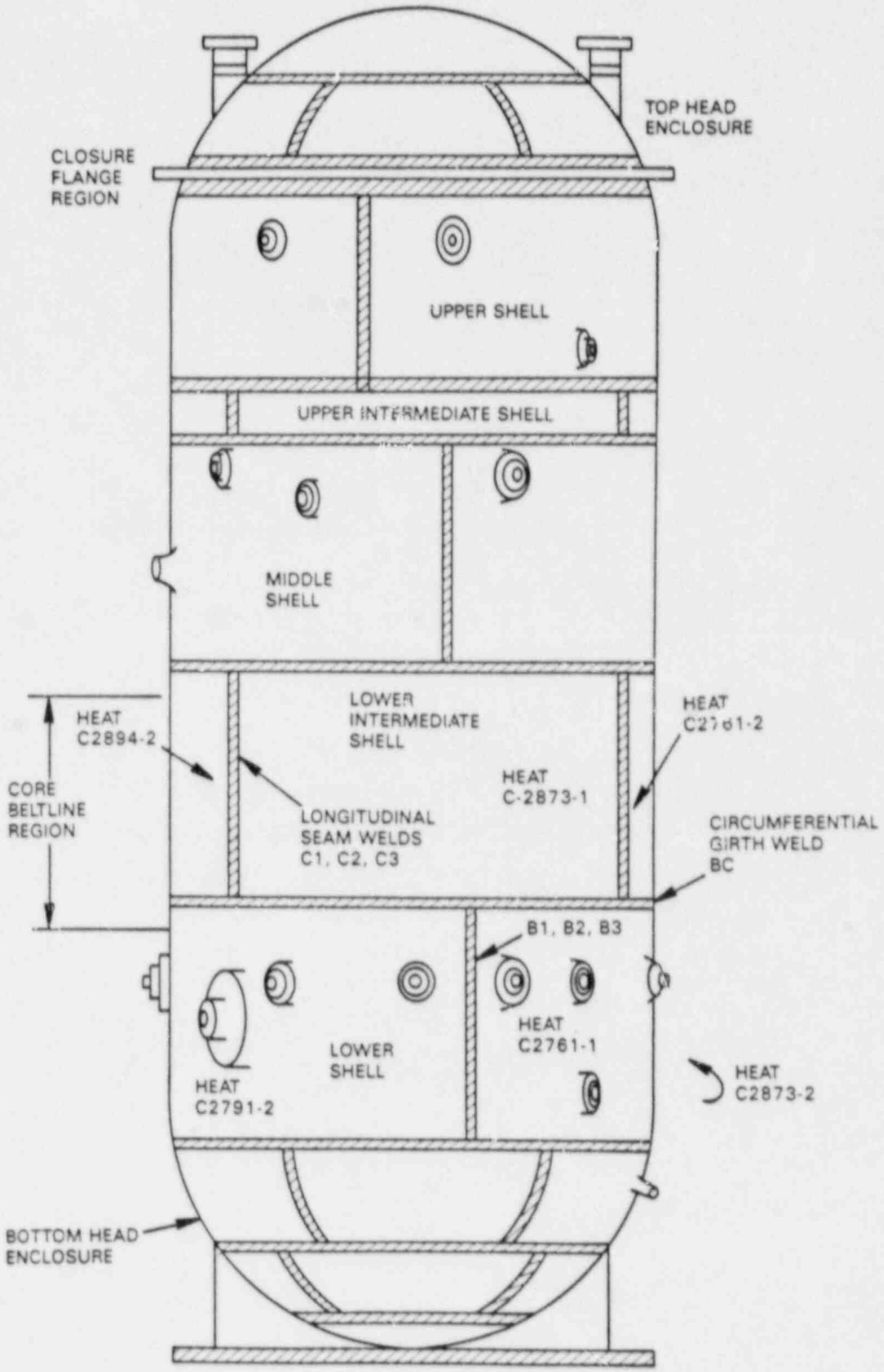

Figure 3-2. Schematic of the RPV Showing Arrangement of Vessel Plates and Welds

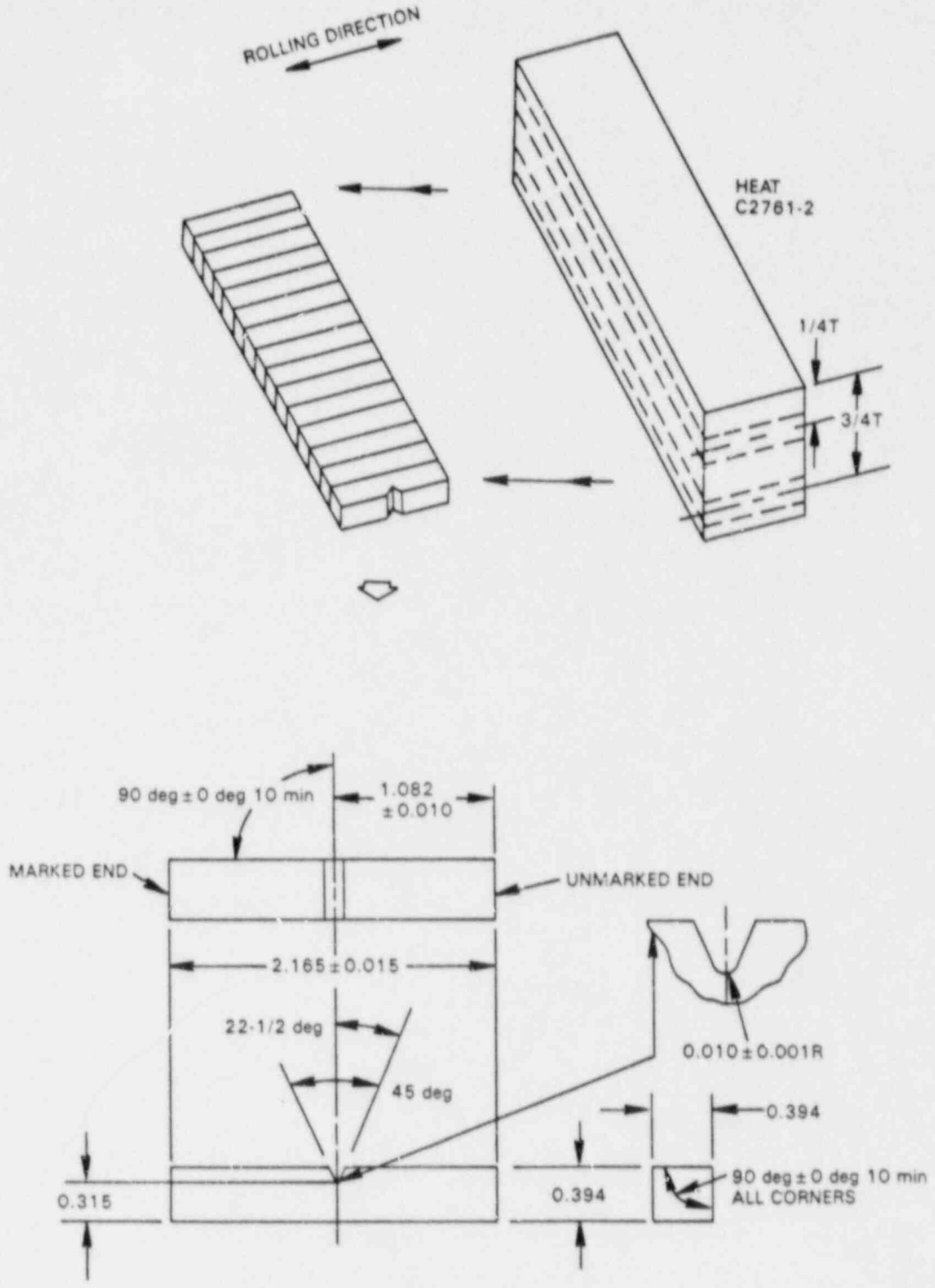

Figure 3-3. Fabrication Method for Base Metal Charpy Specimens

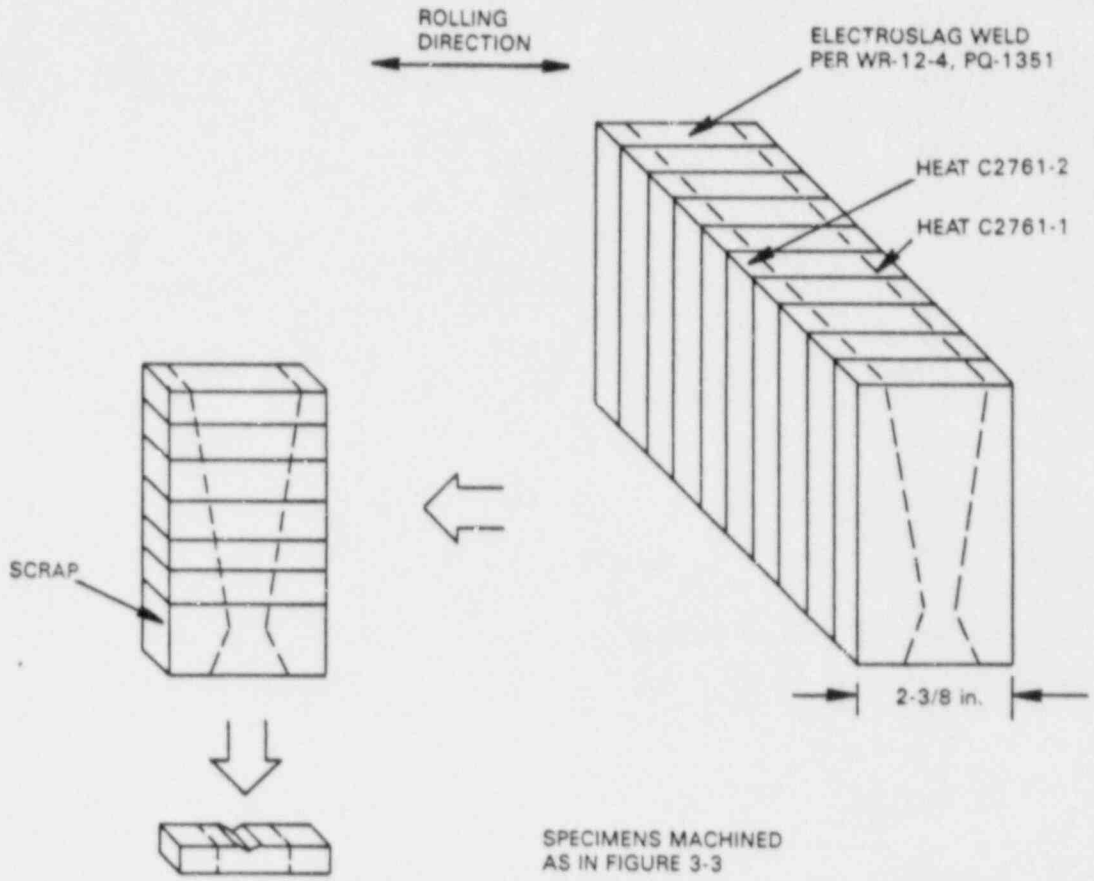

Figure 3-4. Fabrication Method for Weld Metal Charpy Specimens

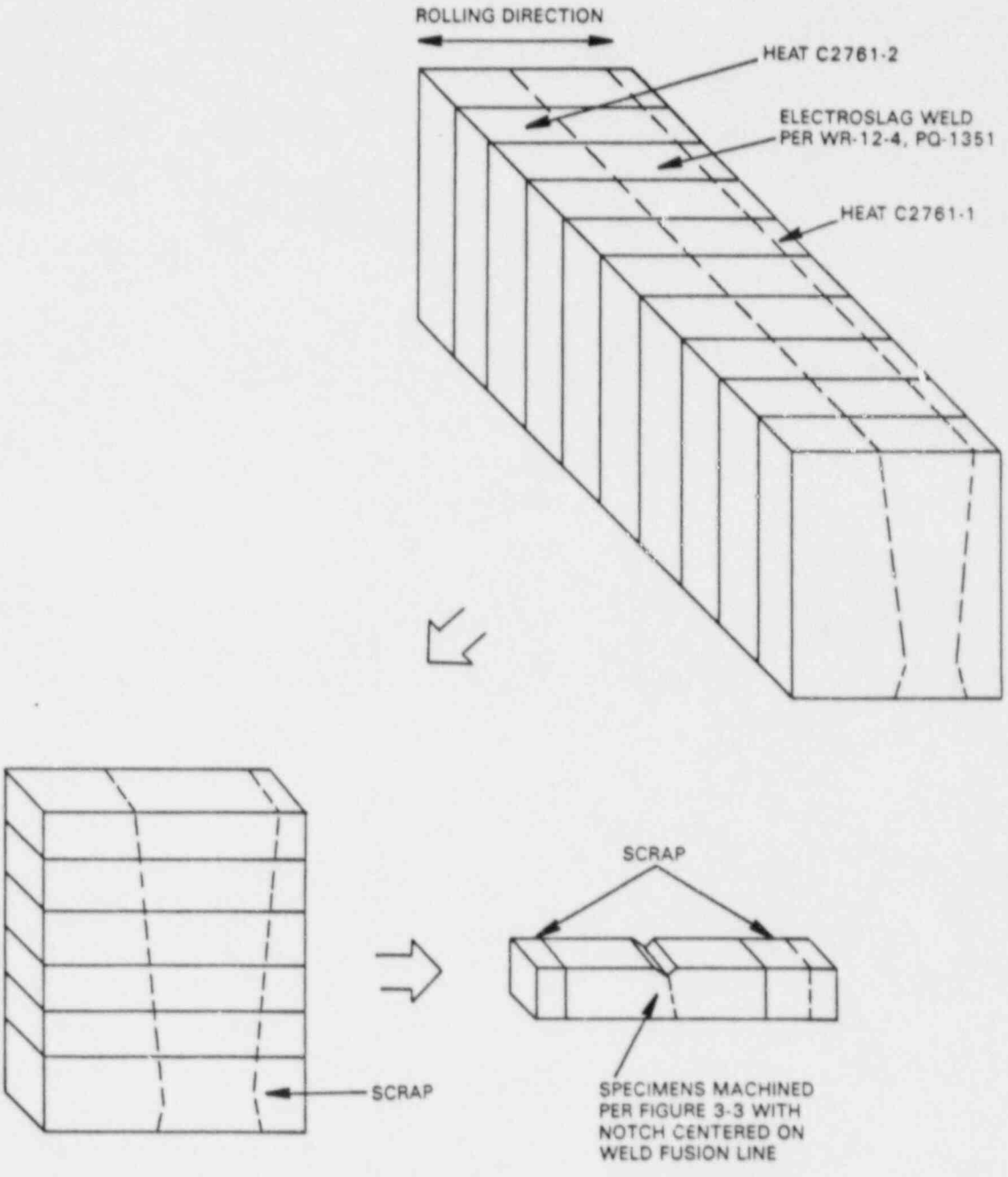

Figure 3-5. Fabrication Method for HAZ Charpy Specimens

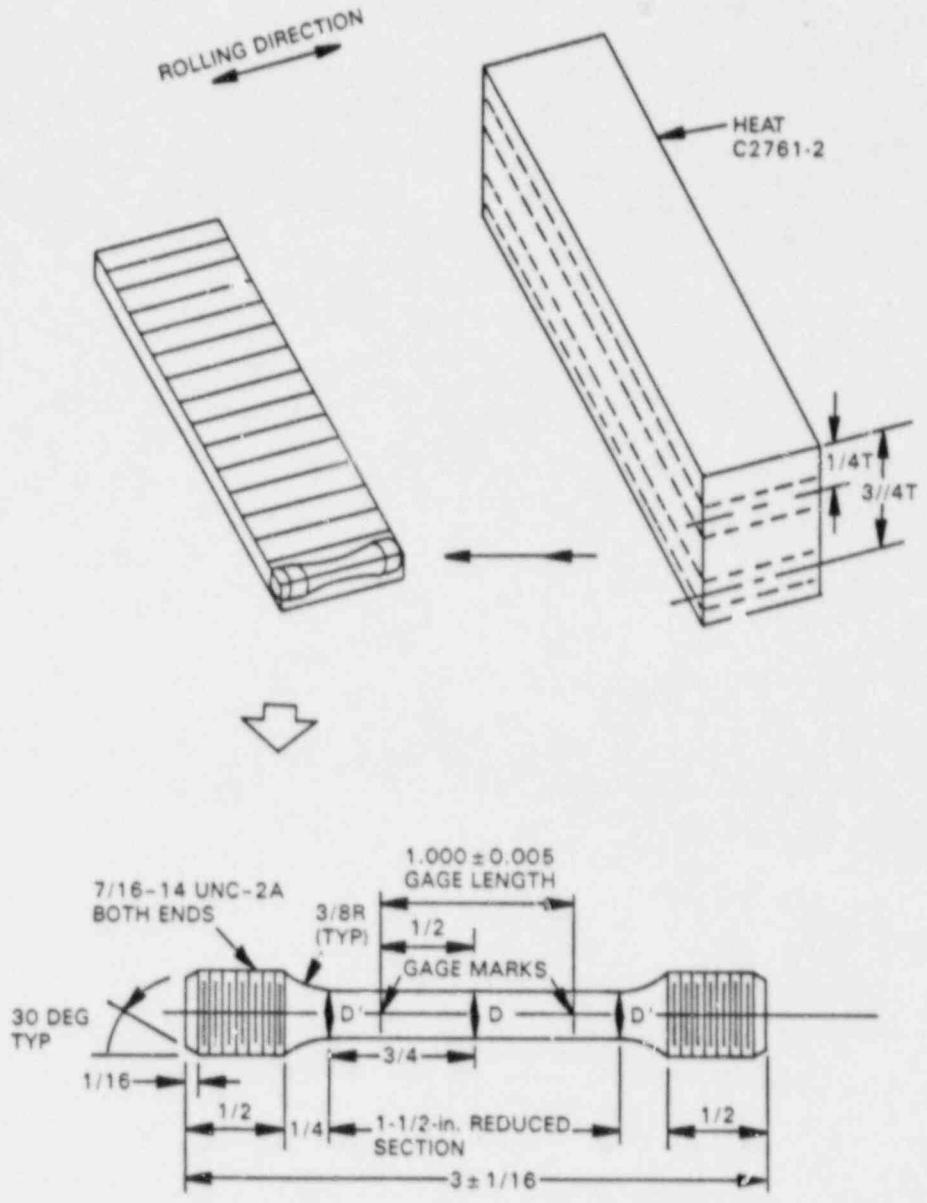

Figure 3-6. Fabrication Method for Base Metal Tensile Specimens

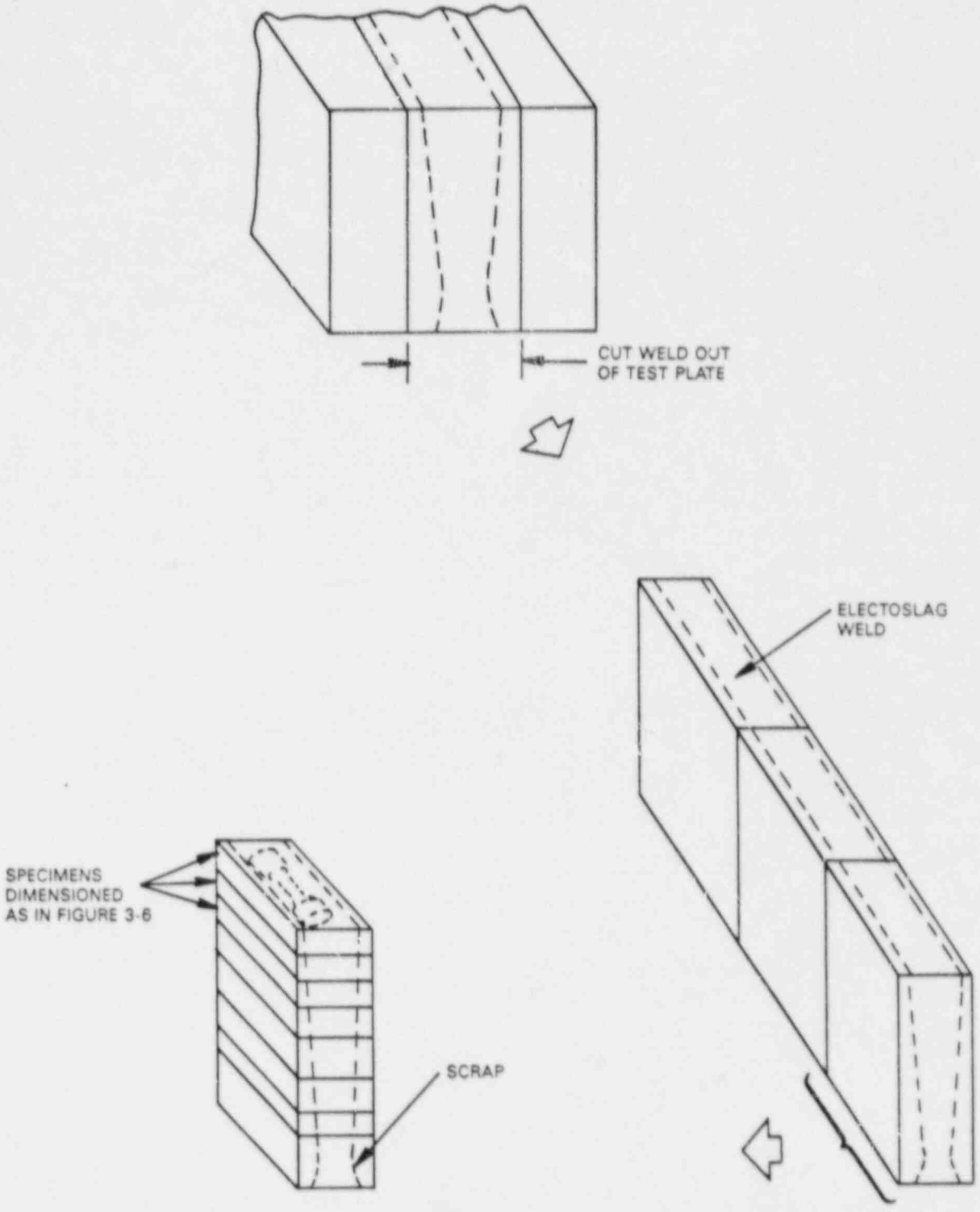

Figure 3-7. Fabrication Method for Weld Metal Tensile Specimens

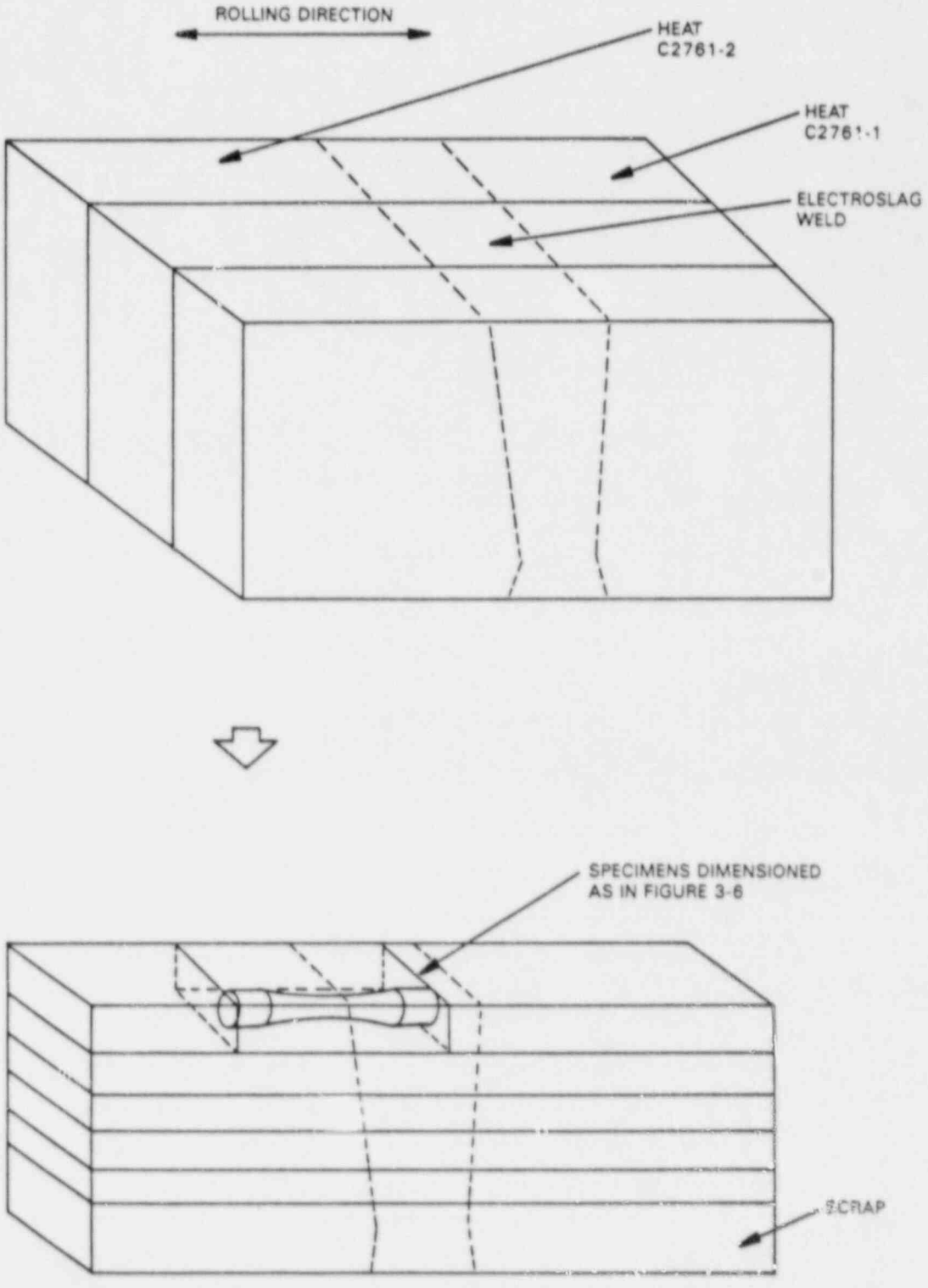

Figure 3-8. Fabrication Method [illegible] sile Specimens

4. PEAK RPV FLUENCE EVALUATION

Flux wires were analyzed to determine flux and fluence received by the surveillance capsule. An analysis combining two-dimensional and one-dimensional flux distribution computer calculations was evaluated to establish the location of peak vessel fluence and the lead factors of the surveillance capsule relative to the peak vessel location.

4.1 FLUX WIRE ANALYSIS

4.1.1 Procedure

The surveillance capsule contained six flux wires: two each of iron, copper, and nickel. Each wire was removed from the capsule, cleaned with dilute acid, weighed, mounted on a counting card, and analyzed for its radioactivity content by gamma spectrometry. Each iron wire was analyzed for Mn-54 content, each copper wire for Co-60 and each nickel wire for Co-58 at a calibrated 4-cm or 10-cm source-to-detector distance with 100-cc and 80-cc Ge(Li) detector systems. The gamma spectrometer was calibrated using NBS material.

To properly predict the flux and fluence at the surveillance capsule from the activity of the flux wires, the periods of full and partial power irradiation and the zero power decay periods were considered. Operating days for each fuel cycle and the reactor average power fraction are shown in Table 4-1. Zero power days between fuel cycles are listed as well.

From the flux wire activity measurements and power history, reaction rates for Fe-54 (n,p) Mn-54, Cu-63 (n,α) Co-60 and Ni-58 (n,p) Co-58 were calculated. The >1 MeV fast flux reaction cross sections for the iron, copper and nickel wires were estimated to be 0.212 barn, 0.00374 barn and 0.276 barn, respectively. These values were obtained from measured cross section functions determined at Vallecitos from more than 65 spectral determinations for BWRs and for the General Electric Test Reactor using activation monitor and spectral unfolding techniques. These data functions are applied to BWR pressure vessel locations based on water gap (fuel to vessel wall) distances. The cross sections for >0.1 MeV flux were determined from the measured 1-[illegible] MeV cross section ratio of 1.6.

4.1.2 Results

The measured activity, reaction rate and determined full-power flux results for the surveillance capsule are given in Table 4-2. The >1 MeV and >0.1 MeV flux values of 7.5×10^8 and 1.2×10^9 n/cm^2-sec from the flux wires were calculated by dividing the reaction rate measurement data by the appropriate cross sections. The corresponding fluence results, 1.8×10^{17} and 2.9×10^{17} n/cm^2 for >1 MeV and >0.1 MeV, respectively, were obtained by multiplying the full-power flux density values by the product of the total seconds irradiated (3.275×10^8 sec) and the full-power fraction (0.726).

Generally, for long-term irradiations, dosimetry results from copper flux wires are considered the most accurate because of Co-60's long half-life (5.27 years). The secondary iron flux monitor reaction yielding Mn-54 gave results very consistent with the copper reaction despite the shorter half-life of 312.5 days for Mn-54. Nickel wire results are least accurate, because of the 70.8 day half life of Co-58. In fact, Co-58 activity is usually so low by the time the flux wires are tested that the nickel wires are not tested. Consistency in results between the iron and copper wire results indicates an accurate power-history evaluation and a consistent core radial power shape.

The accuracies of the values in Table 4-2 for a 2σ deviation are estimated to be:

± 5% for dps/g (disintegrations per second per gram)
± 10% for dps/nucleus (saturated)
± 25% for flux and fluence >1 MeV
± 35% for flux and fluence >0.1 MeV

A set of flux wires from Peach Bottom 2 was evaluated by General Electric in 1978. The >1 MeV flux was 1.05×10^9 n/cm^2-sec. Differences in the current test inputs and methods would decrease that number to about 7.9×10^8 n/cm^2-sec. The result from this study of 7.5×10^8 n/cm^2-sec is slightly lower than the adjusted flux value. Past experiences with dosimeters removed after one fuel cycle have generally shown high results when compared to the ten-year dosimetry. The first cycle dosimetry

reflects power cycling due to testing, and in some cases the initial cores had an atypical power shape in the first fuel cycle, where the peripheral fuel bundles had unusually high power levels. The ten-year results reflect a long period of typical operation, so the results from the current test are considered to be more accurate.

4.2 DETERMINATION OF LEAD FACTORS

The flux wires detect flux at a single location. The wires will therefore reflect the power fluctuations associated with the operation of the plant. However, the flux wires are not necessarily at the location of peak vessel flux. Lead factors are required to relate the flux at the wires' location to the the peak flux. These lead factors are a function of the core and vessel geometry and of the distribution of bundles in the core. Lead factors were generated for the Peach Bottom 2 geometry and operating history. The methods used to calculate the lead factors are discussed below.

4.2.1 Procedure

Determination of the lead factors for the RPV inside wall and at 1/4 T depth was done using a combination of one-dimensional and two-dimensional finite difference computer analysis. The two-dimensional analysis established the relative fluence in the azimuthal direction at the vessel surface and 1/4 T depth. A series of one-dimensional analyses were done to determine the core height of the axial flux peak and its relationship to the surveillance capsule height. The combination of azimuthal and axial distribution results provides the ratio of flux, or the lead factor, between the surveillance capsule location and the peak flux locations.

The two-dimensional DOT IV computer program was used to solve the Boltzman transport equation using the discrete ordinate method on an (R,θ) geometry, assuming a fixed source. Eighth core symmetry was used with periodic boundary conditions at 90° and 135°. Neutron cross sections were determined for 26 energy groups, with angular scattering approximated by a third-order Legendre expansion. A schematic of the two-dimensional vessel model is shown in Figure 4-1. A total of 113 radial intervals and

45 azimuthal intervals were used. The model consists of an inner and outer core region, the shroud water annulus inside and outside the shroud, the vessel wall and an air annulus representing the drywell. Flux as a function of azimuth was calculated, establishing the azimuth of the peak flux and its magnitude relative to the flux at the wires' location of 120°.

The one-dimensional computer code (SN1D) was used to calculate radial flux distribution at several core elevations at the azimuth angle of 115.5°, where the azimuthal peak was determined to exist. The elevation of the peak flux was determined, as well as its magnitude relative to the flux at the surveillance capsule elevation.

4.2.2 Results

The two-dimensional calculation indicated the flux to be a maximum 25.5° past the RPV quadrant references (0°, 90°, etc.). The peak closest to the 120° location of Capsule 2 is at 115.5°, as shown in Figure 4-2. The distribution calculations establish the lead factor between the surveillance capsule location and the peak location at the inner vessel wall. This lead factor is 0.95. The fracture toughness analysis done is based on a 1/4 T depth flaw in the beltline region, so the attenuation of the flux to that depth is considered. The resulting lead factor from the capsule to the 1/4 T depth at the peak location is 1.38.

4.3 ESTIMATE OF 32 EFPY FLUENCE

The fluence at 32 EFPY is estimated by taking the best estimate or upper bound of the measured flux from Table 4-2 and the 1/4 T lead factor. The time period 32 EFPY is 1.01×10^9 seconds. The resulting 32 EFPY fluence values are:

Best Estimate: $(7.5 \times 10^8 \text{ n/cm}^2\text{-s})(1.00)(1.01 \times 10^9 \text{ s})/1.38 = 5.5 \times 10^{17} \text{ n/cm}^2$.

Upper Bound: $(7.5 \times 10^8 \text{ n/cm}^2\text{-s})(1.25)(1.01 \times 10^9 \text{ s})/1.38 = 6.9 \times 10^{17} \text{ n/cm}^2$.

The upper bound fluence was used for analysis purposes in this report.

Table 4-1

SUMMARY OF DAILY POWER HISTORY

Cycle	Cycle Dates	Operating Days	Percent of Full Power	Days Between Cycles
1	2/15/74 - 3/27/76	772	0.634	
				88
2	6/24/76 - 4/27/77	308	0.742	
				140
3	9/15/77 - 9/8/78	359	0.815	
				39
4	10/18/78 - 3/21/80	521	0.862	
				146
5	8/15/80 - 2/19/82	554	0.771	
				132
6	7/2/82 - 4/28/84	667	0.646	
				440
7	7/13/85 - 3/13/87	609	0.715	
		3790	0.726 (average)	

Table 4-2

SURVEILLANCE CAPSULE LOCATION FLUX AND FLUENCE

FOR IRRADIATION FROM 2/15/74 TO 3/13/87

Wire (Element)	Wire Weight (g)	dps/g Element (at end of Irradiation)	Reaction Rate [dps/nucleus (saturated)]	Full Power Flux [a] (n/cm|-s) >1 MeV	Full Power Flux [a] (n/cm|-s) >0.1 MeV	Fluence (n/cm|) >1 MeV	Fluence (n/cm|) >0.1 MeV
Copper 64945	0.3742	8.36×10^{3}	2.80×10^{-18}				
Copper 64946	0.3706	8.49×10^{3}	2.84×10^{-18}				
			Average - 2.82×10^{-18}	7.5×10^{8}	1.2×10^{9}	1.8×10^{17}	2.9×10^{17}
Iron 64945	0.1017	5.74×10^{4}	1.55×10^{-16}				
Iron 64946	0.1041	6.13×10^{4}	1.66×10^{-16}				
			Average - 1.60×10^{-16}	7.6×10^{8}			
Nickel 64945	0.2800	1.14×10^{6}	2.27×10^{-16}				
Nickel 64946	0.2855	1.16×10^{6}	2.33×10^{-16}				
			Average - 2.30×10^{-16}	8.3×10^{8}			

[a] Full power of 3293 MW_t.

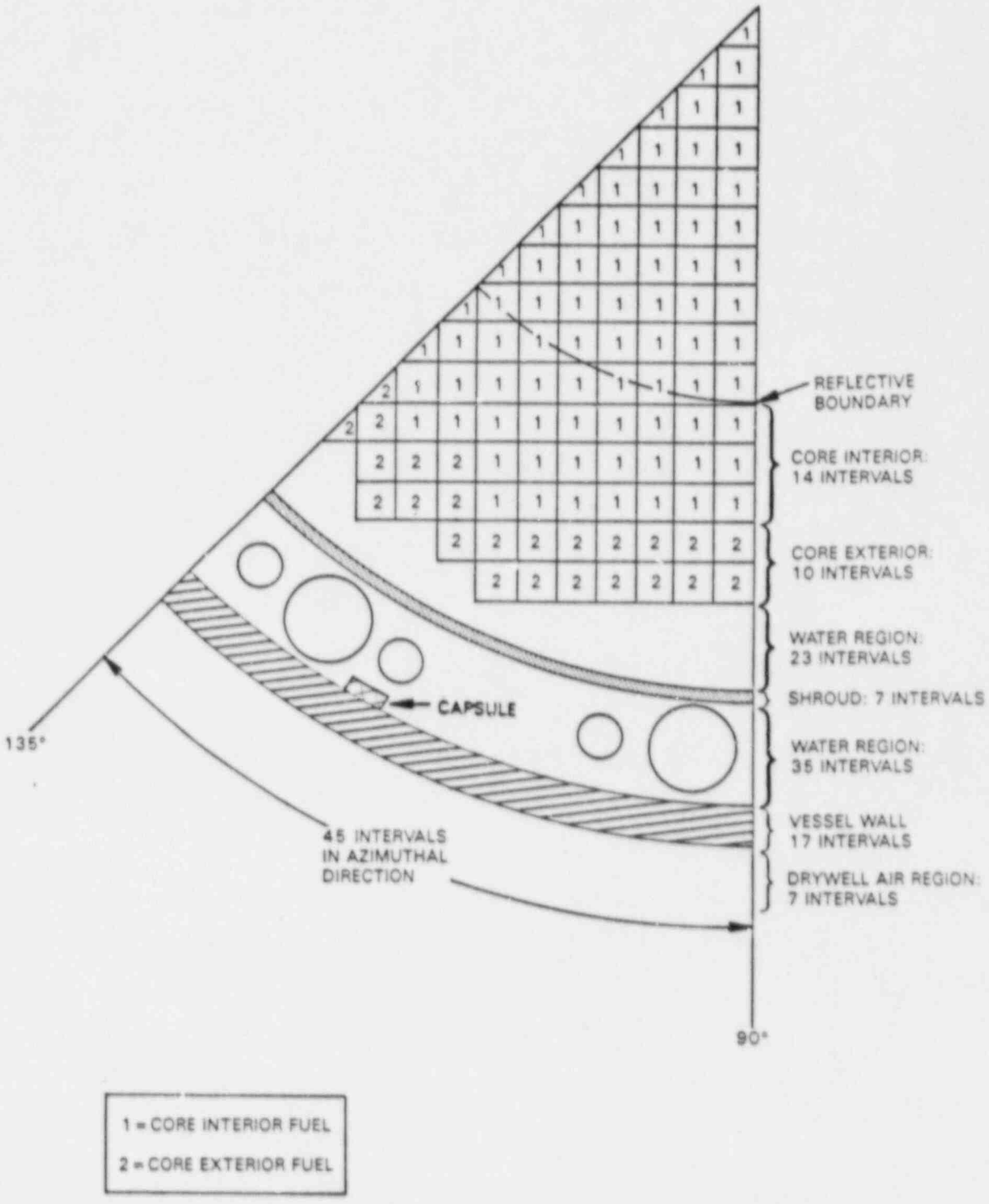

Figure 4-1. Schematic of Model for Two-Dimensional Flux Distribution Analysis

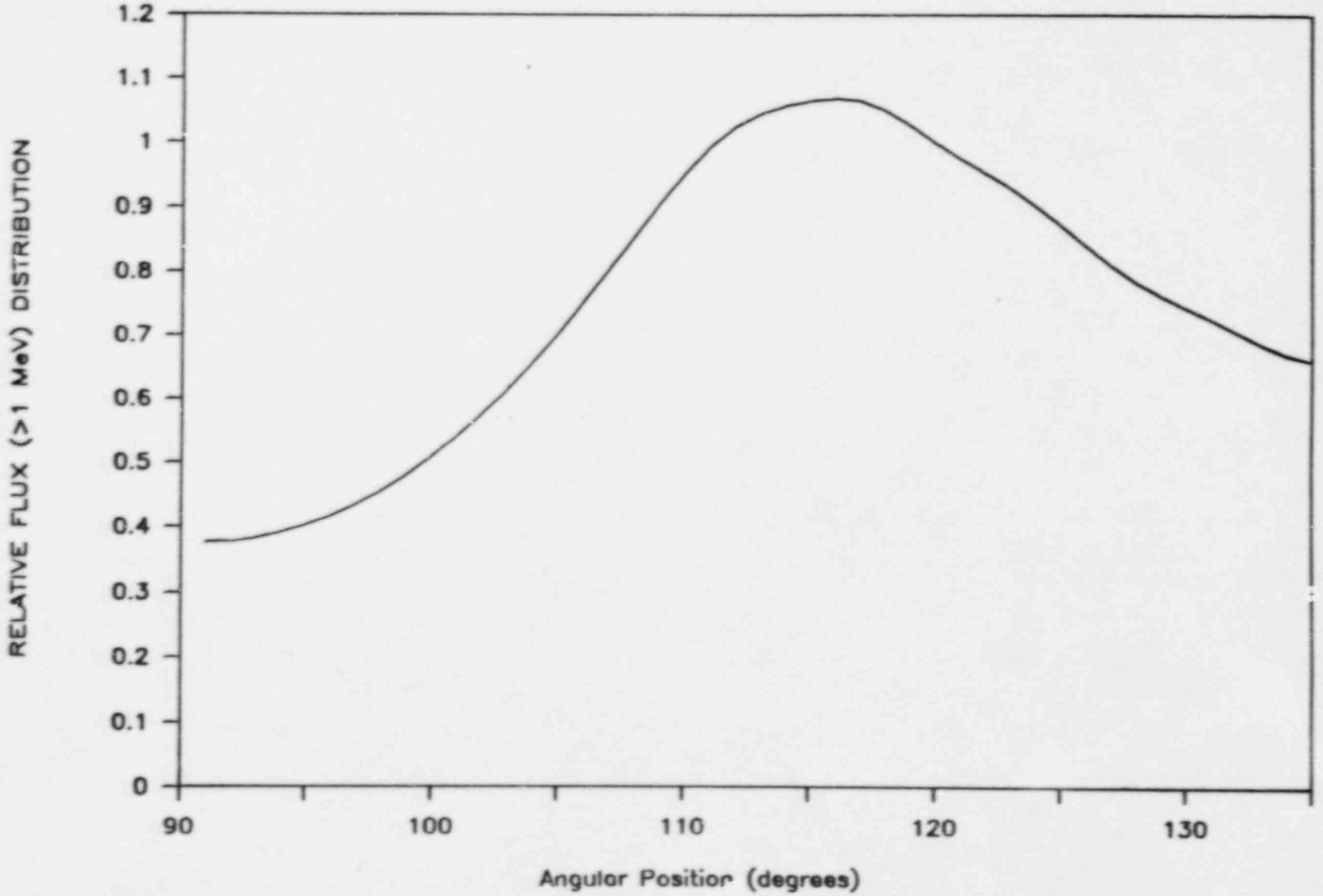

Figure 4-2. Relative Fast Neutron Flux Variation with Angular Position at the Vessel

5. CHARPY V-NOTCH IMPACT TESTING

The 24 Charpy specimens recovered from the surveillance capsule were impact tested at temperatures selected to establish the toughness transition and upper shelf of the irradiated RPV materials. Testing was conducted in accordance with ASTM E23-82 (Reference 11).

5.1 IMPACT TEST PROCEDURE

The testing machine used was a Riehle Model PL-2 impact machine, serial number R-89916. The pendulum has a maximum velocity of 15.44 ft/sec and a maximum available hammer energy of 240 ft-lb. The test apparatus and operator were qualified using U.S. Army Watertown standard specimens. The standards are designed to fail at 70.3 ft-lb and 15.0 ft-lb at a test temperature of -40°F. According to Reference 11, the test apparatus averaged results must reproduce the Watertown design values within an accuracy of ±5% or ±1.0 ft-lb, whichever is greater. The successful qualification of the Riehle machine and operator is summarized in Table 5-1.

Charpy V-Notch tests were conducted at temperatures between -20°F and 300°F. For tests between 70°F and 212°F, the temperature conditioning fluid was water. Methanol was used at temperatures below 70°F. Above 212°F, a silicone oil was used. Cooling of the conditioning fluids was done with liquid nitrogen, and heating by an immersion heater. The fluids were mechanically stirred to maintain uniform temperatures. The fluid temperature was measured with a calibrated chromel-alumel thermocouple. Once at test temperature, the specimens were manually transferred with centering tongs to the Riehle machine and impacted within 5 seconds.

For each Charpy V-Notch specimen tested, test temperature, energy absorbed, lateral expansion, and percent shear were evaluated. Lateral expansion and percent shear were measured according to Reference 11 methods. Percent shear was determined with method one of Subsection 11.2.4.3 of Reference 11, which involves measuring the length and width of the cleavage surface and locating the percent shear value from Tables 1 or 2 of Reference 11.

5.2 IMPACT TEST RESULTS

Eight Charpy V-Notch specimens each of base metal, weld metal and HAZ were tested at temperatures selected to define the toughness transition and upper shelf portions of the fracture toughness curve. Absorbed energy, lateral expansion and percent shear data are listed in Table 5-2 for each material. Plots of absorbed energy data for base, weld, and HAZ metal are presented in Figures 5-1, 5-2 and 5-3, respectively. Lateral expansion plots for base, weld and HAZ metal are given in Figures 5-4, 5-5 and 5-6, respectively.

The data sets are fit with the hyperbolic tangent function developed by Oldfield for the EPRI Irradiated Steel Handbook (Reference 12):

$$Y = A + B * \mathrm{TANH}\,[(T - T_0)/C],$$

where Y = impact energy or lateral expansion
T = test temperature, and
A, B, T_0 and C are determined by non-linear regression.

The TANH function is one of the few continuous functions with a shape characteristic of low alloy steel fracture toughness transition curves.

Photographs were taken of the fracture surfaces for each specimen. The fracture surface photographs were used to evaluate percent shear. The photographs and a summary of test results for each specimen are contained in Appendix B.

5.3 IRRADIATED VERSUS UNIRRADIATED CHARPY V-NOTCH PROPERTIES

As a part of the RPV fabrication test program, Charpy V-Notch testing was done at one temperature, 10°F, on the unirradiated RPV plate materials. Data for the beltline plate from which the base metal specimens were fabricated, (Heat C2761-2) were recovered from QA records. The impact energy data are fit with the TANH function, assuming the same slope as for the irradiated data curve. The results are plotted in Figure 5-7, along with the irradiated data from this test. The surveillance weld material was expected to be the same weld wire heat as that in the beltline electroslag weld, but the chemistry test results in Section 3 are not consistent, so no comparisons were made for weld data.

The irradiated and unirradiated Charpy V-Notch property data are used to estimate the values in Table 5-3: 30 ft-lb, 50 ft-lb and 35 MLE index temperatures and the USE. RT_{NDT} shift values are determined as the change in the temperature at which 30 ft-lb impact energy is achieved, as required in Reference 4. In previous experience, the shift in the transition curve has been approximately equal at the 30 ft-lb and 50 ft-lb levels. The values in Table 5-3 assume this to be the case for the plate material, compensating somewhat for the lack of unirradiated plate data. A decrease in USE could not be estimated for the plate or weld materials because of the lack of unirradiated data.

The shift from initial to adjusted RT_{NDT} for the base metal is compared in Section 7 to analytical values calculated according to Regulatory Guide 1.99, Revision 2.

Table 5-1

QUALIFICATION TEST RESULTS USING
U.S. ARMY WATERTOWN SPECIMENS
(TESTED IN MARCH 1988)

Qualification Test Specimen Identification	Test Temperature (°F)	Energy Absorbed Mechanical Gage (ft-lb)
KK10-0681	-40	69.0
KK10-0525	"	72.5
KK10-0561	"	70.0
KK10-0527	"	68.3
KK10-0662	"	65.5
Average		69.1
Allowable	-40	70.3 ± 3.5 Acceptable
LL5-0203	-40	14.3
LL5-0066	"	16.5
LL5-0493	"	15.0
LL5-0395	"	17.0
LL5-0162	"	15.5
Average		15.7
Allowable	-40	15.0 ± 1.0 Acceptable

Table 5-2

CHARPY V-NOTCH IMPACT TEST RESULTS
FOR IRRADIATED RPV MATERIALS

Specimen Identification	Test Temperature (°F)	Fracture Energy (ft-lb)	Lateral Expansion (mils)	Percent Shear (Method 1) (%)
Base:				
772	-20	22.0	24	6
765	0	47.0	38	18
76K	20	54.5	46	26
77A	40	58.0	50	34
77D	70	81.5	70	40
75M	140	131.0	98	100
75P	200	132.0	92	100
77K	300	136.0	90	100
Weld:				
7BT	-20	15.0	16	1
7AT	20	34.0	32	9
7C1	40	31.0	34	8
7B3	60	53.5	48	31
7BA	70	65.0	58	28
7AM	140	95.5	79	83
7BL	200	108.0	86	100
7B4	300	114.5	88	100
HAZ:				
7D1	-20	24.0	21	4
7J3	20	47.0	45	12
7DK	40	52.0	44	26
7J1	60	75.0	64	50
7D3	70	55.0	49	25
7DU	140	102.5	80	83
7JA	200	116.0	87	100
7DL	300	152.0	87	100

Table 5-3

SIGNIFICANT RESULTS OF IRRADIATED AND
UNIRRADIATED CHARPY V-NOTCH DATA

Material	Index Temperature (°F)			Upper[a] Shelf Energy (ft-lb)
	E-30 ft-lb	E-50 ft-lb	MLE-35 mil	L/T
Unirradiated Plate	-42	-9		
Irradiated Plate	-12	20	2	136/88
Difference	30	29		
Irradiated Weld	21	56	32	115

[a] Longitudinal (L) USE is read directly from Figures 5-1 and 5-2. Transverse (T) plate USE is taken as 65% of the longitudinal USE, according to Reference 6. L/T USE values are equal for weld metal, which has no orientation effect.

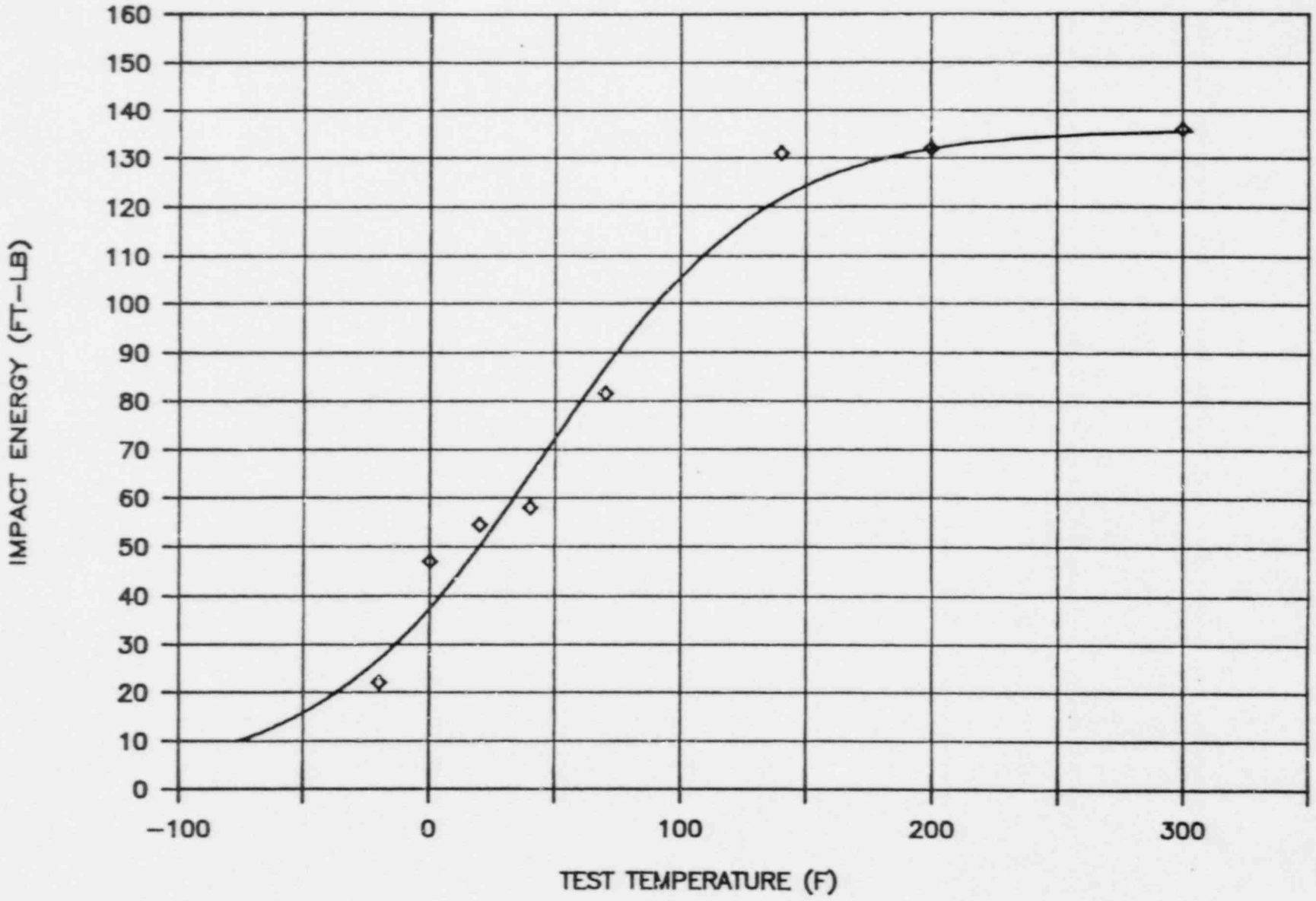

Figure 5-1. Irradiated Base Metal Impact Energy

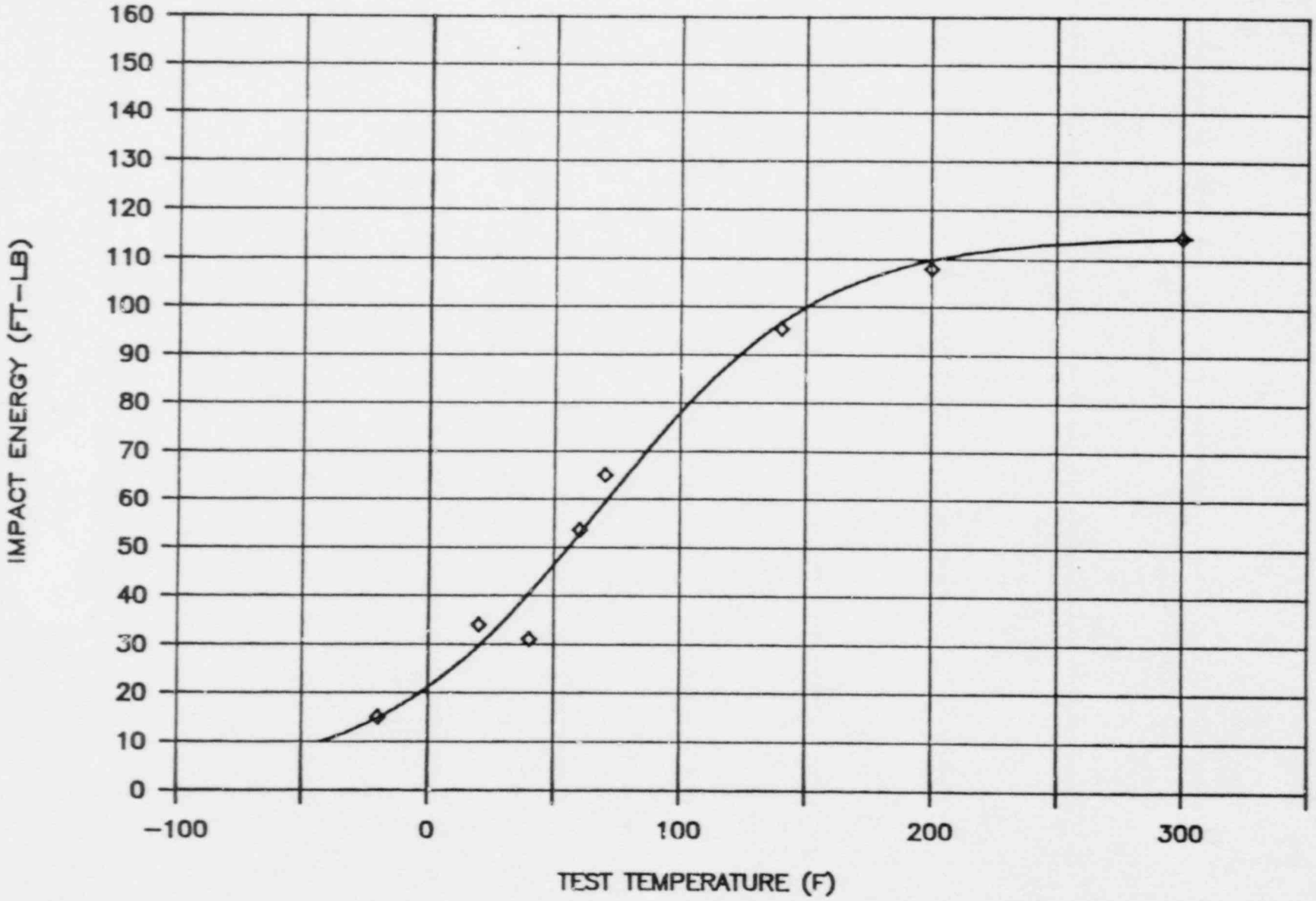

Figure 5-2. Irradiated Weld Metal Impact Energy

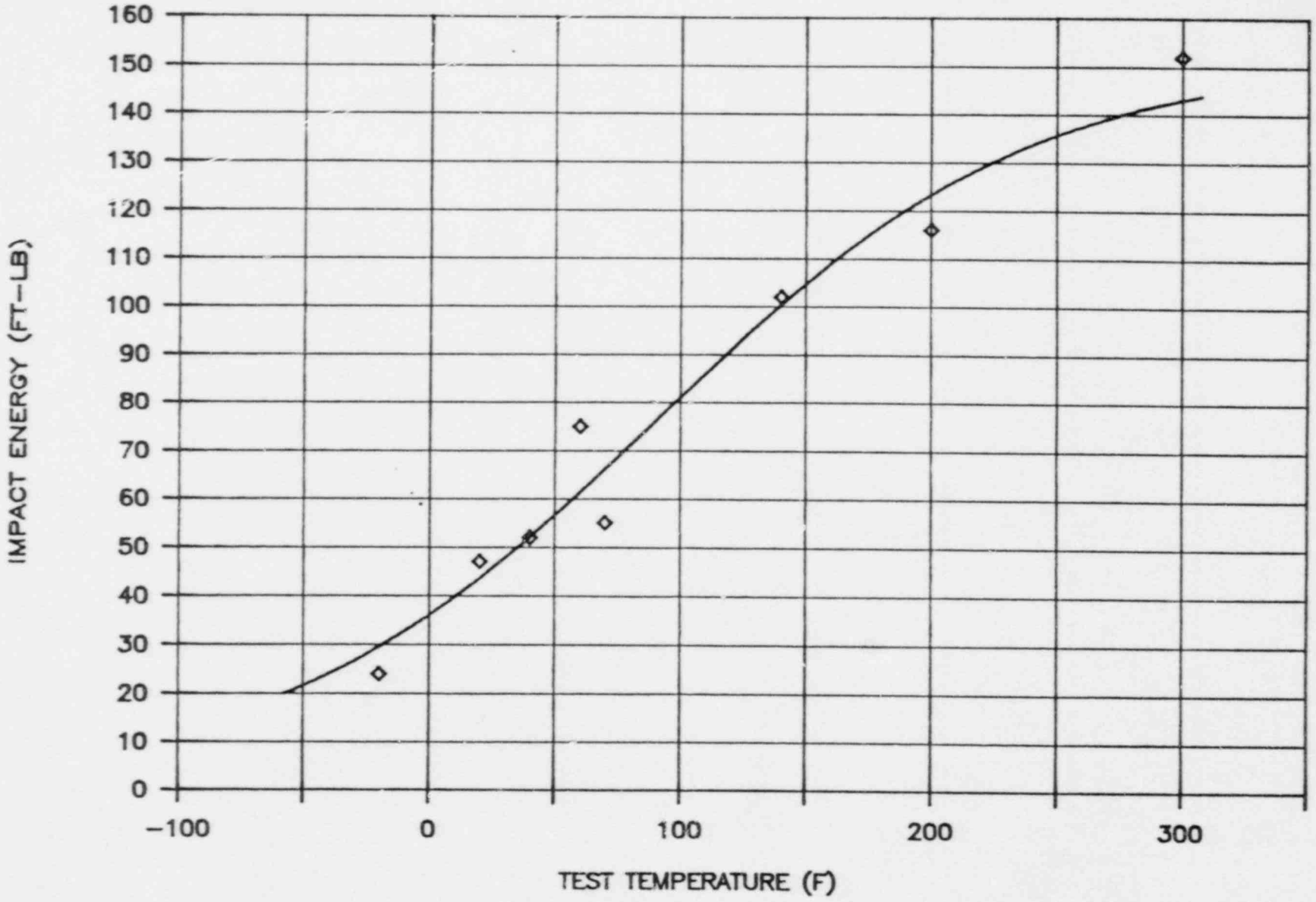

Figure 5-3. Irradiated HAZ Impact Energy

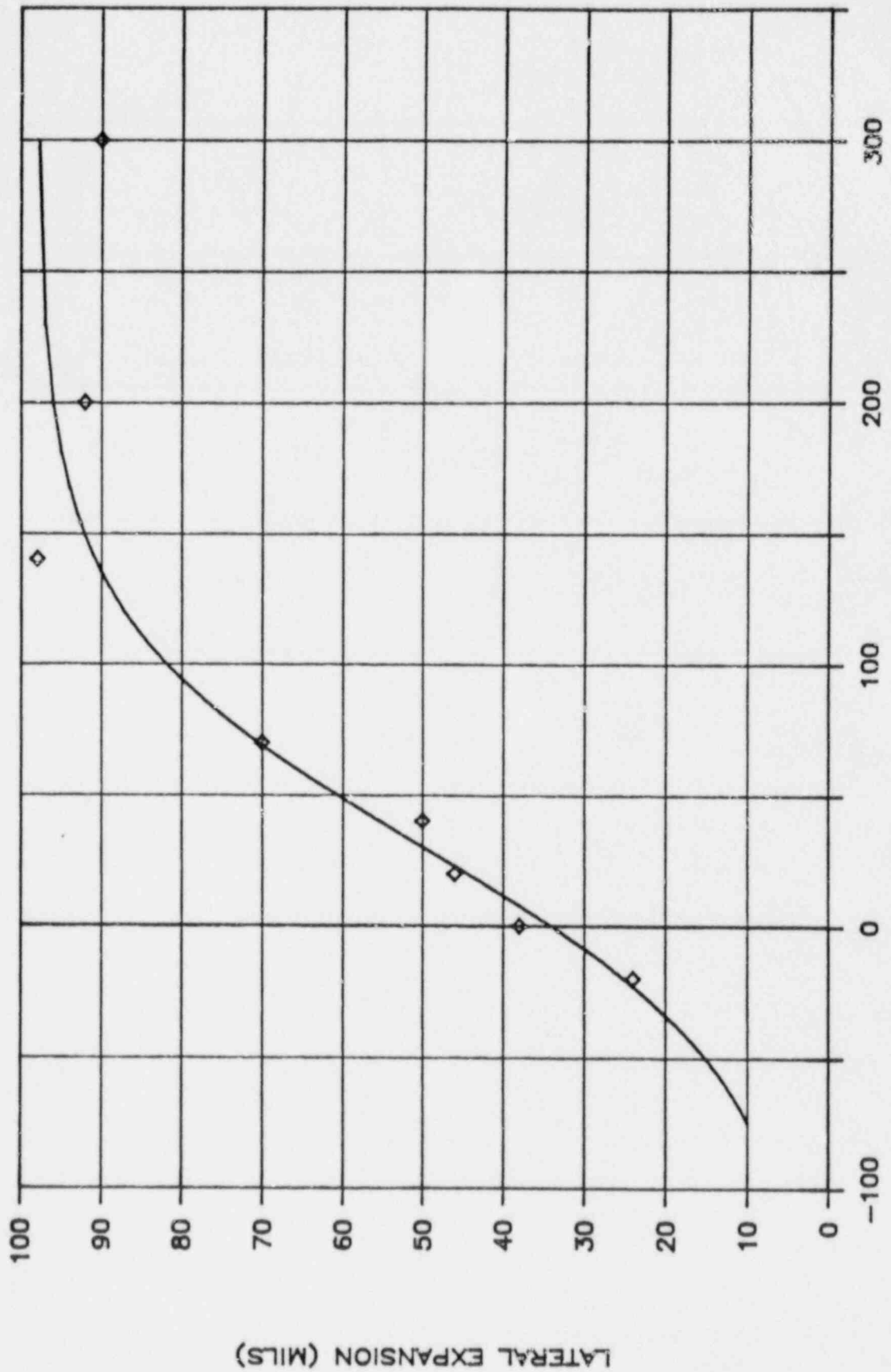

Figure 5-4. Irradiated Base Metal Lateral Expansion

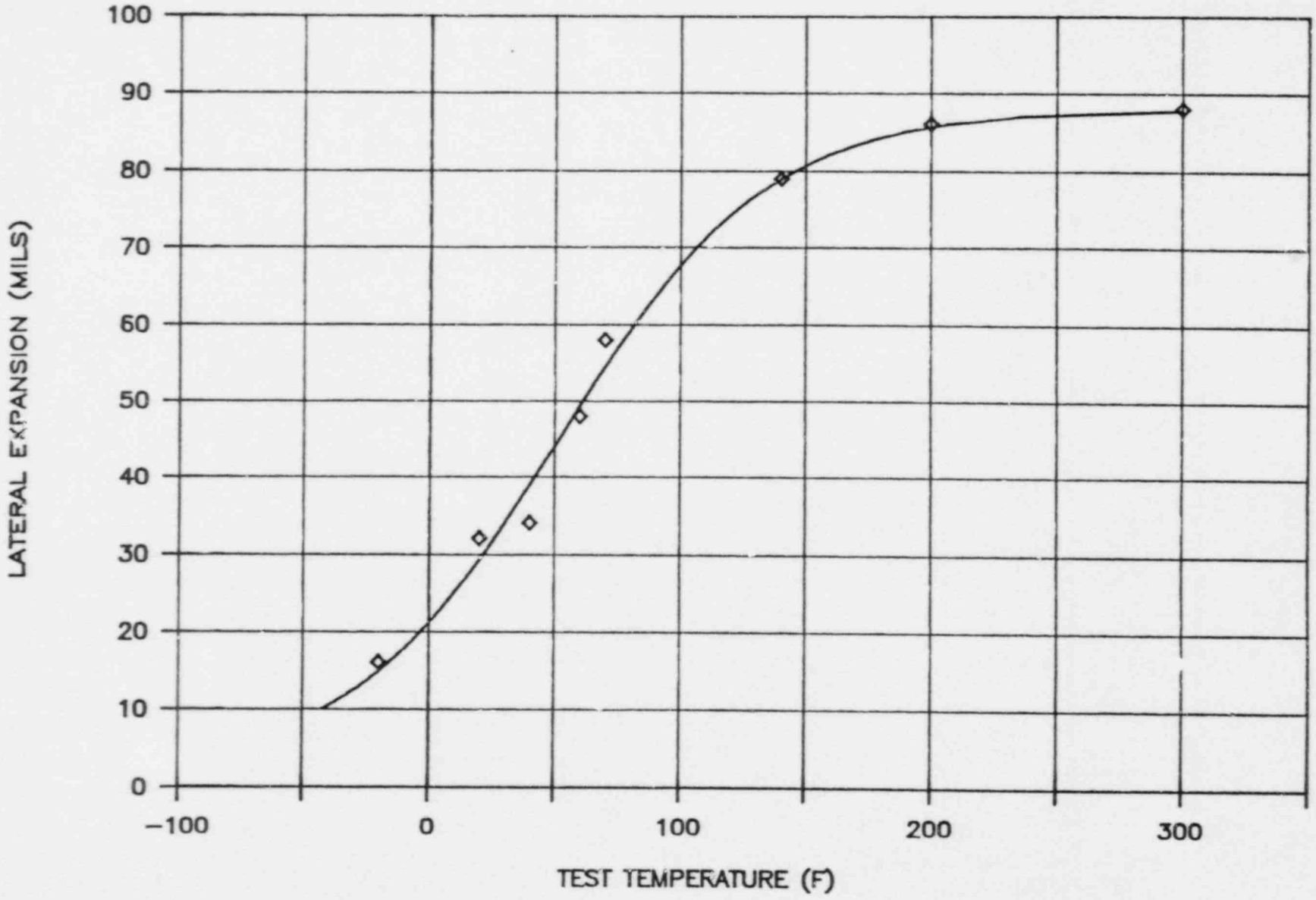

Figure 5-5. Irradiated Weld Metal Lateral Expansion

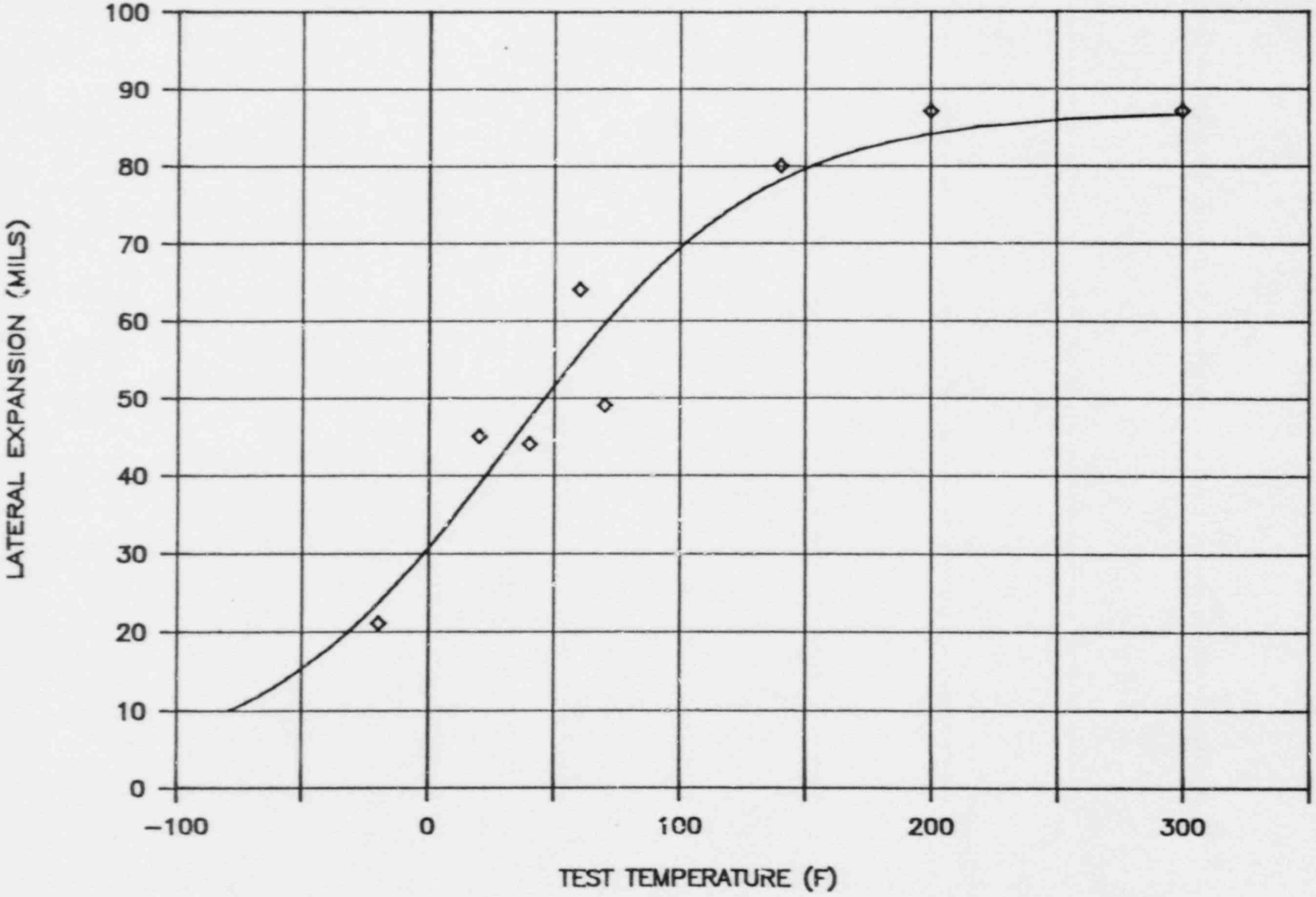

Figure 5-6. Irradiated HAZ Lateral Expansion

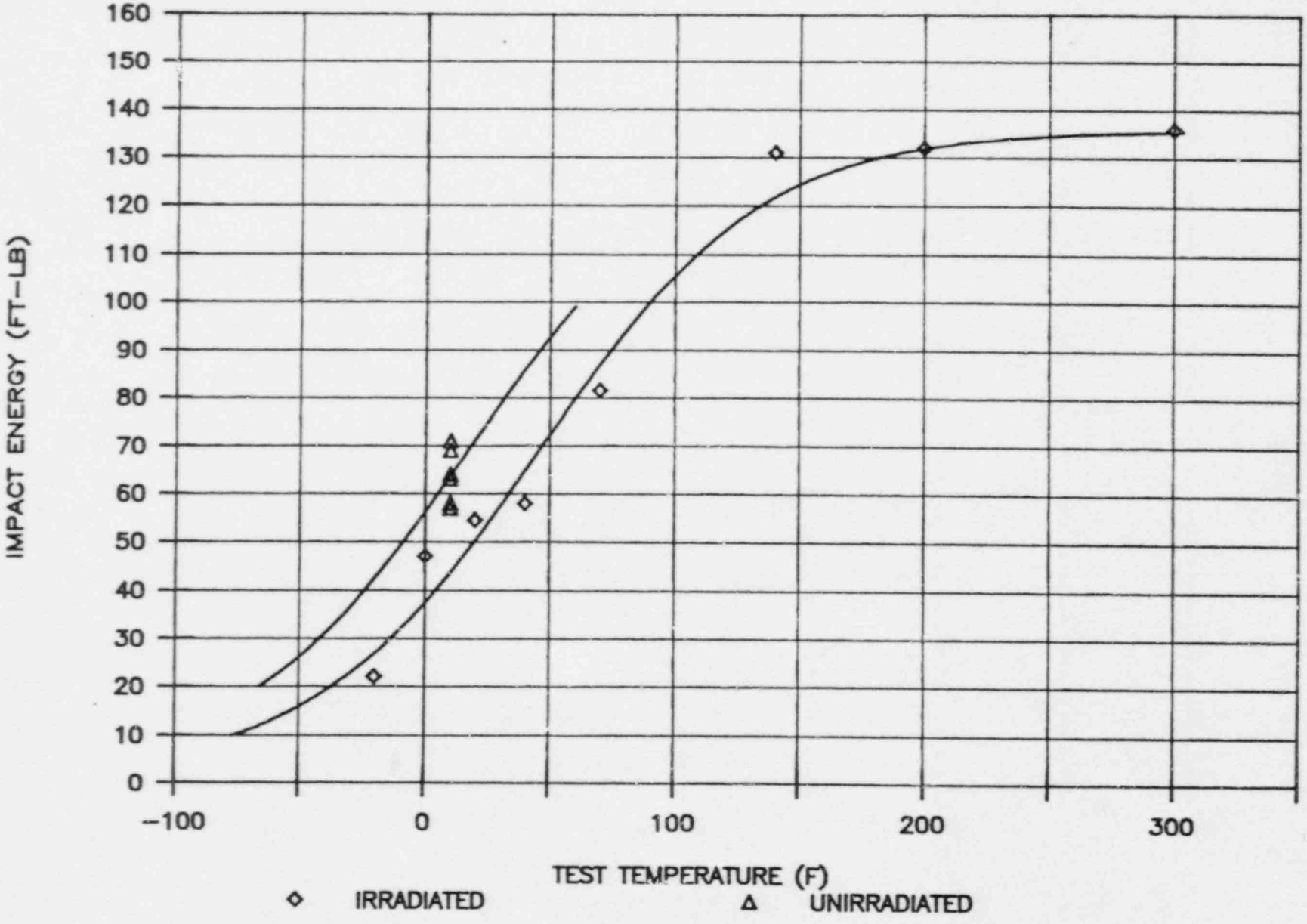

Figure 5-7. Comparison of Unirradiated and Irradiated Base Metal Impact Energy

6. TENSILE TESTING

Eight round bar tensile specimens were recovered from the surveillance capsule. Uniaxial tensile tests were conducted in air at room temperature, RPV operating temperature, and onset of upper shelf temperature. Tests were conducted in accordance with ASTM E8-81 (Reference 13).

6.1 PROCEDURE

All tests were conducted using a screw-driven Instron test frame equipped with a 20-kip load cell and special pull bars and grips. Heating was done with a Satec resistance clamshell furnace centered around the specimen load train. Test temperature was monitored and controlled by a chromel-alumel thermocouple spot-welded to an Inconel clip that was friction-clipped to the surface of the specimen at its midline. Before the elevated temperature tests, a profile of the furnace was conducted at the test temperature of interest using an unirradiated steel specimen of the same geometry. Thermocouples were spot-welded to the top, middle, and bottom of a central 1 inch gage of this specimen. In addition, the clip-on thermocouple was attached to the midline of the specimen. When the target temperatures of the three thermocouples were within ±5°F of each other, the temperature of the clip-on thermocouple was noted and subsequently used as the target temperature for the irradiated specimens.

All tests were conducted at a calibrated crosshead speed of 0.005 inch/min until well past yield, at which time the speed was increased to 0.05 inch/min until fracture. A one inch span knife edge extensometer was attached directly to each specimen's central gage region and was used to monitor gage extension during test.

The test specimens were machined with a minimum diameter of 0.250 inch at the center of the gage length. The three base metal specimens were tested at room temperature (RT = 70°F), onset of upper shelf temperature (estimated at 130°F), and RPV operating temperature (550°F).

The three weld metal specimens were tested at room temperature, onset of upper shelf temperature (estimated at 180°F) and 550°F. The two HAZ specimens were tested at room temperature and 550°F. The yield strength (YS) and ultimate tensile strength (UTS) were calculated by dividing the nominal area (0.0491 $in.^2$) into the 0.2% offset load and into the maximum test load, respectively. The values listed for the uniform and total elongations were obtained from plots that recorded load versus specimen extension and are based on a one inch gage length. Reduction of area (RA) values were determined from post-test measurements of the necked specimen diameters using a calibrated blade micrometer and employing the formula:

$$RA = 100\% * (A_o - A_f)/A_c$$

After testing, each broken specimen was photographed end-on showing the fracture surface and lengthwise showing fracture location and local necking behavior.

6.2 RESULTS

Tensile test properties of YS, UTS, RA, uniform elongation (UE) and total elongation (TE) are presented in Table 6-1. Shown in Figure 6-1 is a stress-strain curve for a 550°F base metal specimen typical of the stress-strain characteristics of all the specimens tested. Shown graphically in Figures 6-2 and 6-3 are the data in Table 6-1. Photographs of fracture surfaces and necking behavior are given in Figures 6-4, 6-5 and 6-6 for base, weld and HAZ specimens, respectively. The base, weld and HAZ materials generally follow the trend of decreasing properties with increasing temperature. The nick in specimen 7K3 appears to have made little difference in the results.

6.3 IRRADIATED VERSUS UNIRRADIATED TENSILE PROPERTIES

Unirradiated tensile test data were recovered from QA records for the surveillance specimen plate (Heat C2761-2), as shown in Table 3-2. The unirradiated data provide average values of YS, UTS, RA and TE at room temperature. These are compared in Table 6-2 to the irradiated base metal specimen RT data to determine the degree of irradiation effect. The trends of increasing YS and UTS and of decreasing TE and RA, characteristic of irradiation embrittlement, are seen in the base metal data.

Table 6-1

TENSILE TEST RESULTS FOR IRRADIATED RPV MATERIALS

Specimen Number	Material	Test Temp (°F)	Yield Strength (ksi)	Ultimate Strength (ksi)	Uniform Elongation (%)	Total Elongation (%)	Reduction of Area (%)
7K1	Base	69	67.9	92.9	9.0	19.0	69.3
7K3 [a]	Base	130	67.5	89.7	8.9	17.5	64.8
7JE	Base	550	62.9	89.4	9.2	17.9	58.5
7KK	Weld	71	64.2	87.6	10.1	20.0	67.8
7KD	Weld	180	70.0	81.7	8.6	18.4	62.1
7KL	Weld	550	58.1	80.8	8.8	17.2	69.5
7LA	HAZ	72	62.5	85.7	7.5	16.1	65.8
7LE	HAZ	550	59.4	80.6	6.4	14.4	64.4

[a] Specimen was nicked, but fracture results appear reasonably unaffected.

Table 6-2

COMPARISON OF UNIRRADIATED AND IRRADIATED
TENSILE PROPERTIES AT ROOM TEMPERATURE

	Yield Strength (ksi)	Ultimate Strength (ksi)	Total Elongation (%)	Reduction of Area (%)
Base (Heat C2761-2):				
Unirradiated	67.0	91.8	29.3	70.5
Irradiated	67.9	92.9	19.0	69.3
Difference [a]	1.3%	1.2%	-54.2%	-1.7%

[a] Difference = [(Irradiated - Unirradiated)/Irradiated] * 100%

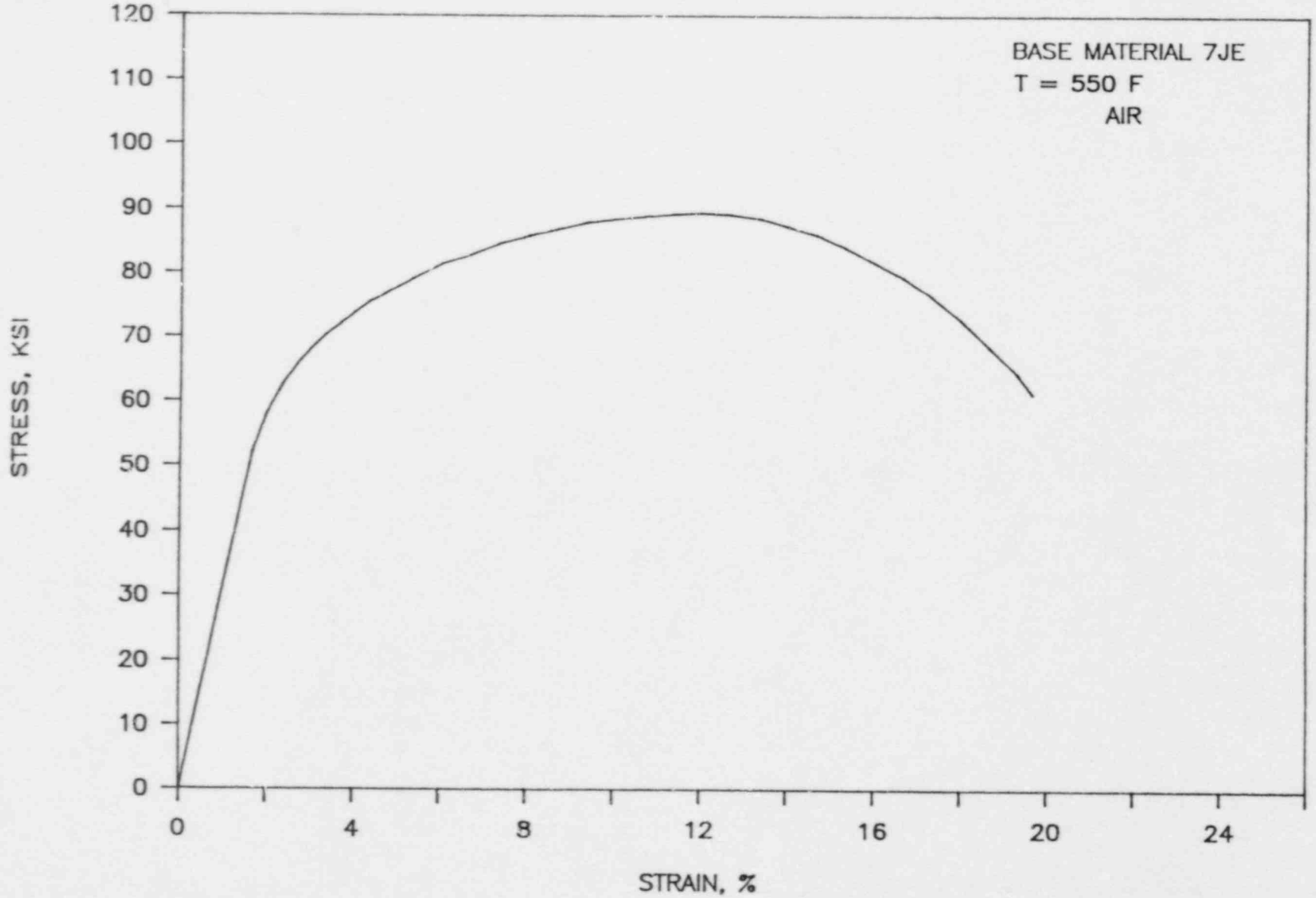

Figure 6-1. Typical Engineering Stress versus Percent Strain for Irradiated RPV Materials

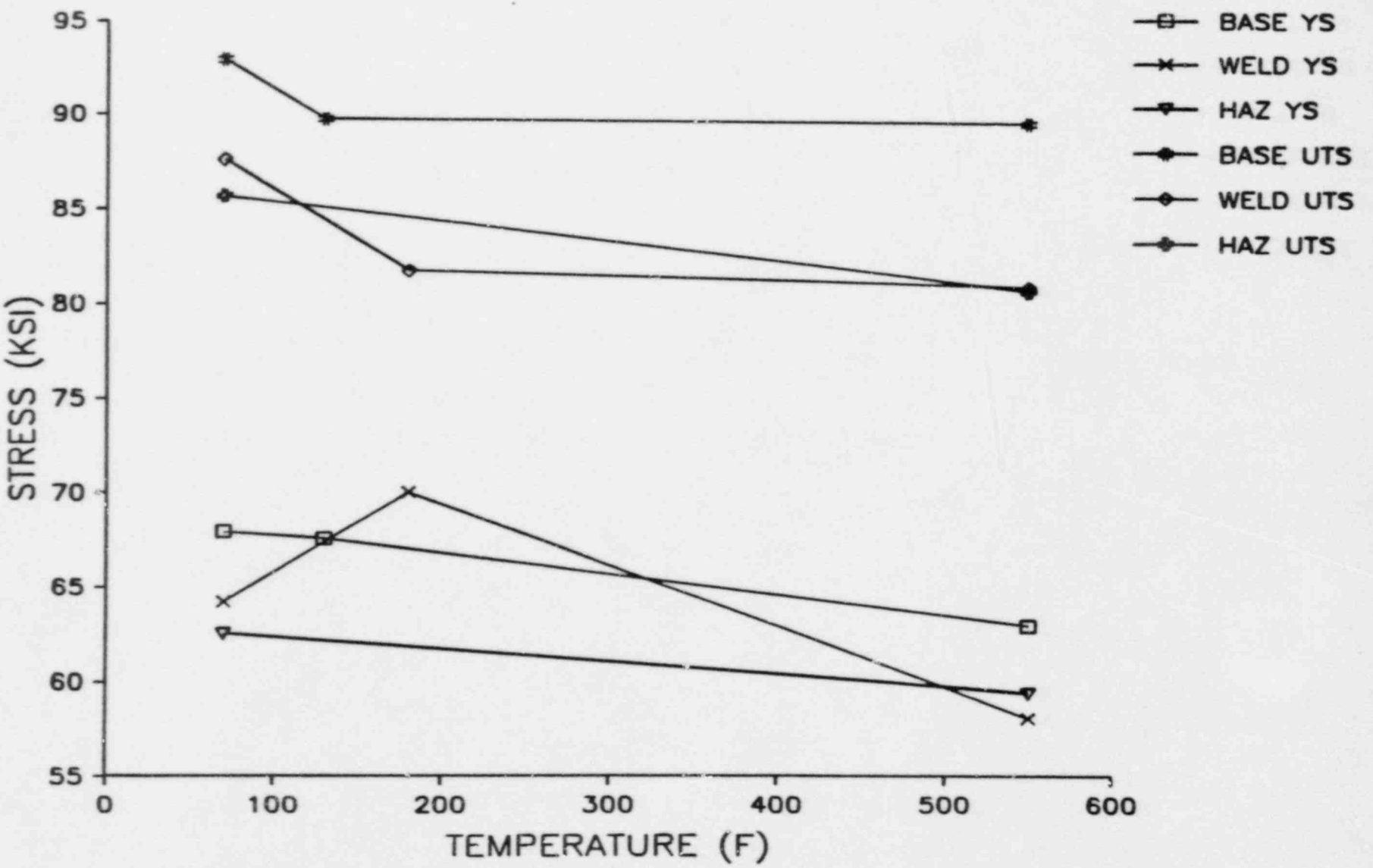

Figure 6-2. Strength versus Test Temperature for Irradiated Base, Weld and HAZ Tensile Specimens

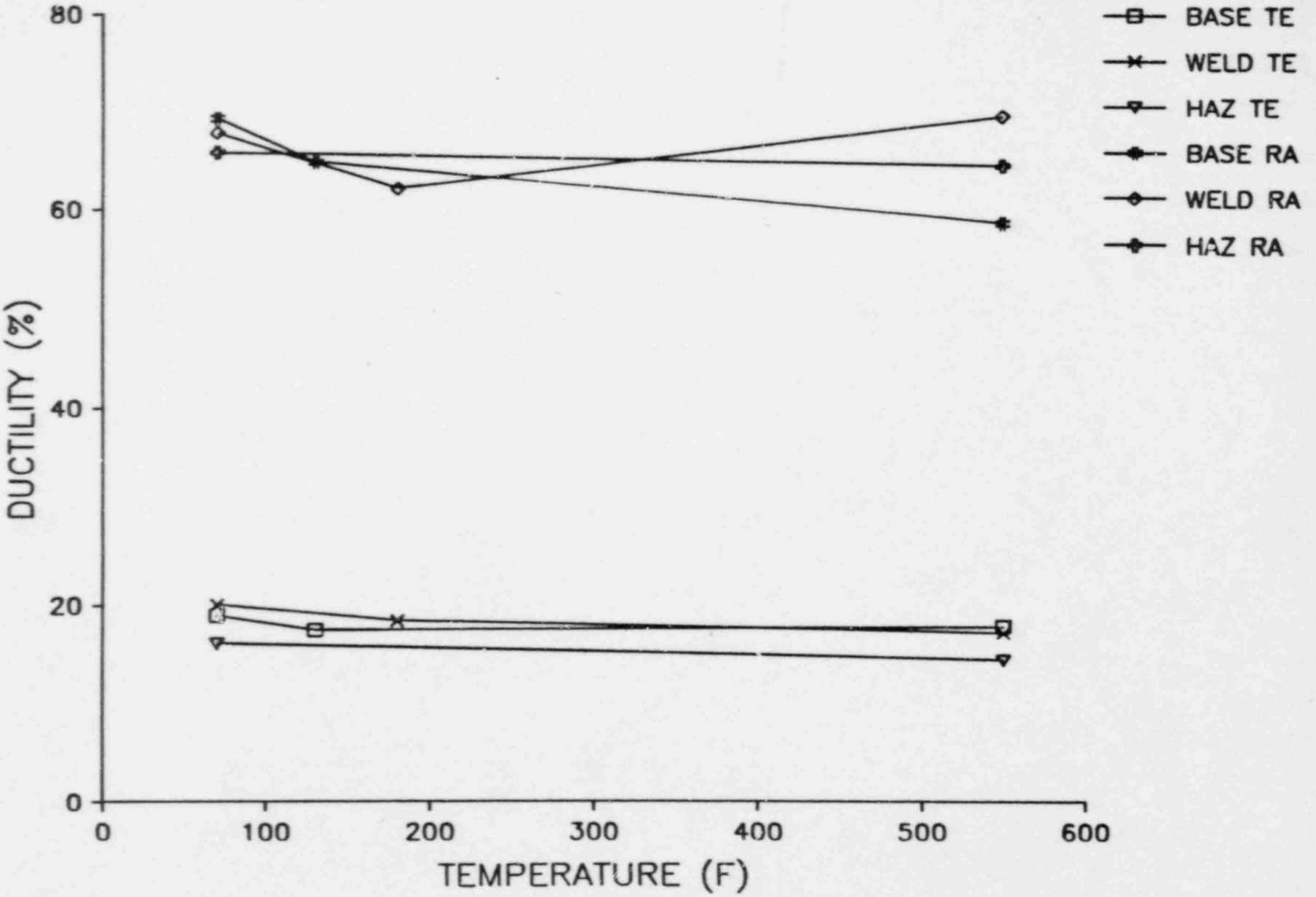

Figure 6-3. Ductility versus Test Temperature for Irradiated Base, Weld and HAZ Tensile Specimens

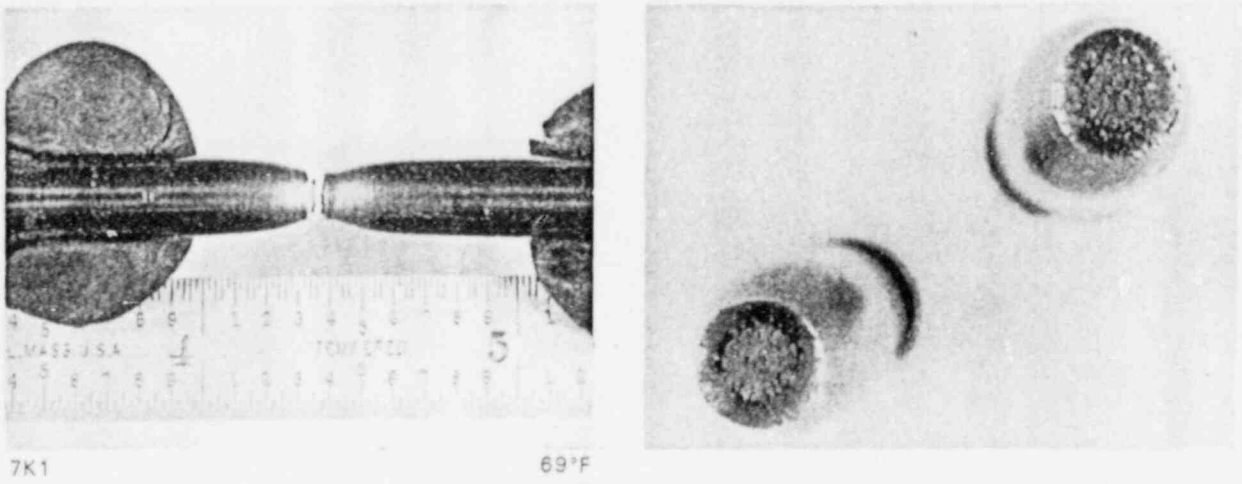

7K1 69°F

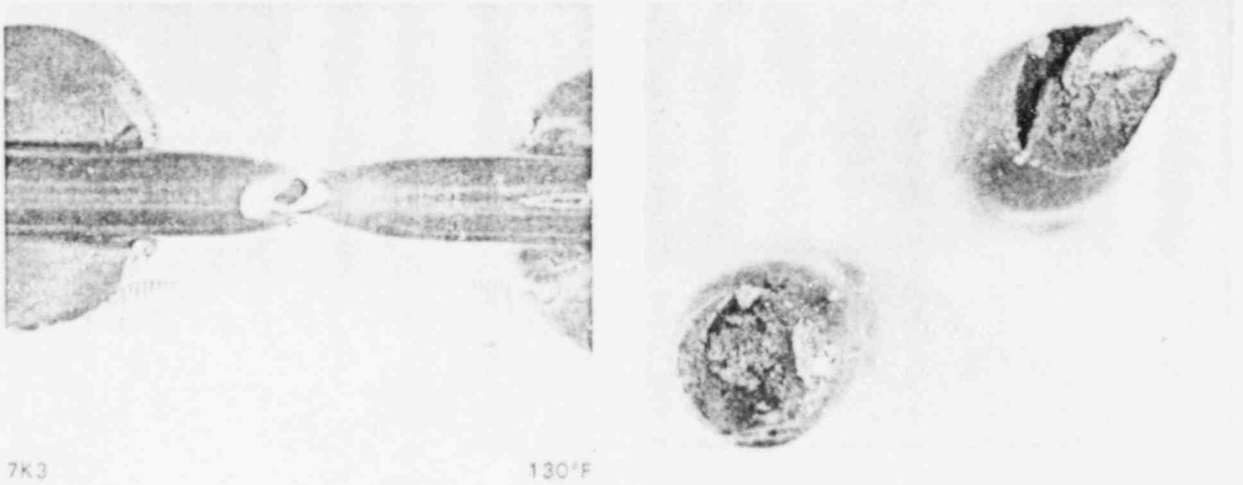

7K3 130°F

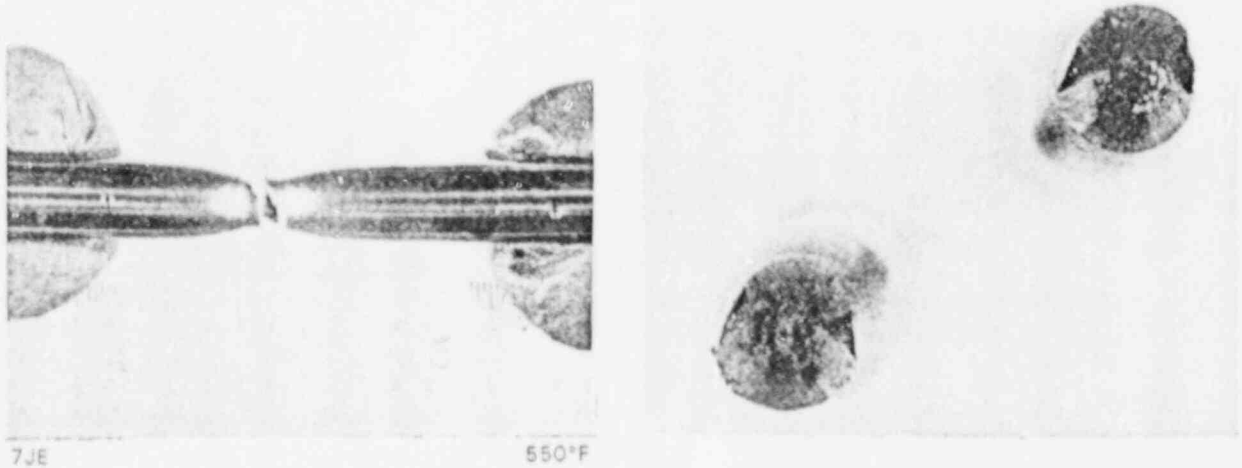

7JE 550°F

Figure 6-4. Fracture Location, Necking Behavior, and Fracture Appearance for Irradiated Base Metal Tensile Specimens

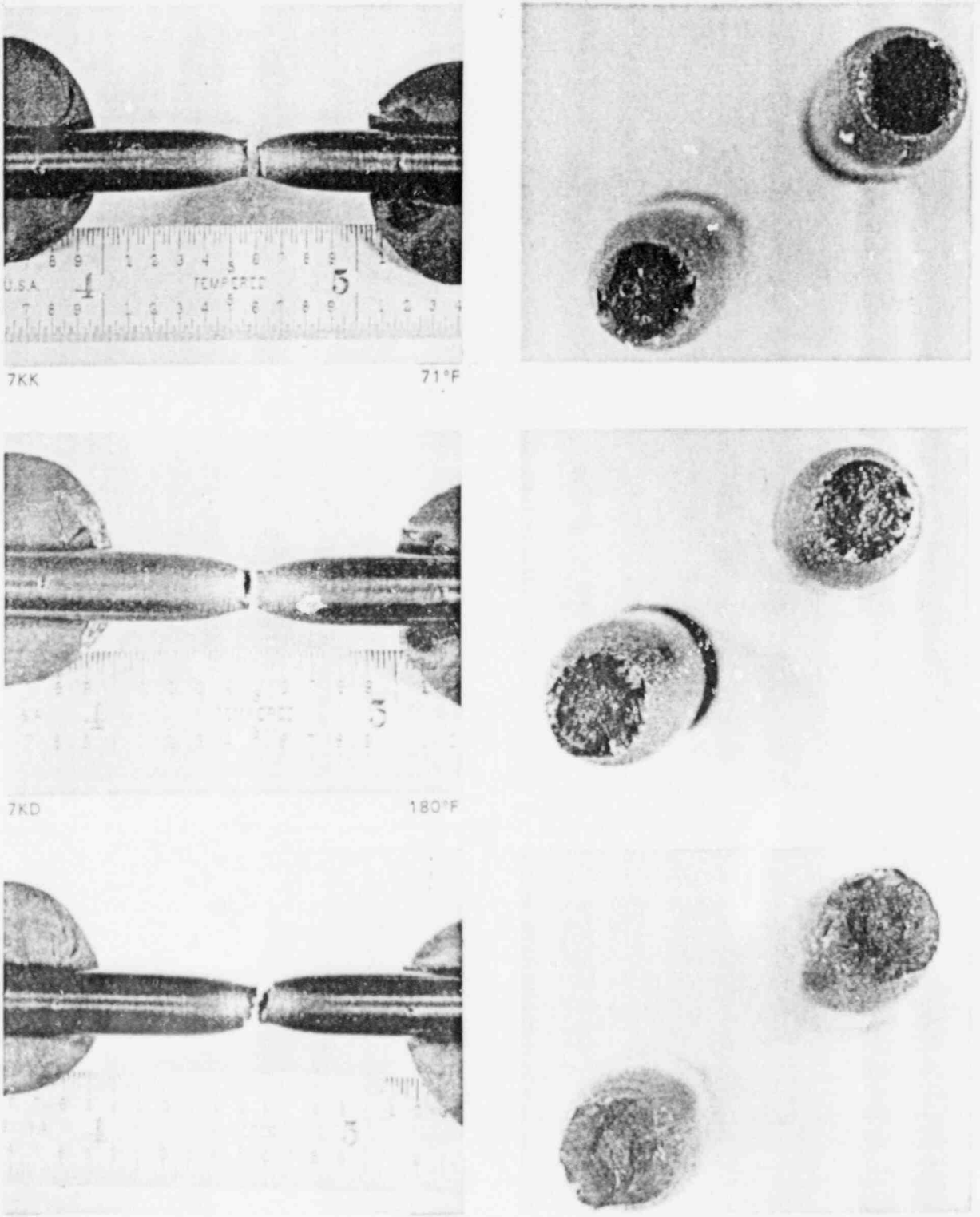

Figure 6-5. Fracture Location, Necking Behavior, and Fracture Appearance for Irradiated Weld Metal Tensile Specimens

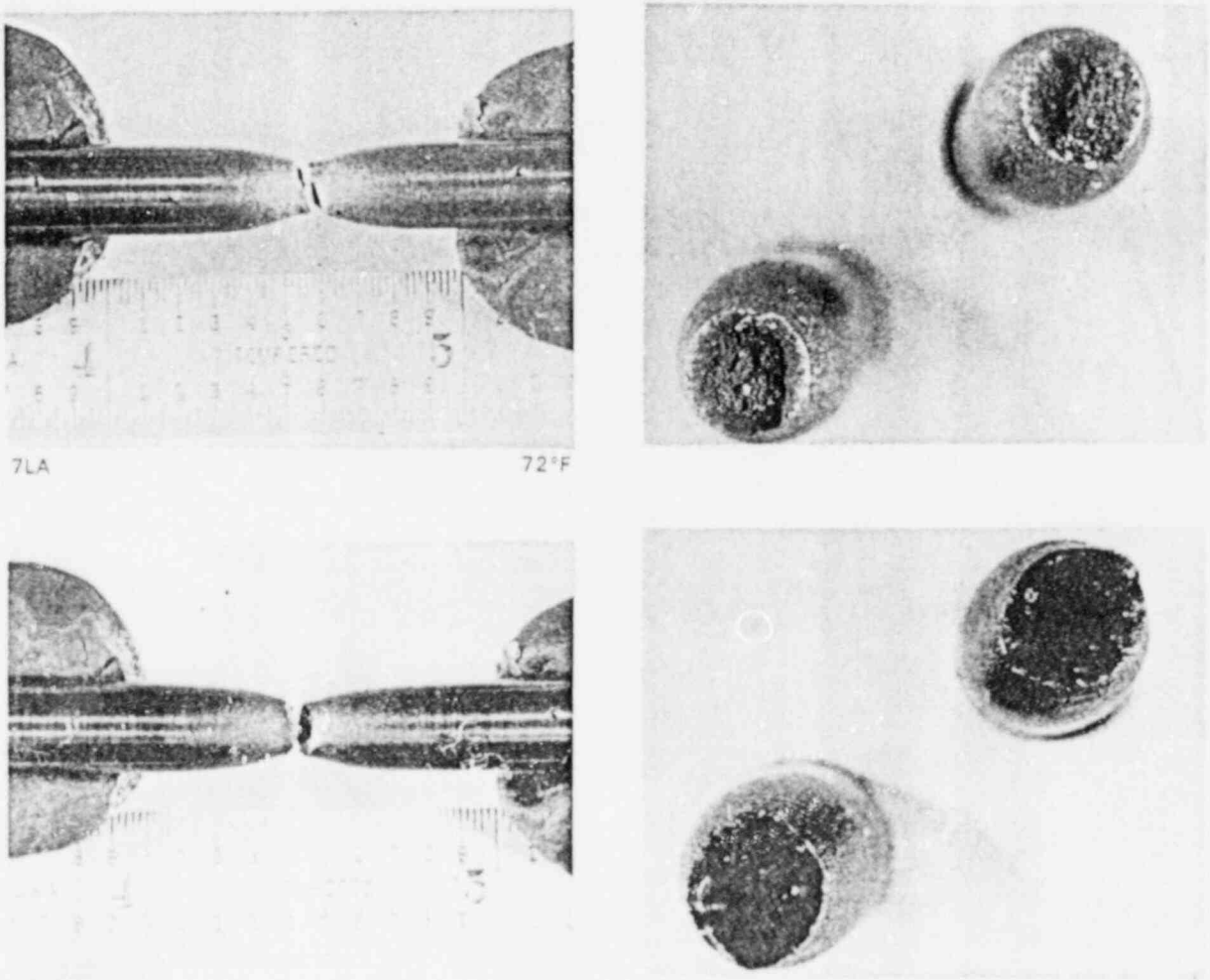

Figure 6-6. Fracture Location, Necking Behavior, and Fracture Appearance for Irradiated HAZ Tensile Specimens

7. DEVELOPMENT OF OPERATING LIMITS CURVES

7.1 BACKGROUND

Operating limits for pressure and temperature are required for three categories of operation: (a) hydrostatic pressure tests and leak tests, referred to as Curve A; (b) non-nuclear heatup/cooldown and low-level physics tests, referred to as Curve B; and (c) core critical operation, referred to as Curve C. There are three vessel regions that affect the operating limits: the closure flange region, the core beltline region, and the remainder of the vessel, or non-beltline regions. The closure flange region limits are controlling at lower pressures primarily because of Reference 1 requirements. The non-beltline and beltline region operating limits are evaluated according to procedures in References 1 and 2, with the beltline region minimum temperature limits increasing as the vessel is irradiated.

7.2 NON-BELTLINE REGIONS

Non-beltline regions are those locations that receive too little fluence to cause any RT_{NDT} increase. Non-beltline components include the nozzles, the closure flanges, some shell plates, top and bottom head plates and the control rod drive (CRD) penetrations. Detailed stress analyses of the non-beltline components were performed for the BWR/6. The analyses took into account all mechanical loadings and thermal transients anticipated. Detailed stresses were used according to Reference 2 to develop plots of allowable pressure (P) versus temperature relative to the reference temperature ($T - RT_{NDT}$). These results are applicable to the Peach Bottom 2 vessel components, since the Peach Bottom 2 geometries are not significantly different from BWR/6 configurations and the mechanical and thermal loadings are comparable.

The non-beltline region results were established by adding the highest RT_{NDT} for the non-beltline discontinuities to the P versus (T - RT_{NDT}) curves for the most limiting BWR/6 components, which are the CRD penetration and feedwater nozzle. Shown in Figures 7-1 through 7-3 are the Peach Bottom 2 unique calculated non-beltline operating limits for Curves A, B, and C, respectively. The BWR/6 component curves are adjusted to reflect the limiting non-beltline RT_{NDT} of the Peach Bottom 2 vessel, which is 52°F for the bottom head torus plates.

7.3 CORE BELTLINE REGION

The pressure-temperature (P-T) limits for the unirradiated beltline region are shown in Figures 7-1 through 7-3. As the beltline fluence increases during operation, these curves shift to the right by an amount discussed in Subsection 7.6. Typically, the beltline curves shift to become more limiting than the non-beltline curves. The stress intensity factors calculated for the beltline region according to Reference 2 procedures are based on a combination of pressure and thermal stresses. The pressure stresses were calculated using thin-walled cylinder equations. Thermal stresses were calculated assuming the through-wall temperature distribution of a flat plate subjected to a 100°F/hr thermal gradient. An initial RT_{NDT} of -6°F for the limiting plate is used to adjust the (T - RT_{NDT}) values from Figure G-2210-1 of Reference 2.

7.4 CLOSURE FLANGE REGION

Reference 1 sets several minimum requirements for pressure and temperature in the closure flange region in addition to those outlined in Reference 2. In some cases, the results of analysis for other regions exceed these requirements and they do not affect the shape of the P-T curves. However, some closure flange requirements from Reference 1 do impact the curves. In addition, General Electric recommends 60°F margin on the required bolt preload temperature.

As stated in Paragraph G-2222(c) of Reference 2, for application of full bolt preload and reactor pressure up to 20% of hydrostatic test pressure, the RPV metal temperature must be at RT_{NDT} or greater. The GE practice is to require (RT_{NDT} + 60°F) for bolt preload, for two reasons:

a. The original ASME Code of construction requires (RT_{NDT} + 60°F); and

b. The highest stressed region during boltup is the closure flange region, and the flaw size assumed in that region (0.24 inches) is less than 1/4 T. This flaw size is detectable using ultrasonic testing (UT) techniques. In fact, References 14 and 15 report that a flaw in the closure flange region of 0.09 inch can be reliably detected using UT.

For Peach Bottom 2, (RT_{NDT} + 60°F), or 70°F, is consistent with the allowable LST for the bolting material. Furthermore, (RT_{NDT} + 60°F) is a requirement for Curve C, as described in paragraph IV.A.3 of Reference 1.

Reference 1, paragraph IV.A.2, sets temperature minimum requirements for pressure above 20% hydrotest pressure base on the RT_{NDT} of the closure region. Curve A temperature must be no less than (RT_{NDT} + 90°F) and Curve B temperature no less than (RT_{NDT} + 120°F). The Curve A requirement causes a 30°F shift at 20% hydrotest pressure (312 psig) as shown in Figure 7-1. The Curve B requirement has no impact on Figure 7-2 because the analytical results for the feedwater nozzle require that temperature be greater than (RT_{NDT} + 120°F) at 312 psig.

7.5 CORE CRITICAL OPERATION REQUIREMENTS OF 10CFR50, APPENDIX G

Curve C, the core operation curve shown in Figure 7-3 is generated from Figure 7-2, accounting for the requirements of Reference 1, paragraph IV.A.3. Essentially paragraph IV.A.3 requires that core critical P-T limits be 40°F above any Curve A or B limits. Curve B is more limiting than Curve A, so Curve C is Curve B plus 40°F. The (RT_{NDT} + 60°F) minimum permissible temperature mentioned in Subsection 7.4 for Curve C is an exception for BWRs, allowing critical operation at temperatures below the hydrostatic test temperature.

7.6 EVALUATION OF RADIATION EFFECTS

The impact on adjusted reference temperature (ART) due to irradiation in the beltline materials is determined according to the methods in Reference 5, as a function of neutron fluence and the element contents of copper (Cu) and nickel (Ni). The specific relationship from Reference 5 is:

$$\text{ART} = \text{Initial } RT_{NDT} + \text{SHIFT} + \text{Margin} \qquad (7\text{-}1)$$

where:

$$\text{SHIFT} = [CF]*f^{(0.28 - 0.10 \log f)} \qquad (7\text{-}2)$$

$$\text{Margin} = 2*(\sigma_I^2 + \sigma_\Delta^2)^{1/2} \qquad (7\text{-}3)$$

CF = chemistry factor from Tables 1 or 2 of Reference 5,
f = fluence (n/cm^2) divided by 10^{19},
σ_I = standard deviation on initial RT_{NDT},
σ_Δ = standard deviation on RT_{NDT} shift, is 28°F for welds and 17°F for base material, except that σ_Δ need not exceed 0.50 times the SHIFT value.

The limiting beltline plate and weld are determined based on the Cu-Ni content and initial RT_{NDT} of the materials. Calculations based on the information in Tables 3-1 and 3-2 show the following:

Limiting plate: 0.12%Cu, 0.57%Ni, Initial RT_{NDT} = -6°F, σ_I = 0°F
Limiting weld: 0.21%Cu, 0.21%Ni, Initial RT_{NDT} = -45°F, σ_I = 16.4°F

This material information is used to evaluate irradiation shift versus fluence.

7.6.1 Measured Versus Predicted Surveillance Shift

Table 5-3 presents an estimated measured shift for the base metal of 30°F. The predicted shift of the surveillance plate can be determined with Equation 7-2. Assuming the best estimate fluence for the surveillance capsule of 1.8×10^{17} n/cm^2, the predicted value of (SHIFT + Margin) is 26°F for the plate.

Reference 5 states that surveillance data may be used in place of Equations 7-2 and 7-3 when two sets of credible data are available. This is only the first set of data for Peach Bottom 2. Furthermore, the estimated shift measurement presented in this report does not meet the requirements for "credible data" discussed in Reference 5. Therefore, determinations of ART for the purposes of developing pressure-temperature curves are based on Reference 5 predictions.

7.6.2 ART Versus EFPY

Equations 7-1 through 7-3 can be plotted as a function of EFPY for the base metal and weld metal. Subsection 4.3 concludes that the 32 EFPY 1/4 T fluence is 6.9×10^{17} n/cm^2. Figure 7-4 shows the ART for the limiting plate and weld materials, based on the initial RT_{NDT} values and chemistry data in Subsection 7.6. As shown in the figure, the plate is the limiting beltline material through 32 EFPY, because of its higher initial RT_{NDT}.

7.6.3 Fracture Toughness Conditions at 32 EFPY

Paragraph IV.B of Reference 1 sets limits on the ART and on the upper shelf energy (USE) of the beltline materials. The ART must be less than 200°F, and the USE must be above 50 ft-lb. Based on Figure 7-4, the ART values at 32 EFPY of 43°F for the weld and 51°F for the plate are acceptable.

Calculations of decrease in USE, using Reference 5, are summarized in Table 7-1. The equivalent transverse USE of the plate material is taken as 65% of the longitudinal USE, according to Reference 6. The weld metal USE has no transverse/longitudinal correction because weld metal has no

orientation effect. The surveillance plate result is used as the measured reference data for USE, because USE data were not obtained for the unirradiated condition. The highest Charpy energy value from Appendix A was assumed as the USE for the electroslag weld material. Extrapolating to the 32 EFPY fluence according to Reference 5, the predicted USE for the plate is 86 ft-lb, and for the weld is 80 ft-lb. There were no USE data available in fabrication records for the other beltline plates or the circumferential weld. Typical plate material of the type used in the Unit 2 beltline, for which USE data are known, indicate that the Unit 2 plates have adequate USE, especially considering the copper contents of the plates and the low fluence predicted for 32 EFPY. Similarly, given the low copper, low fluence and typical USE of submerged arc welds, the circumferential weld is expected to have adequate USE. Therefore, irradiation effects are not severe enough to necessitate RPV annealing before 32 EFPY.

7.7 OPERATING LIMITS CURVES VALID TO 32 EFPY

The ART selected for the core beltline curves depends on the amount of operation for which the curves will be valid. Operation to 32 EFPY was assumed because, in reviewing the shift in beltline curves, it was determined that the non-beltline curves are still limiting at 32 EFPY. The beltline ART for 32 EFPY estimated with Figure 7-4 is 51°F, based on the plate material. Adjusting the unirradiated beltline curves in Figures 7-1 through 7-3, with their initial RT_{NDT} of -6°F, the beltline limits are at least 20°F lower than the non-beltline limits. Therefore, the 32 EFPY limits are the non-beltline region curves, as shown in Figures 7-5, 7-6 and 7-7, respectively.

The beltline shift is based strictly on predictions of Regulatory Guide 1.99, Revision 2. The surveillance data are not factored into the shift calculations because the Regulatory Guide requires two credible data points for each material, and Peach Bottom 2 now has only one data point for plate material. When the second surveillance capsule is tested, around 15 EFPY, the pressure-temperature curves may require revision to account for the beltline shift as predicted by the surveillance [illegible] results at that time.

7.E REACTOR OPERATION VERSUS OPERATING LIMITS

For most reactor operating conditions, pressure and temperature are at saturation conditions, which are in the operating zone of the limits curves. The most severe unplanned transient is an upset condition consisting of several transients which result in a SCRAM. The worst combination of pressure and temperature during this postulated event is 1180 psig with temperatures in the lower head at 250°F. At the same time, the steam space coolant temperature is still nearly 550°F. Steam space coolant temperature is used to identify the appropriate curve to be applied. In this case, the core is not critical and, according to the steam space coolant temperature, there is no significant cooldown occurring, so the hydrostatic pressure curve applies (Curve A). As seen for Curve A in Figure 7-5, at 1180 psi the minimum transient temperature in the vessel of 250°F lies in the safe operating zone. Therefore, violation of the operating limits curves is only a concern in cases where operator interaction occurs, such as hydrostatic pressure testing and initiation of criticality.

Table 7-1

ESTIMATE OF UPPER SHELF ENERGY FOR BELTLINE MATERIALS

Identification	% Cu	Upper Shelf (ft-lb) Longitudinal/Transverse		
		Unirradiated	f=1.8x10^{17}	f=6.9x1017
Plate:				
Heat C2761-2	0.11	-	136[a]/88	132/86
Weld:				
Heat 37C065	0.21	99[b]	-	80

[a] USE value taken from surveillance test data. Other USE values are calculated using Reference 5.

[b] USE value taken from fabrication test data in Appendix A.

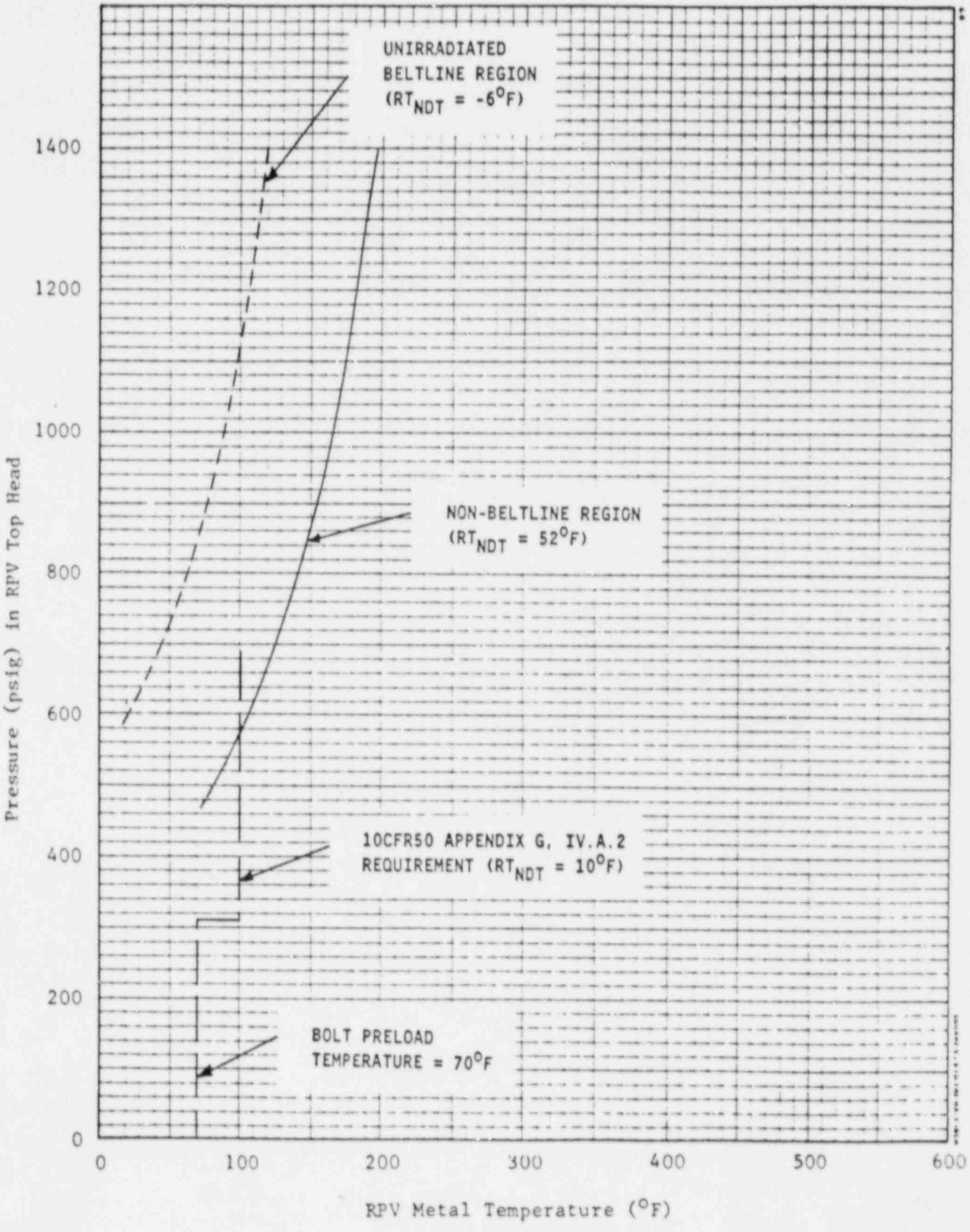

Figure 7-1. Components of Operating Limits Curve for Pressure Tests (Curve A)

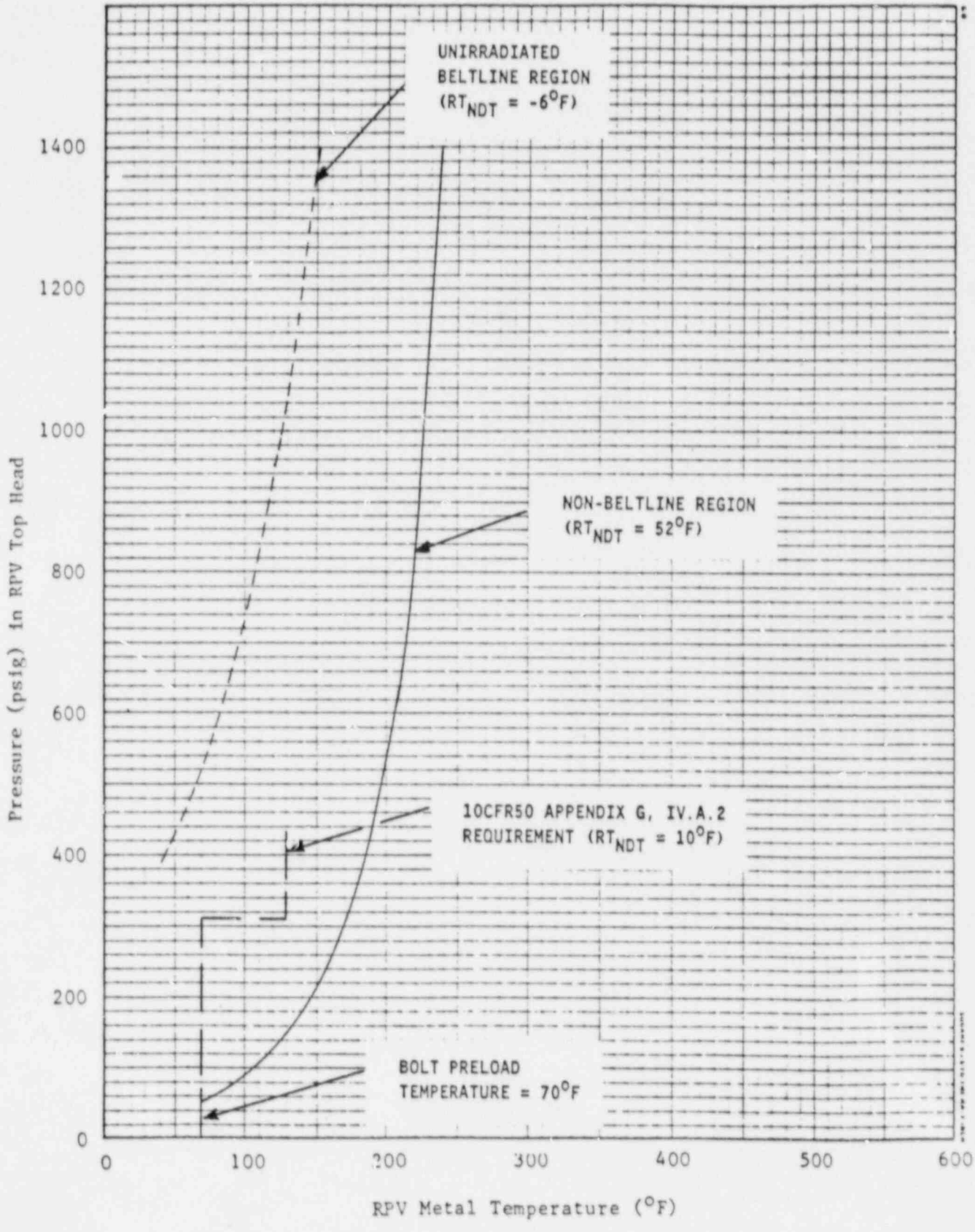

Figure 7-2. Components of Operating Limits Curve for Non-Nuclear Heatup/Cooldown (Curve B)

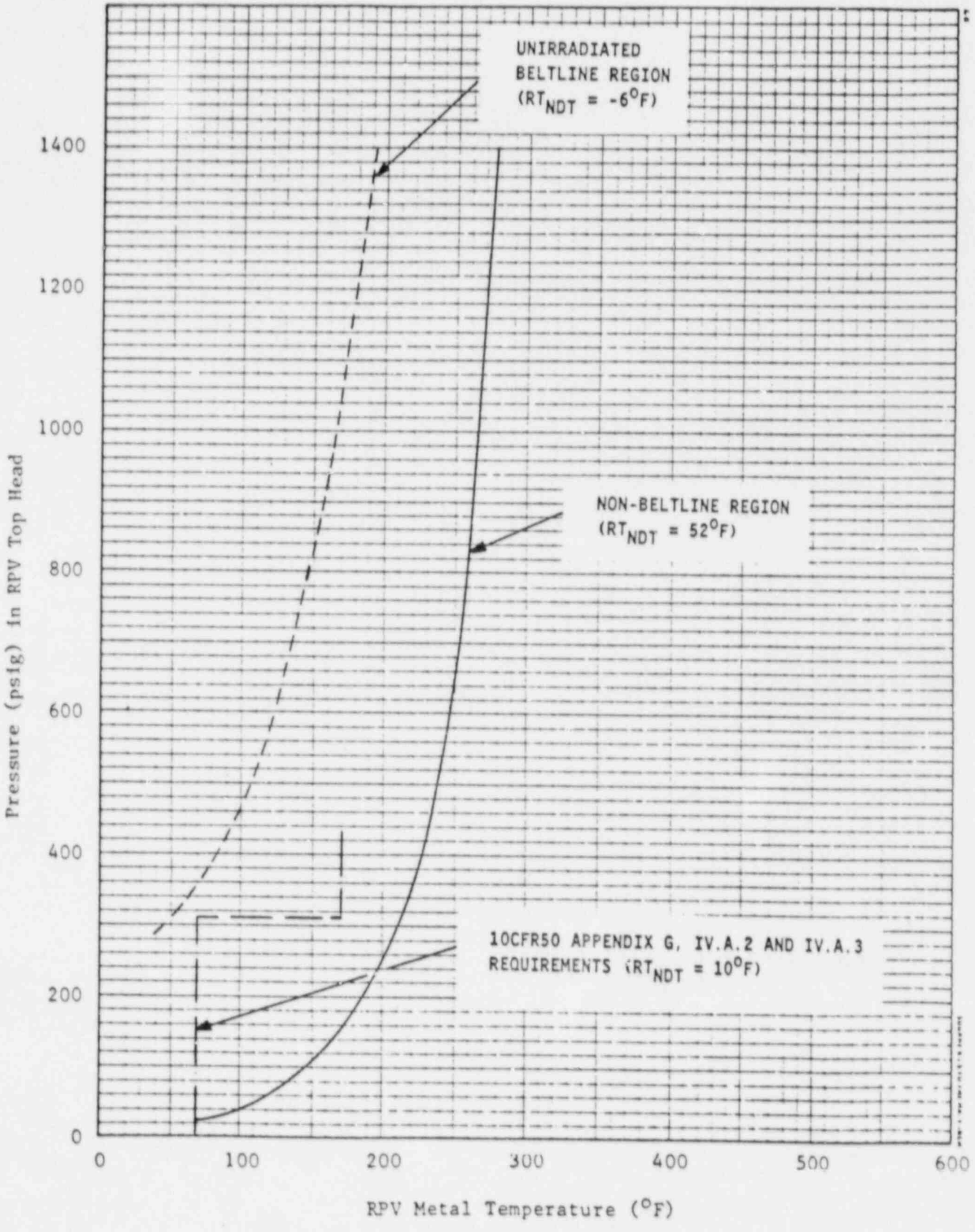

Figure 7-3. Components of Operating Limits Curve for Core Critical Operation (Curve C)

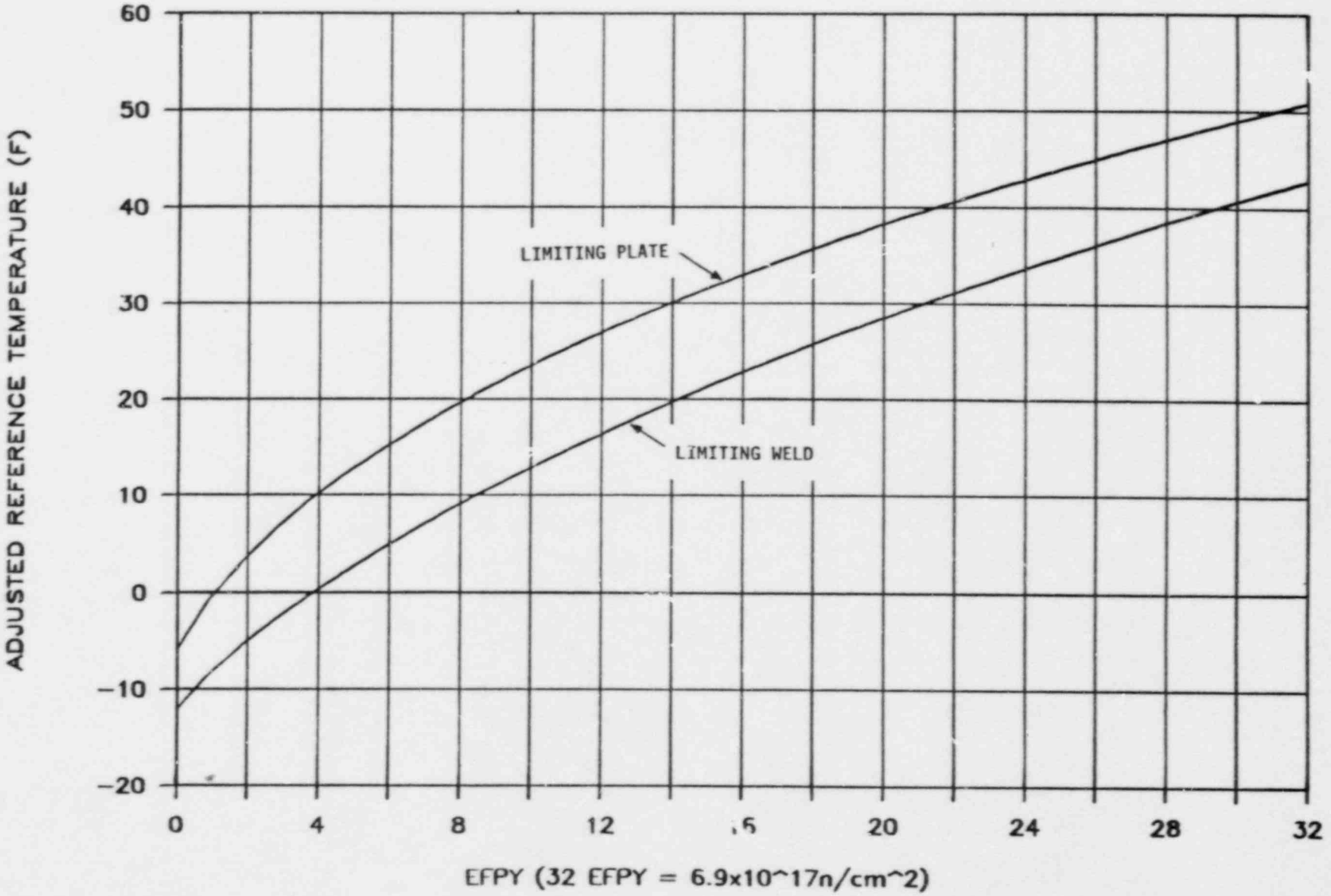

Figure 7-4. Adjusted Reference Temperature of Limiting Plate and Weld

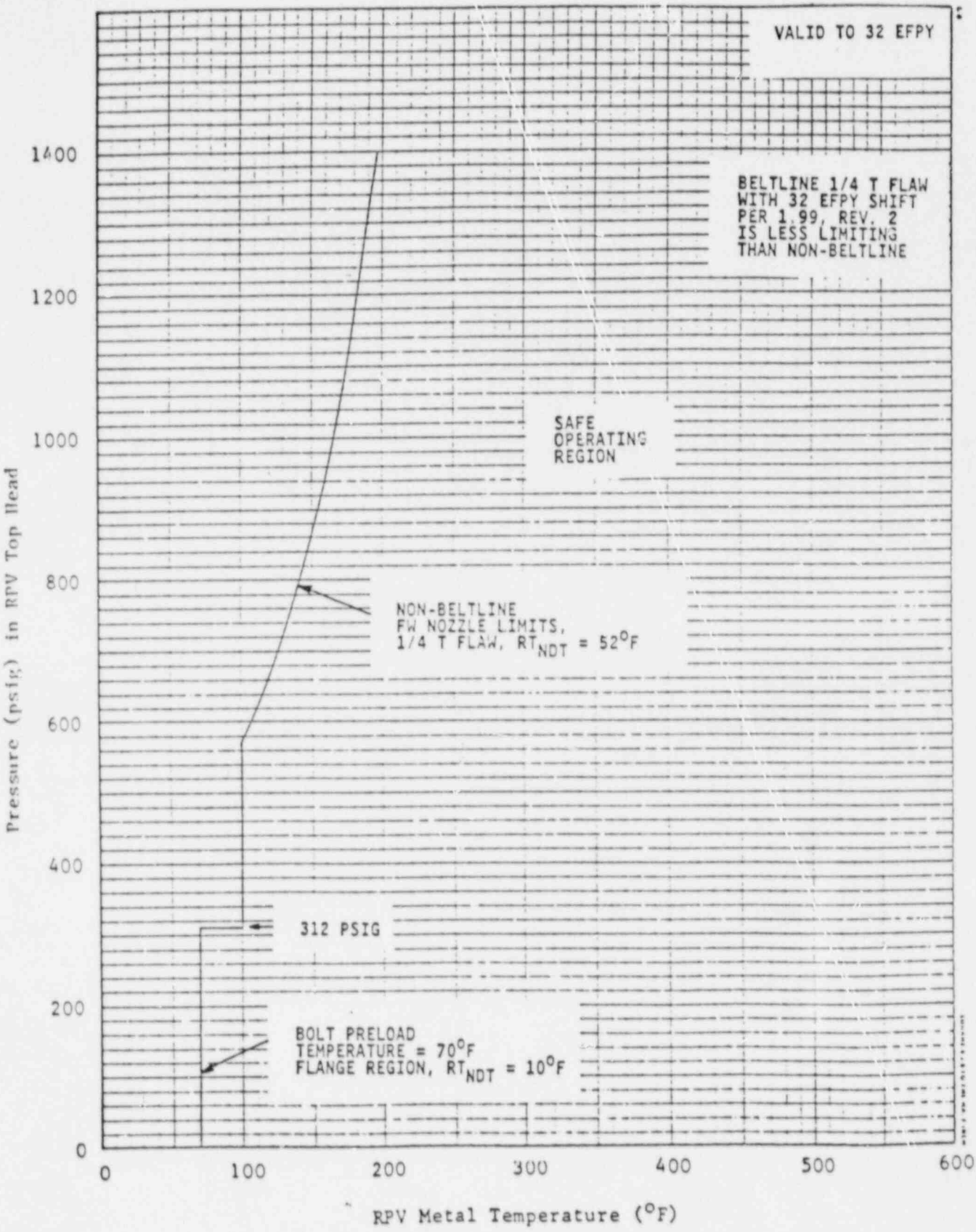

Figure 7-5. Minimum Temperature for Pressure Tests Such as Required by Section XI

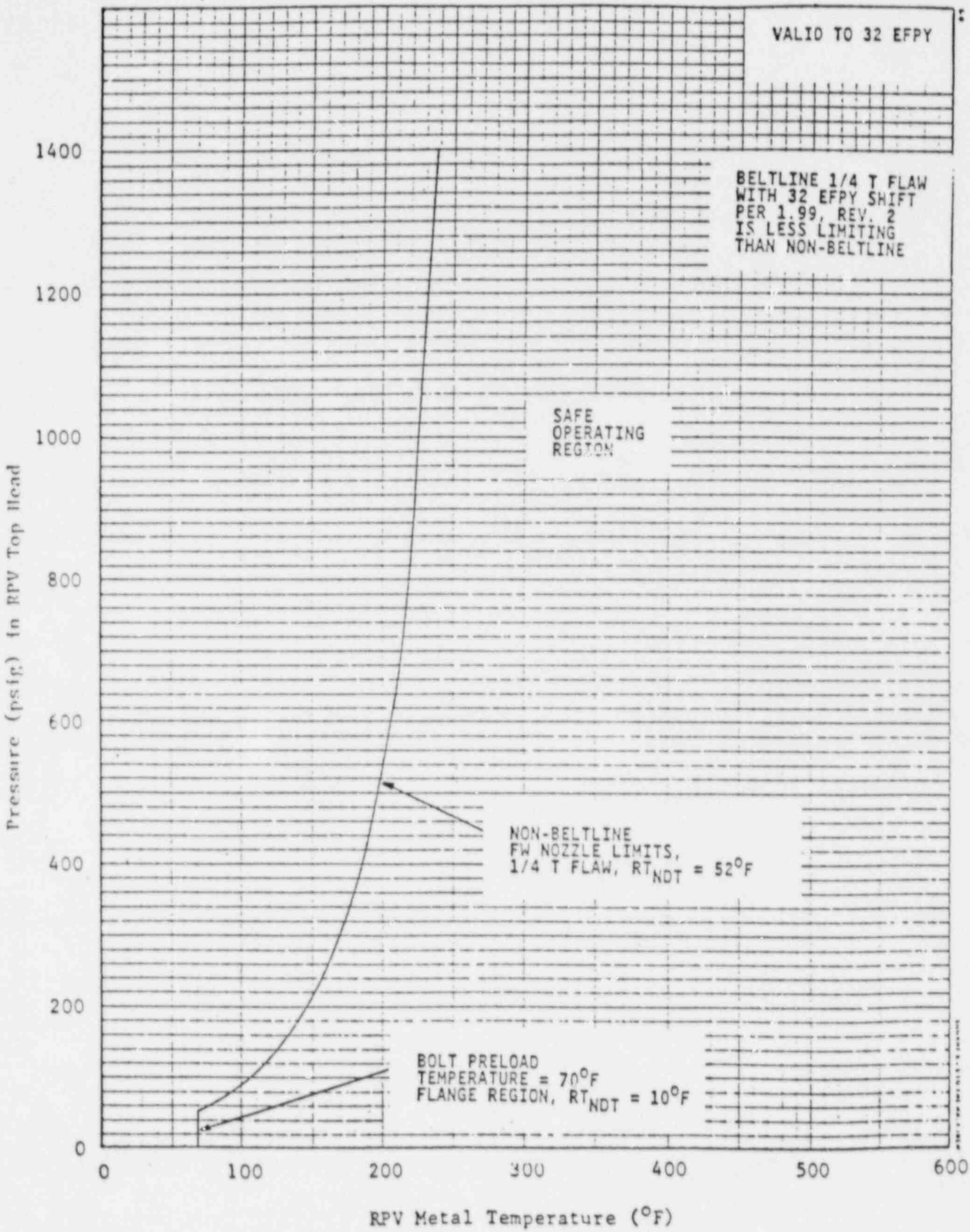

Figure 7-6. Minimum Temperature for Mechanical Heatup or Cooldown Following Nuclear Shutdown

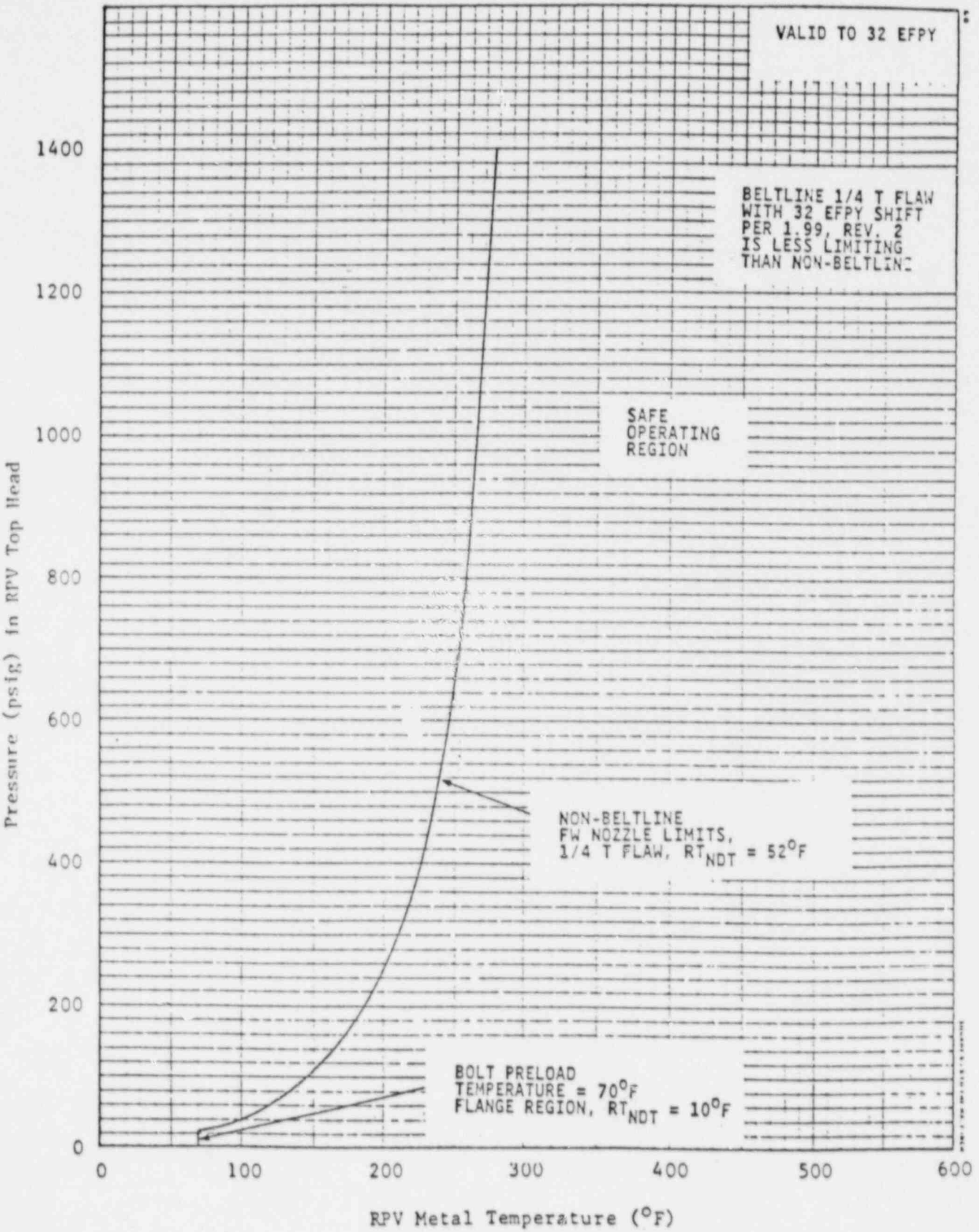

Figure 7-7. Minimum Temperature for Core Operation (Criticality)

8. REFERENCES

1. "Fracture Toughness Requirements," Appendix G to Part 50 of Title 10 of the Code of Federal Regulations, July 1983.

2. "Protection Against Non-Ductile Failure," Appendix G to Section III of the ASME Boiler & Pressure Vessel Code, Addenda to and including Winter 1987.

3. "Reactor Vessel Material Surveillance Program Requirements," Appendix H to Part 50 of Title 10 of the Code of Federal Regulations, July 1983.

4. "Conducting Surveillance Tests for Light Water Cooled Nuclear Power Reactor Vessels," Annual Book of ASTM Standards, E185-82, July 1982.

5. "Radiation Embrittlement of Reactor Vessel Materials," USNRC Regulatory Guide 1.99, Draft Revision, August 1987.

6. "Fracture Toughness Requirements," USNRC Branch Technical Position MTEB 5-2, Revision 1, July 1981.

7. "Capsule Basket," General Electric Drawing 117C4048, Revision 1, October 1969.

8. Schmidt, C. L., "Test Results from Electroslag Weld Prolongations - 610-0139 Units 1 and 2," Babcock & Wilcox Manufacturing Engineering Report No. 1, October 1968.

9. Hodge, J. M., "Properties of Heavy Section Nuclear Reactor Steels," Welding Research Council Bulletin 217, July 1976.

10. "Reactor Pressure Vessel," GE Purchase Specification 21A1111, Revision 9, August 1970.

11. "Standard Methods for Notched Bar Impact Testing of Metallic Materials," Annual Book of ASTM Standards, E23-82, March 1982.

12. "Nuclear Plant Irradiated Steel Handbook," EPRI Report NP-4797, September 1986.

13. "Standard Methods of Tension Testing of Metallic Materials," Annual Book of ASTM Standards, E8-81.

14. "Ultrasonic Examination for Cracks in the Top Head Flange," CBI Nuclear, Development Report 74-9047, December 1975.

15. "Ultrasonic Examination for Cracks in the Shell Flange," CBI Nuclear, Development Report 74-9056, November 1975.

APPENDIX A

DETERMINATION OF ELECTROSLAG WELD PROPERTIES

Babcock & Wilcox performed testing on nine electroslag weld prolongations from the Peach Bottom 2 vessel, all made from the same weld heat. The data are evaluated in this appendix to determine conservative values of weld chemistry and initial RT_{NDT} representative of the welds.

A.1 ELECTROSLAG WELD CHEMISTRY

The weld chemistry analyses are summarized in Table A-1. The average element values were used as representative values, except for copper and nickel, where the maximum recorded values were assumed.

A.2 ELECTROSLAG WELD RT_{NDT}

Nine sets of Charpy data from the prolongation tests for Peach Bottom 2 welds are plotted in Figures A-1 through A-9. The testing was not done with the objective of defining a full Charpy curve, so upper shelf values are not available. The data sets were fit with the function

Energy = A + B * TANH [(T - T_0) / C], where

T = test temperature, °F

A, B, C and T_0 are constants.

The highest and lowest Charpy energies recorded were 99 ft-lb and 2 ft-lb, respectively. For purposes of curve fitting, these were assumed to be the upper and lower shelf values, thus setting the values of A and B. The values of C and T_0 were determined by nonlinear regression to provide a best fit to the transition regions of the curves.

The TANH curve fit values of 50 ft-lb are tabulated in Table A-2. These values were averaged to arrive at the mean RT_{NDT} value of -45°F. Determination of the standard deviation is shown in Table A-2 as well.

Table A-1

ELECTROSLAG WELD CHEMISTRY TEST RESULTS

Test Weld No.	C	Mn	P	S	Si	Cr	Ni	Mo	Cu	V	AS
1	.18	1.40	.014	.012	.09	.05	.21	.53	.16	.01	.002
2	.17	1.43	.016	.012	.10	.06	.21	.54	.19	.01	.001
3	.17	1.41	.014	.012	.08	.05	.19	.53	.20	.01	.001
4	.16	1.37	.015	.011	.08	.04	.14	.51	.21	.01	.001
5	.18	1.41	.015	.012	.09	.04	.16	.52	.16	.01	.002
6	.17	1.38	.014	.011	.08	.04	.16	.53	.19	.01	.001
7	.16	1.43	.015	.016	.09	.06	.19	.53	.18	-	-
8	.16	1.44	.016	.015	.09	.05	.19	.54	.17	-	-
9	.17	1.45	.014	.014	.09	.05	.19	.54	.19	-	-
Average	.17	1.41	.015	.013	.09	.05	.18	.53	.18	.01	.001

Representative Chemistry:

C	Mn	P	S	Si	Cr	Ni	Mo	Cu	V	AS
.17	1.41	.015	.013	.09	.05	.21	.53	.21	.01	.001

Table A-2

DETERMINATION OF ELECTROSLAG WELD RT_{NDT}

Test Weld No.	Index Temperature T_{50}	Variation $(T_{50} - \overline{T_{50}})^2$
1	18.8	11.51
2	3.0	155.45
3	31.7	265.76
4	32.1	277.63
5	26.7	126.39
6	-20.7	1303.77
7	15.9	0.20
8	12.5	8.40
9	18.9	11.78
Sum	138.9	2160.89

Mean:

$$\overline{T_{50}} = 138.9 / 9 = 15.4°F, \text{ so}$$

$$RT_{NDT} = (\overline{T_{50}} - 60°F) = \boxed{-45°F}$$

Standard Deviation:

$$\sigma_I = [\ (1/8) * \sum_{1}^{9} (T_{50} - \overline{T_{50}})^2\ ]^{1/2}$$

$$\sigma_I = \boxed{16.44°F}$$

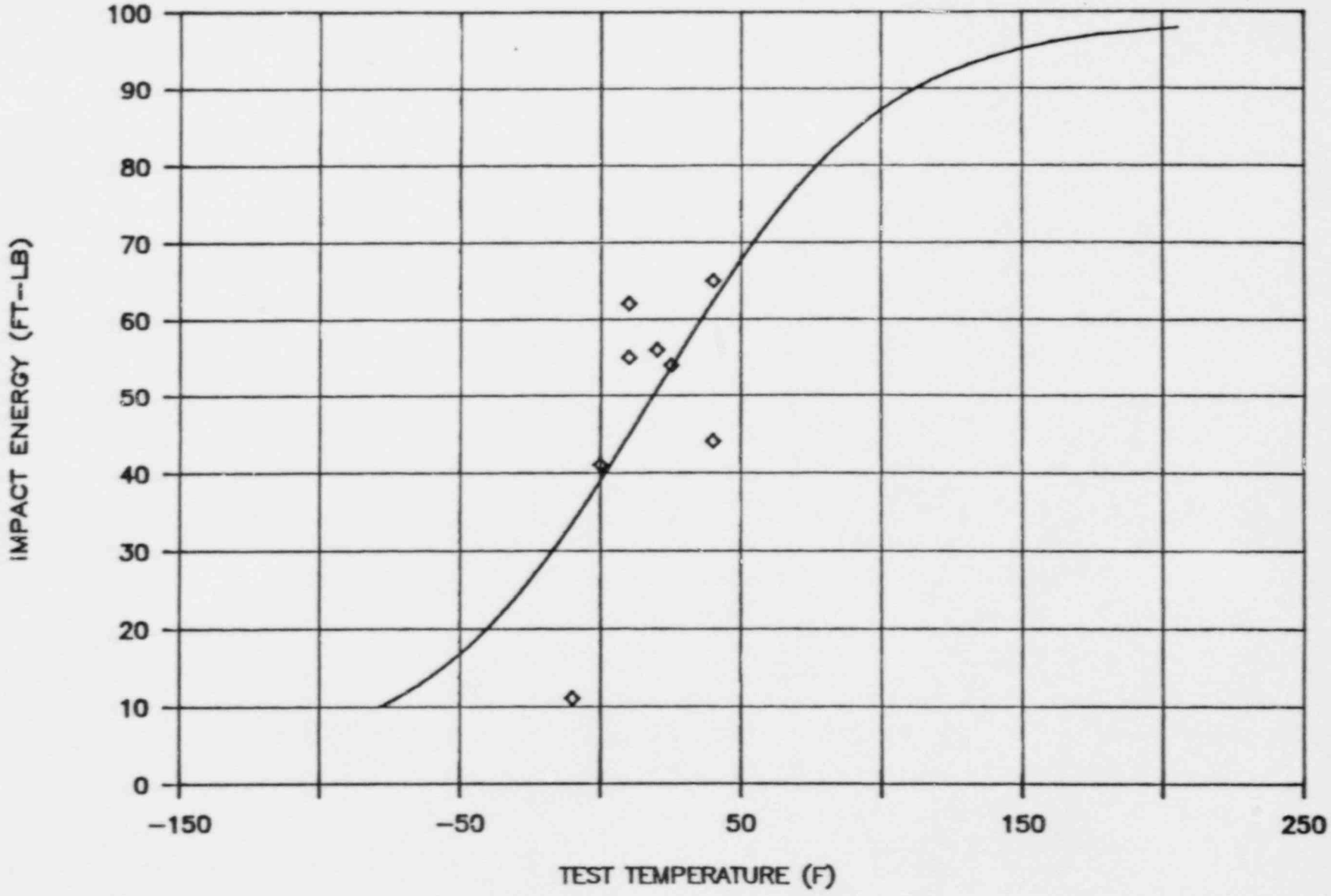

Figure A-1. Charpy Impact Energy Data for Electroslag Weld - Test Weld 1

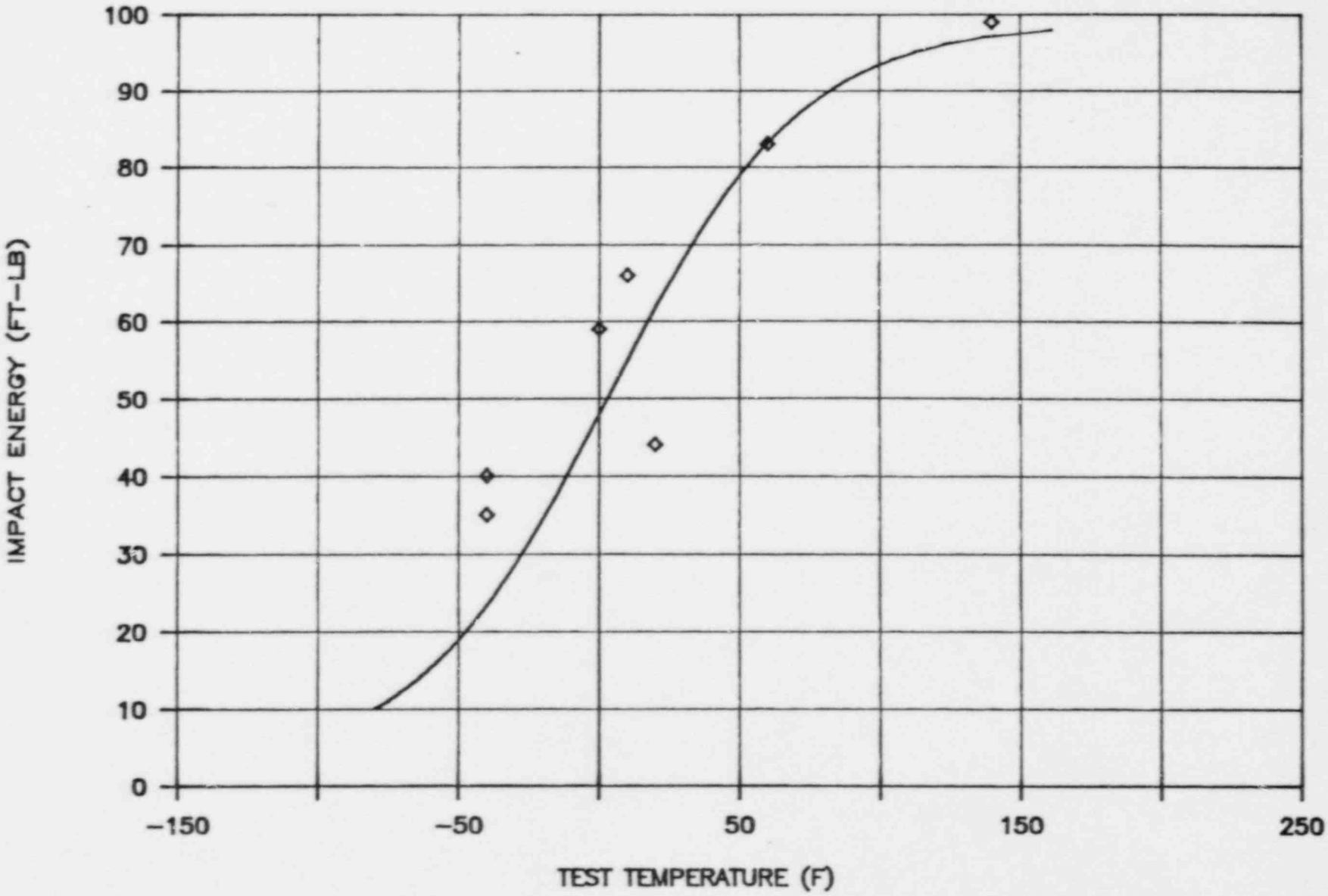

Figure A-2. Charpy Impact Energy Data for Electroslag Weld - Test Weld 2

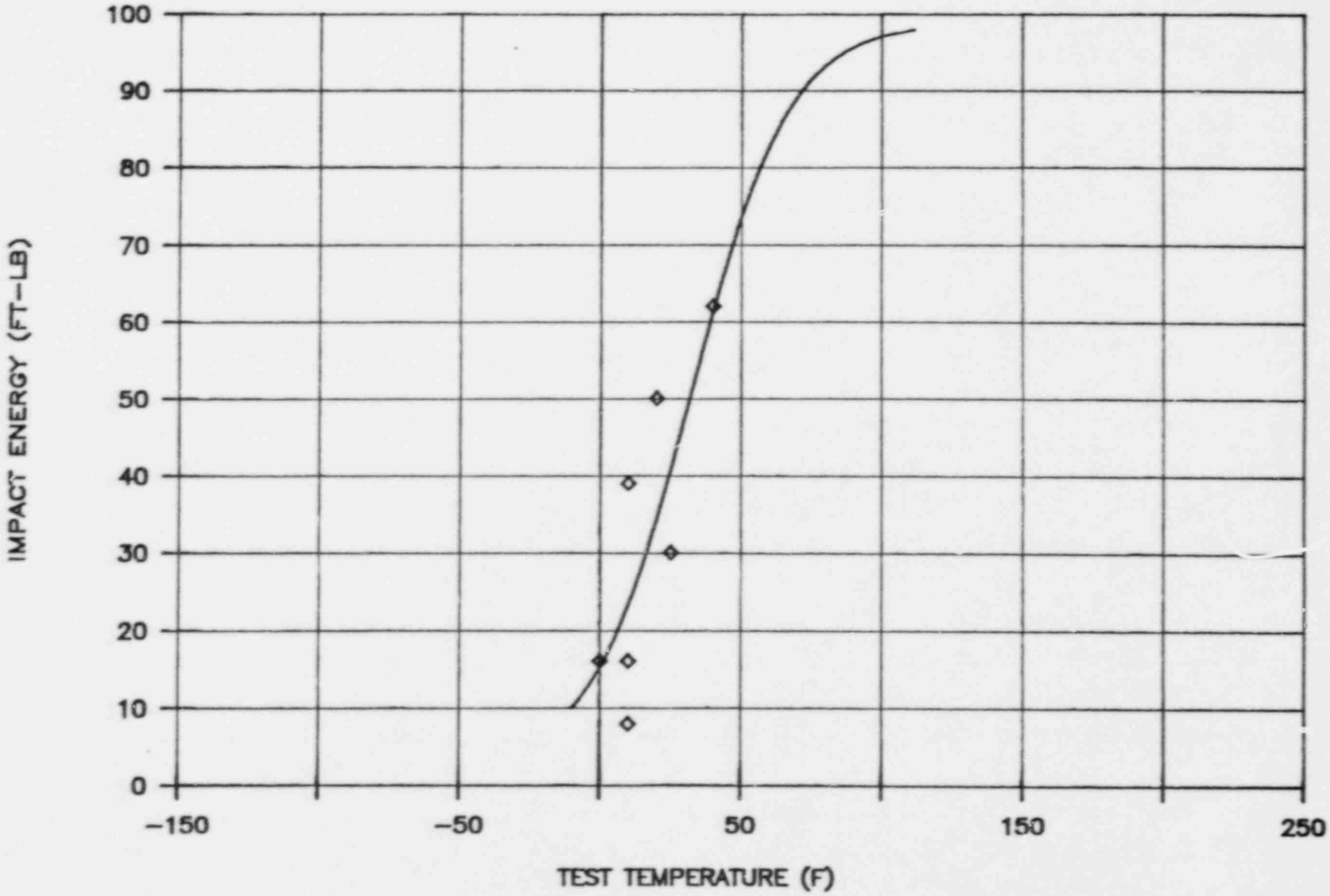

Figure A-3. Charpy Impact Energy Data for Electroslag Weld - Test Weld 3

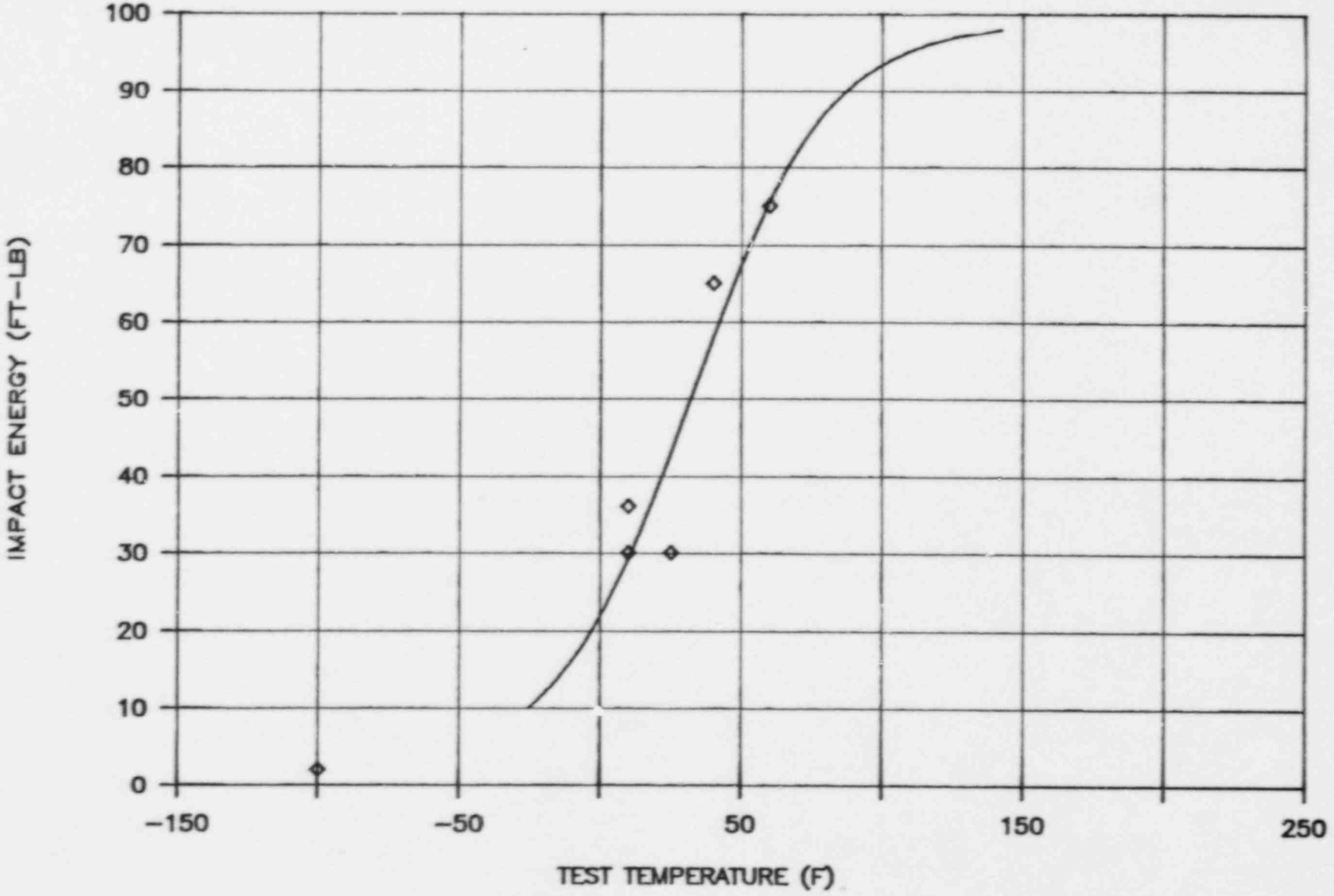

Figure A-4. Charpy Impact Energy Data for Electroslag Weld - Test Weld 4

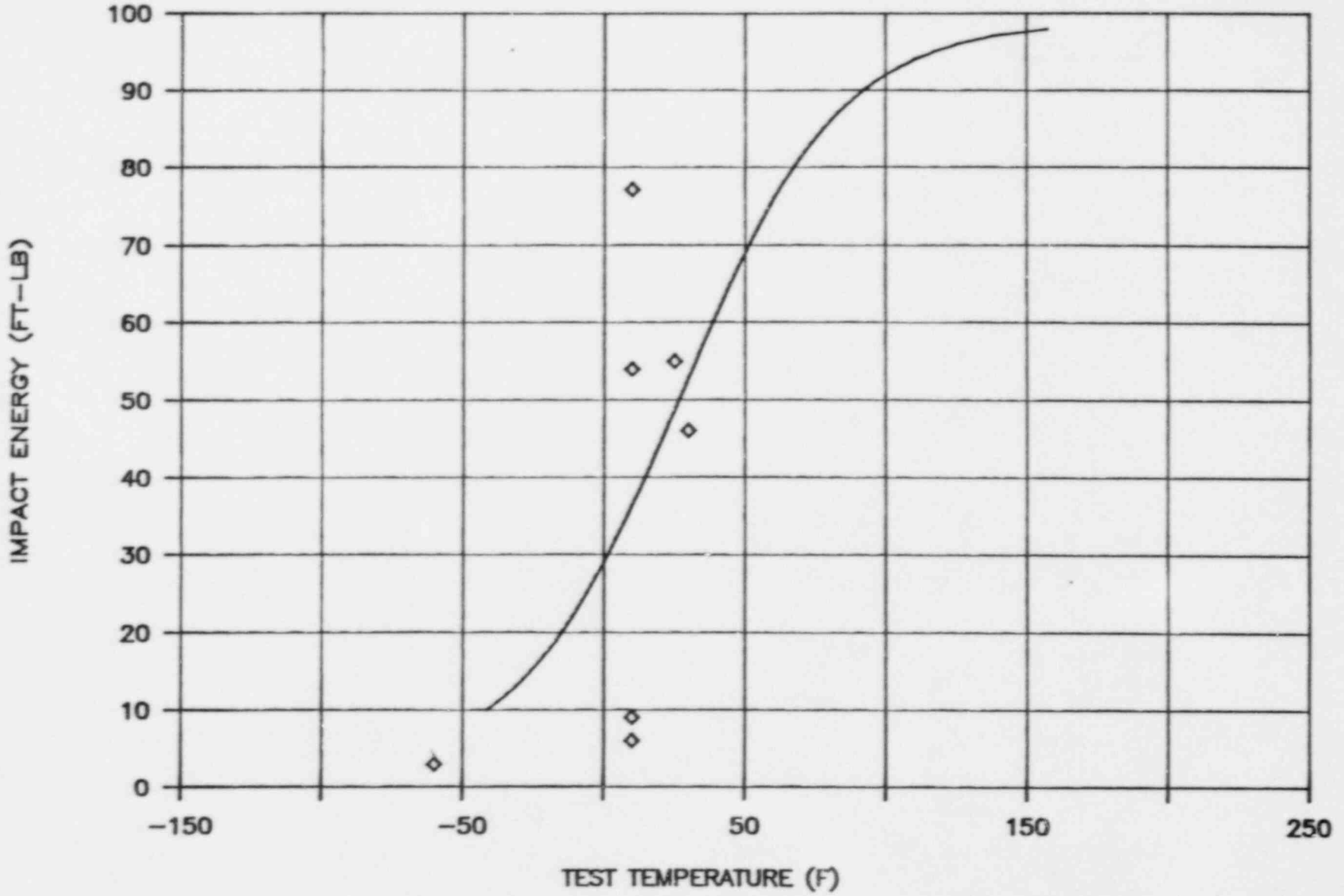

Figure A-5. Charpy Impact Energy Data for Electroslag Weld - Test Weld 5

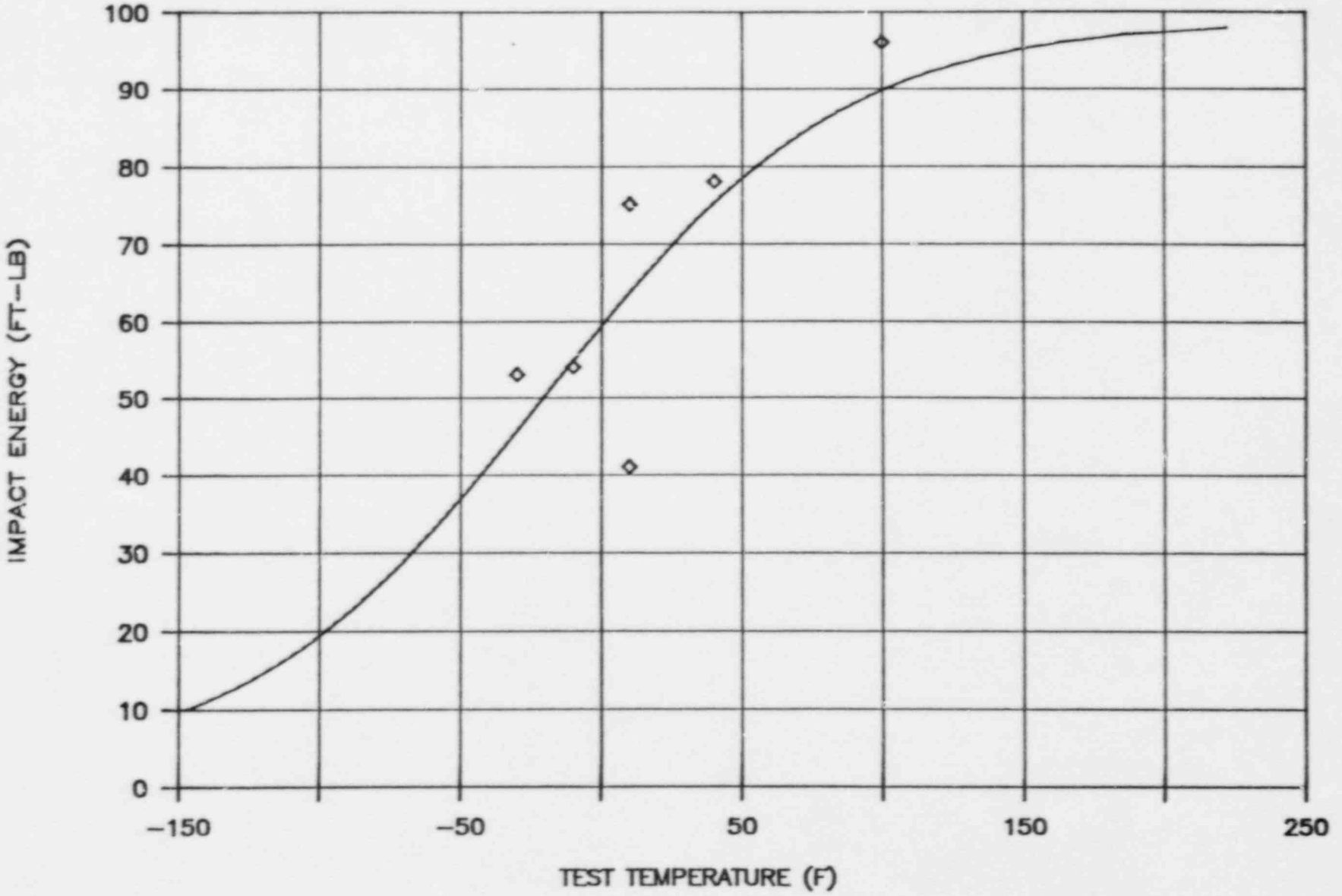

Figure A-6. Charpy Impact Energy Data for Electroslag Weld - Test Weld 6

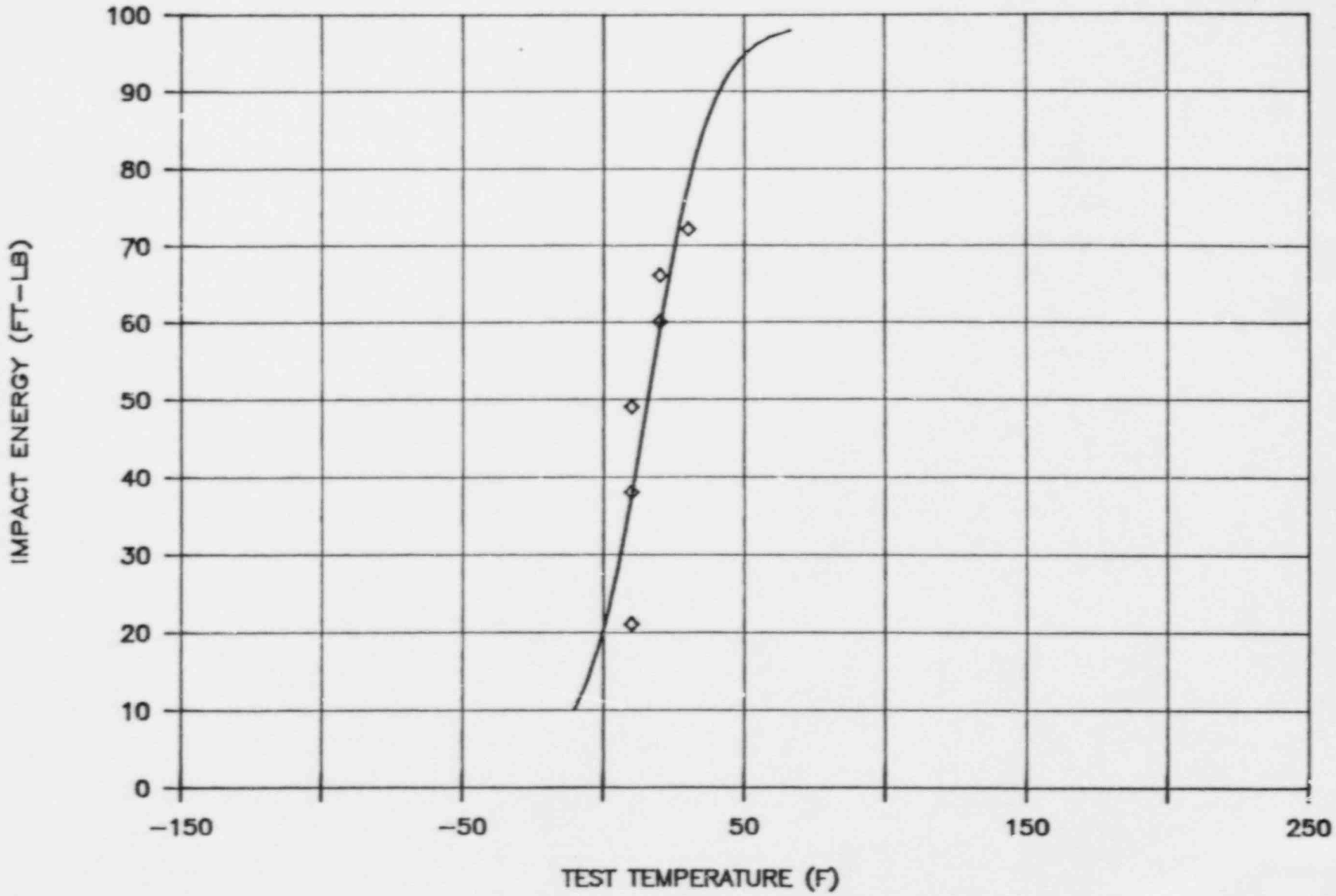

Figure A-7. Charpy Impact Energy Data for Electroslag Weld - Test Weld 7

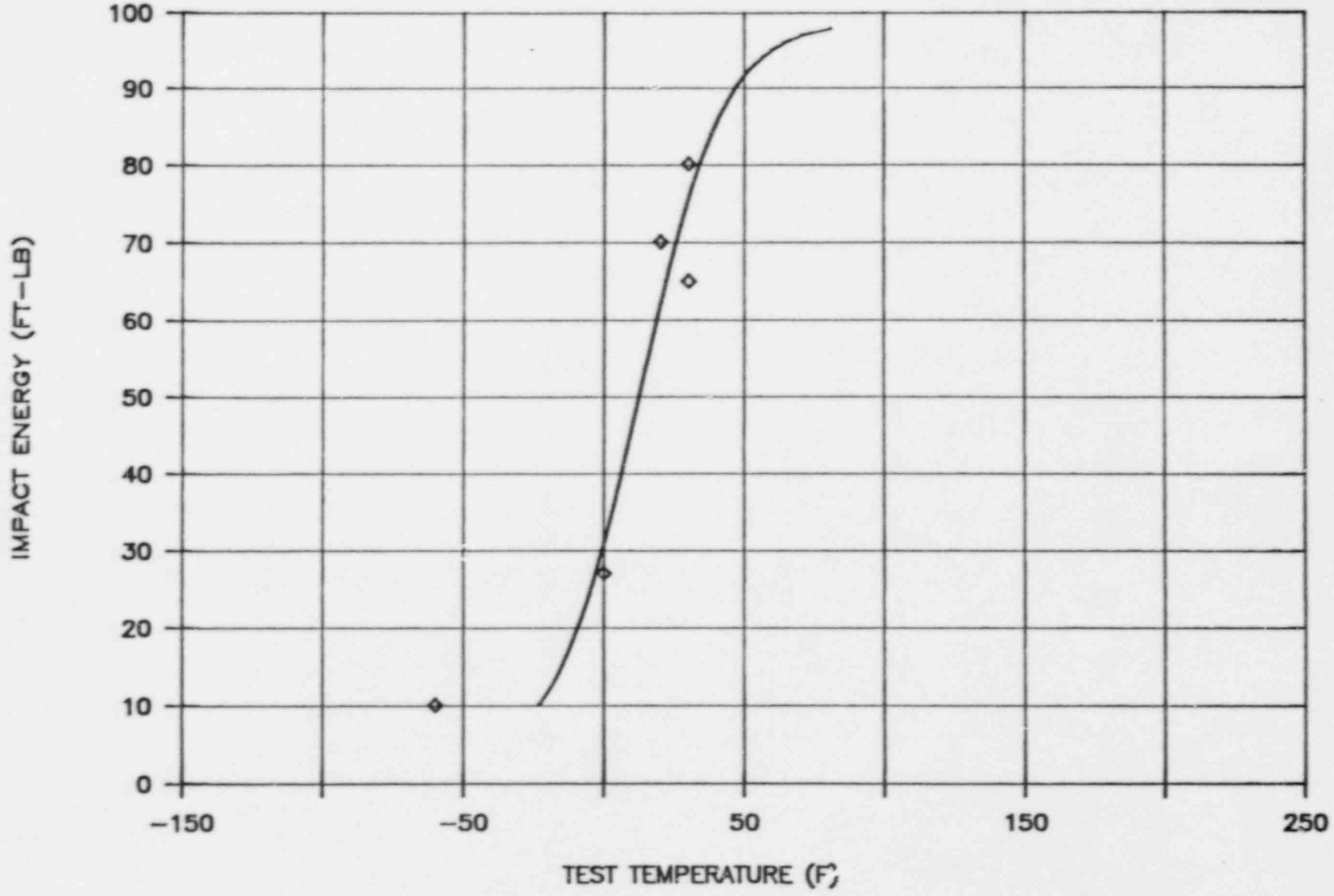

Figure A-8. Charpy Impact Energy Data for Electroslag Weld - Test Weld 8

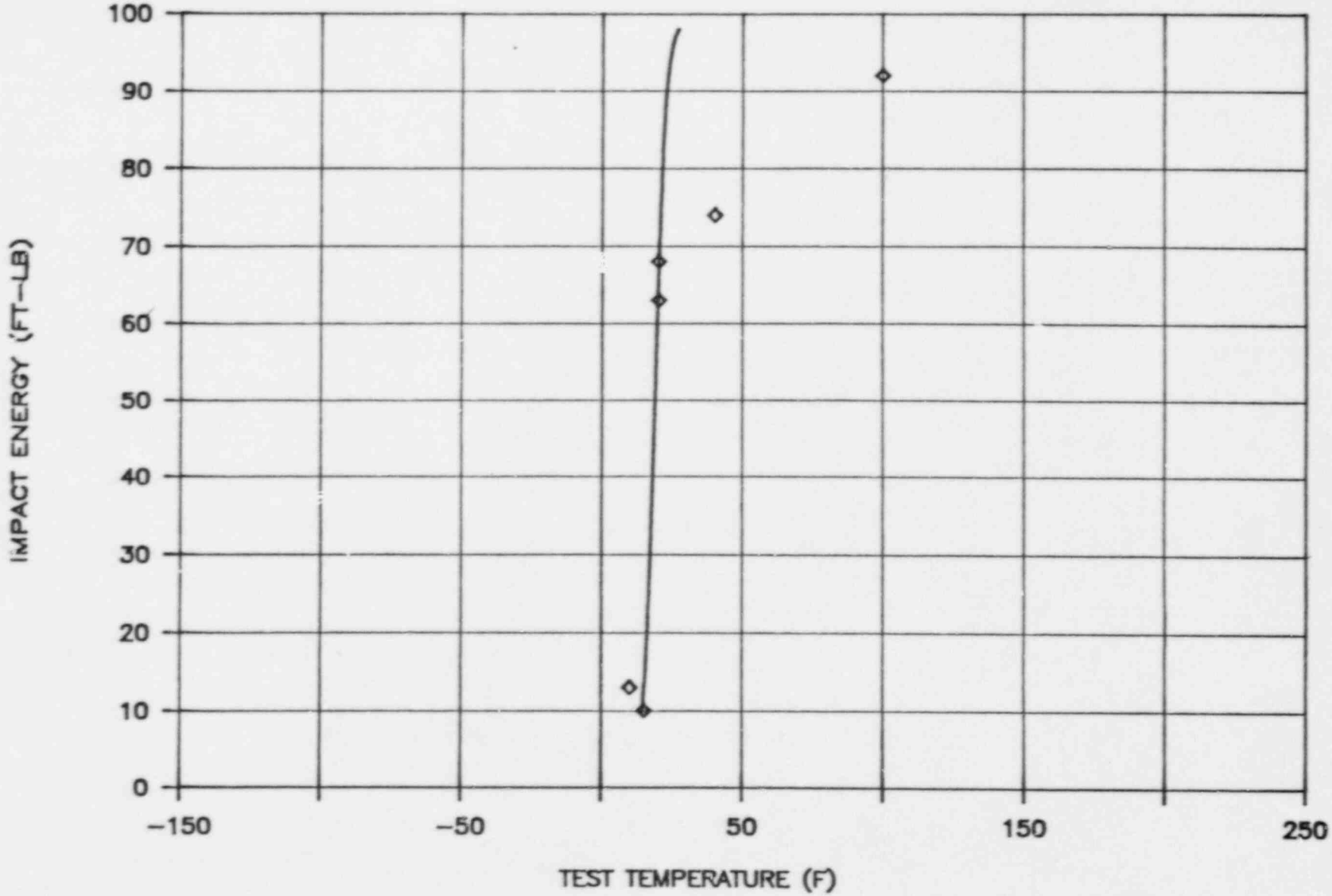

Figure A-9. Charpy Impact Energy Data for Electroslag Weld - Test Weld 9

APPENDIX B

CHARPY V-NOTCH FRACTURE SURFACE PHOTOGRAPHS

Photographs of each Charpy specimen fracture surface were taken to facilitate the determination of percent shear, and to comply with the requirements of ASTM E185-82. The pages following show the fracture surface photographs along with a summary of the Charpy test results for each specimen. The pictures are arranged by increasing test temperature for each material, with the materials in the order of base, weld and HAZ.

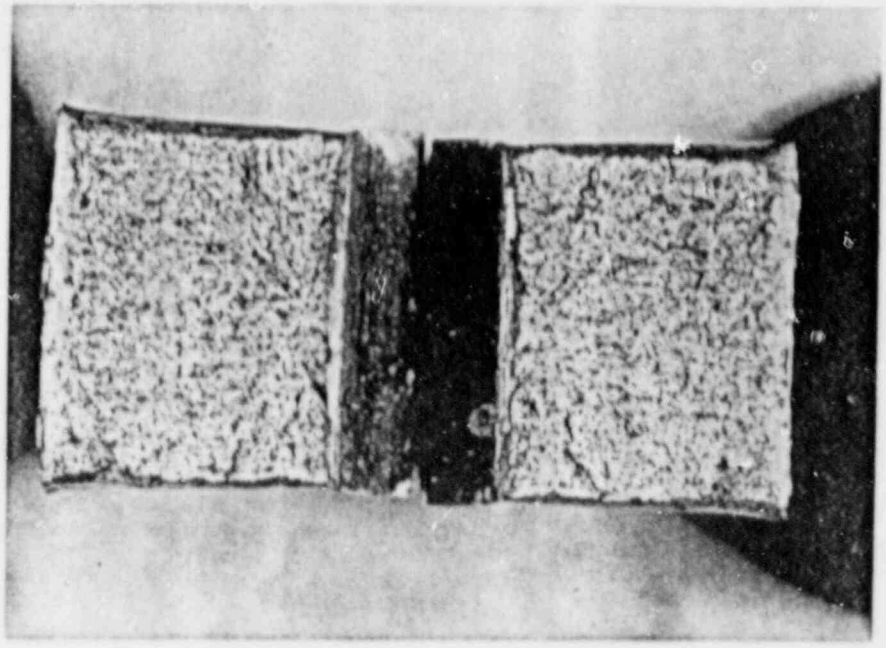

BASE:	772	MLE:	24
TEMP:	-20°F	% SHEAR:	6
ENERGY:	22.0 ft-lb		

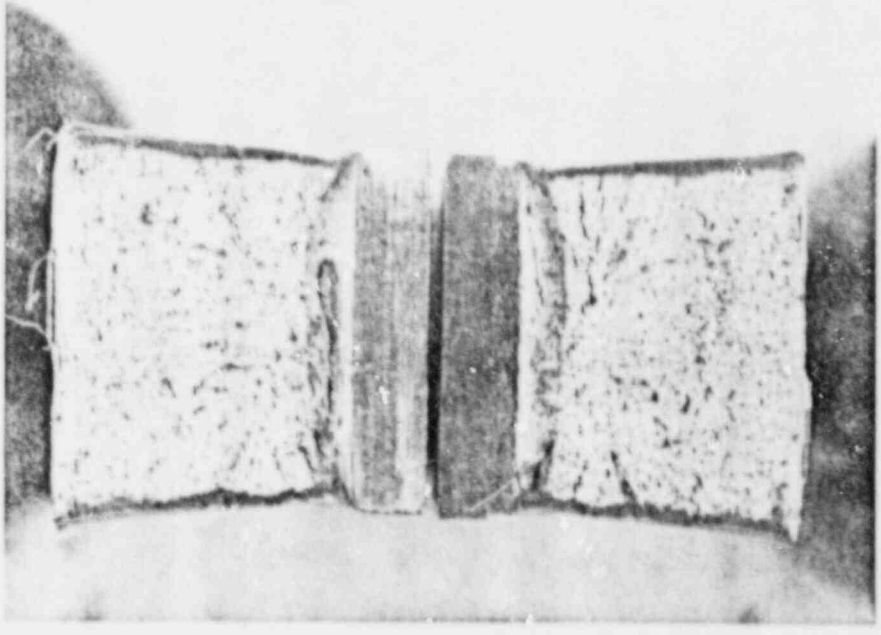

BASE:	765	MLE:	38
TEMP:	0°F	% SHEAR:	18
ENERGY:	47.0 ft-lb		

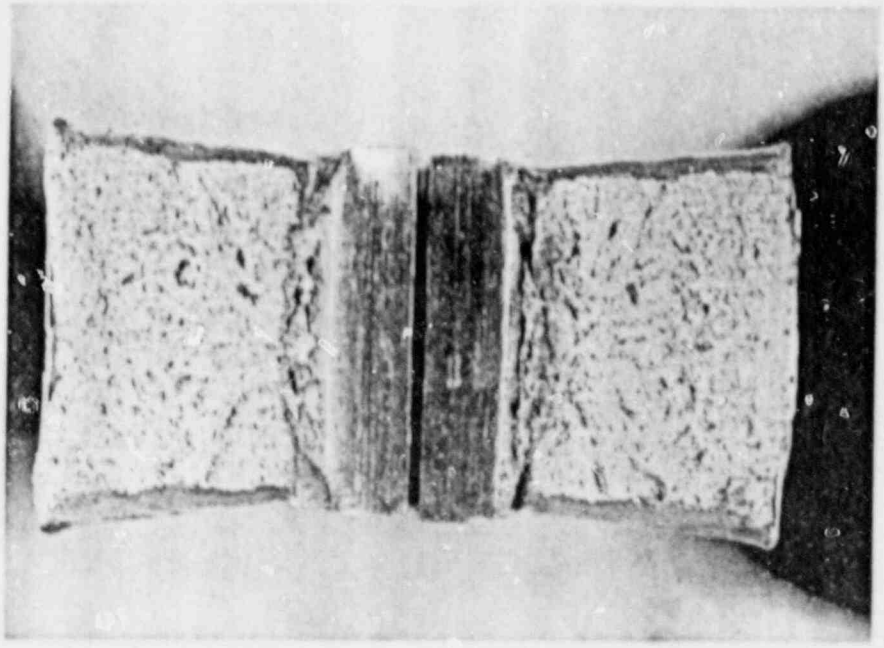

BASE:	76K	MLE:	46
TEMP:	20°F	% SHEAR:	26
ENERGY:	54.5 ft-lb		

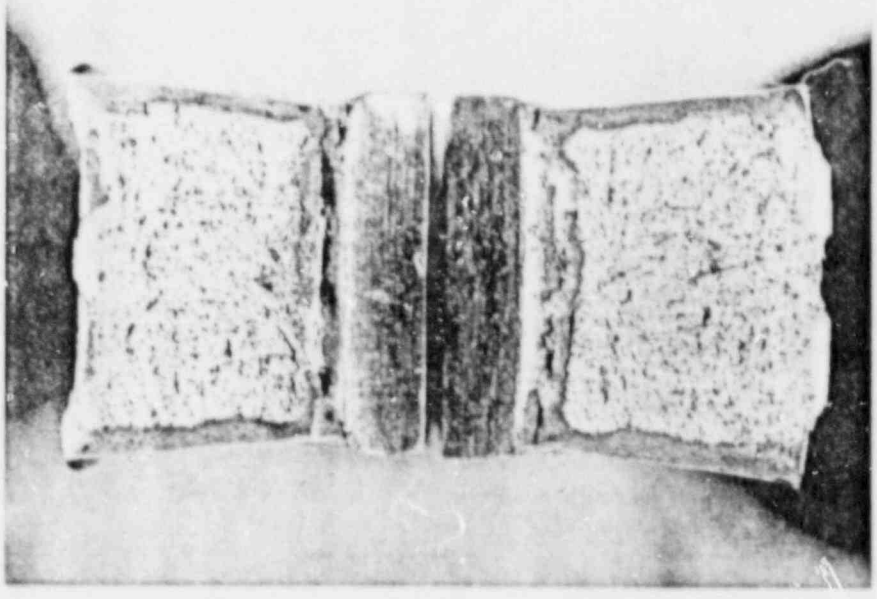

BASE:	77A	MLE:	50
TEMP:	40°F	% SHEAR:	34
ENERGY:	58.0 ft-lb		

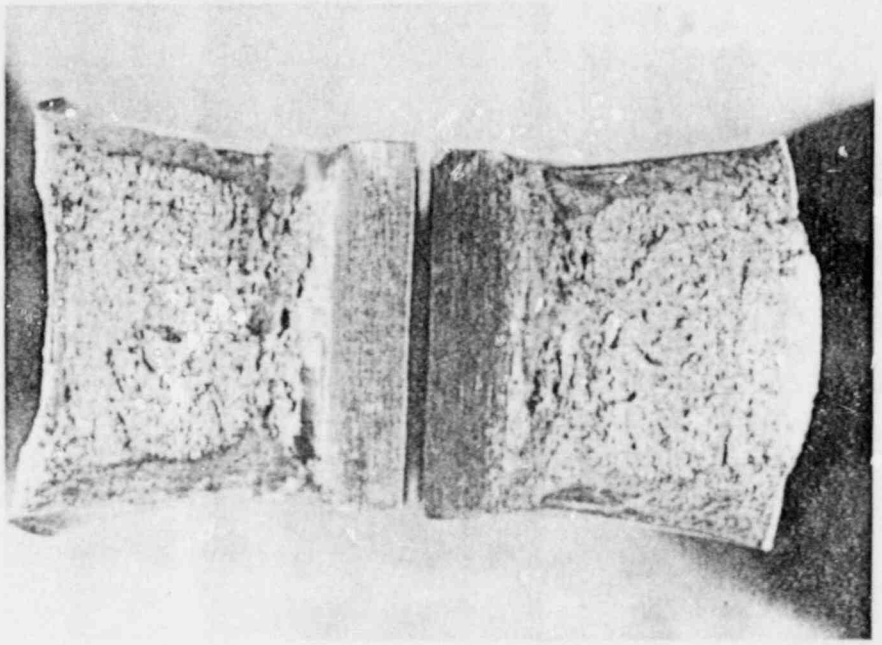

BASE:	77D	MLE:	70
TEMP:	70°F	% SHEAR:	40
ENERGY:	81.5 ft-lb		

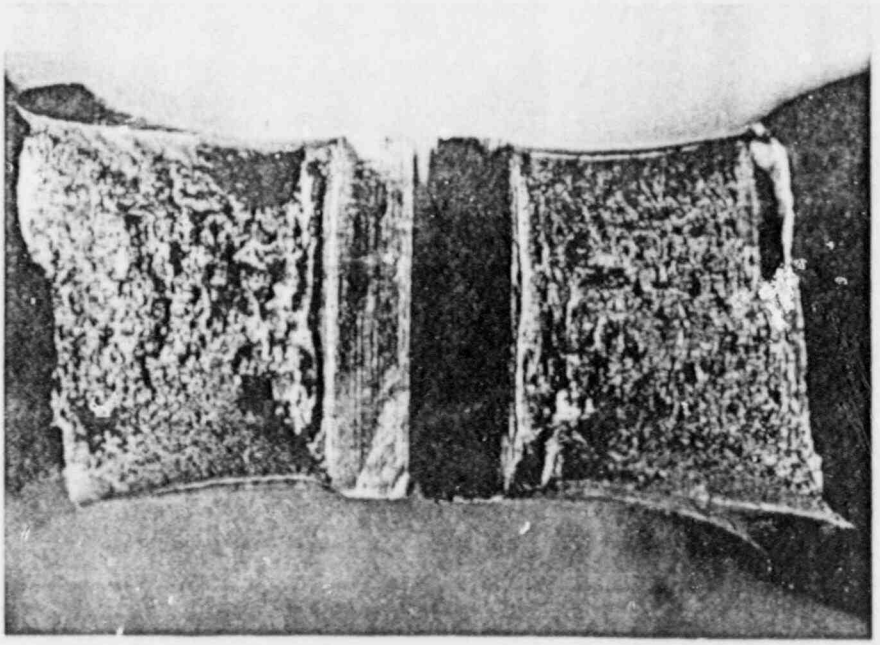

BASE:	75M	MLE:	98
TEMP:	140°F	% SHEAR:	100
ENERGY:	131.0 ft-lb		

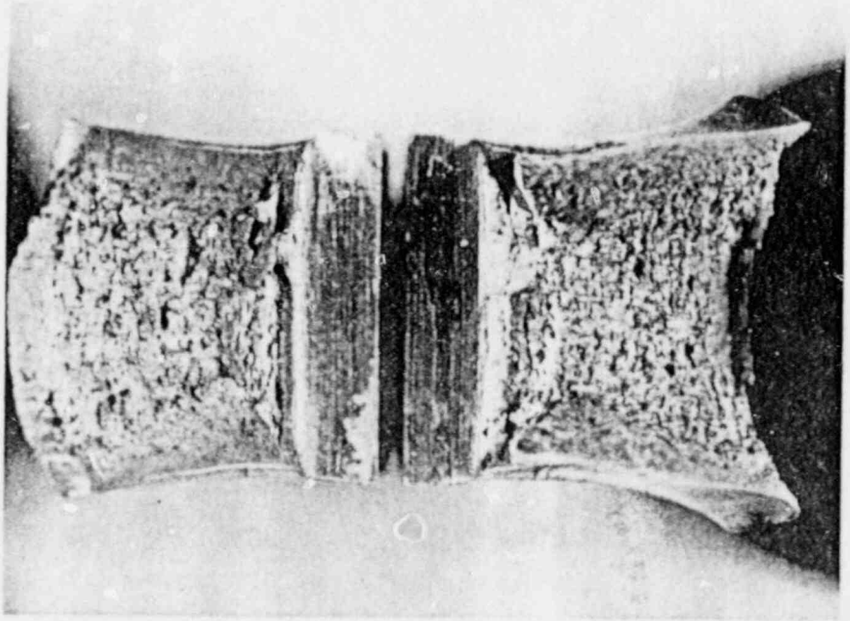

BASE: 75P
TEMP: 200°F
ENERGY: 132.0 ft-lb

MLE: 92
% SHEAR: 100

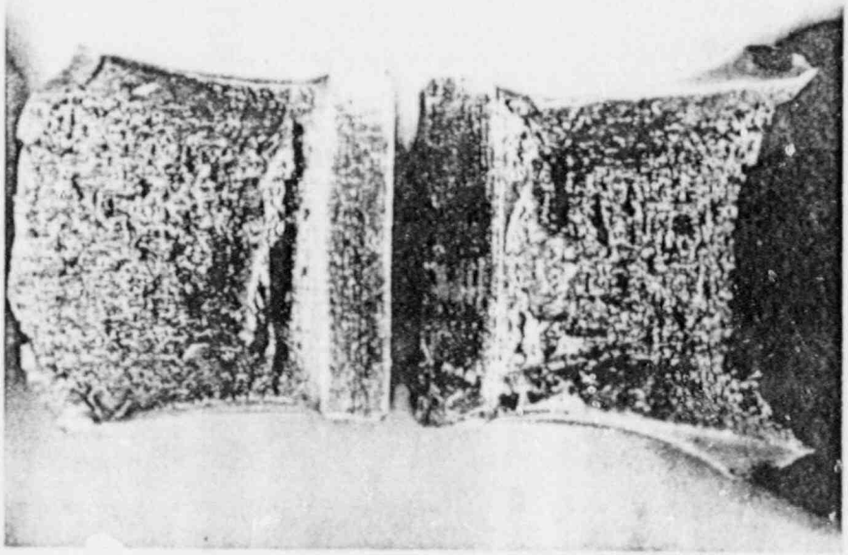

BASE: 77K
TEMP: 300°F
ENERGY: 136.0 ft-lb

MLE: 90
% SHEAR: 100

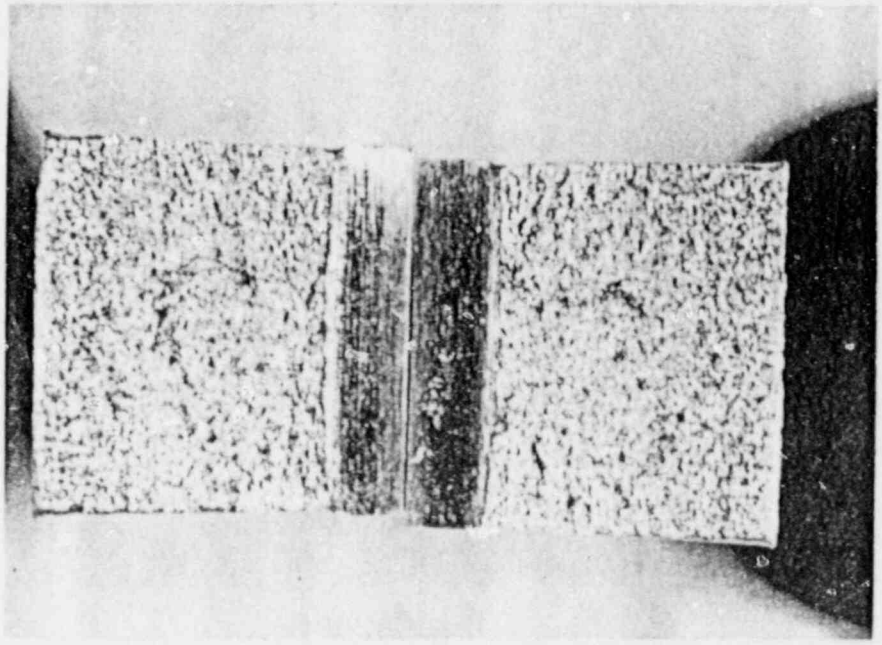

WELD:	7BT	MLE:	16
TEMP:	- 20°F	% SHEAR:	1
ENERGY:	15.0 ft-lb		

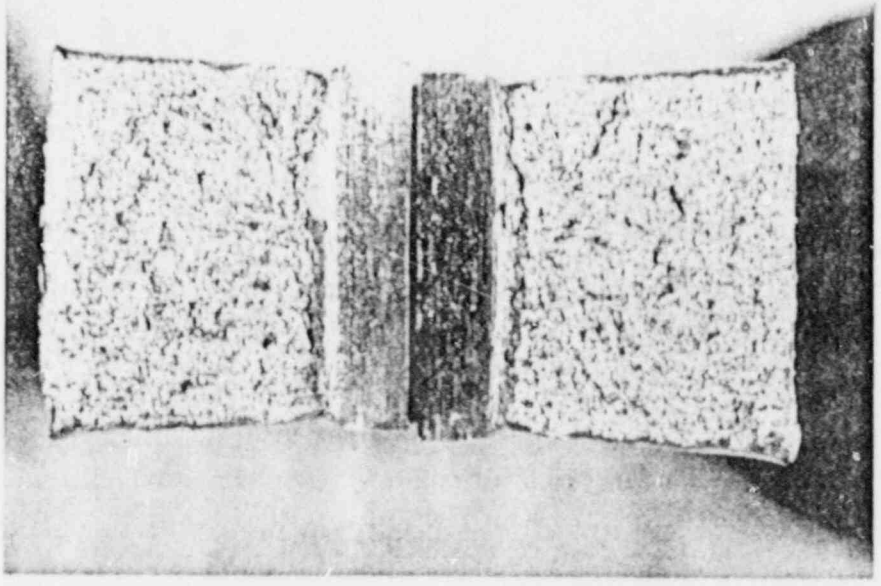

WELD:	7AT	MLE:	32
TEMP:	20°F	% SHEAR:	9
ENERGY:	34.0 ft-lb		

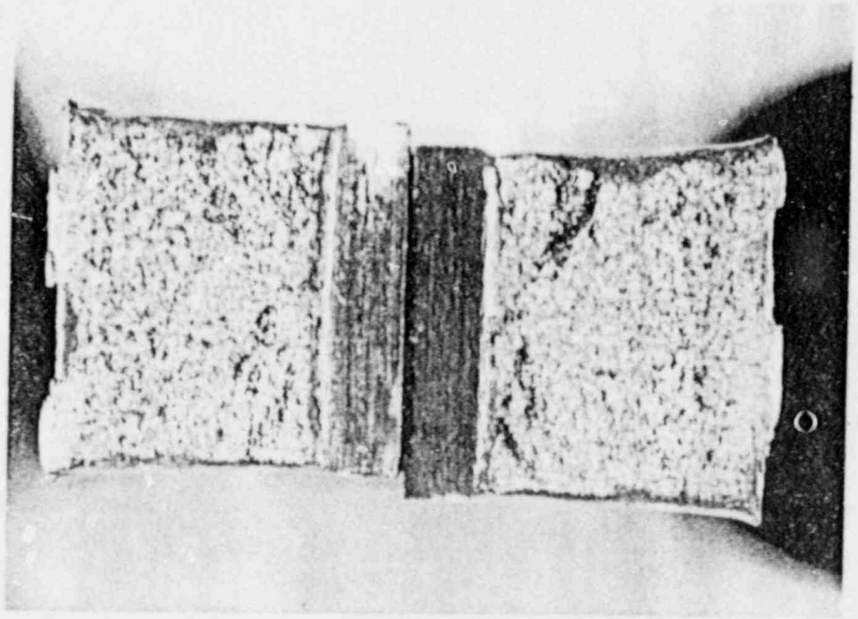

WELD:	7C1	MLE:	34
TEMP:	40°F	% SHEAR:	8
ENERGY:	31.0 ft-lb		

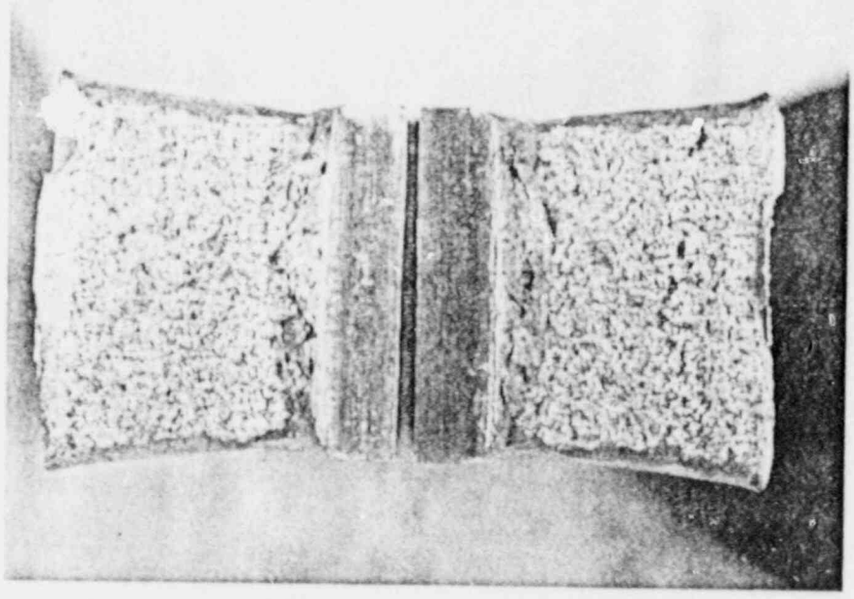

WELD:	7B3	MLE:	48
TEMP:	60°F	% SHEAR:	31
ENERGY:	53.5 ft-lb		

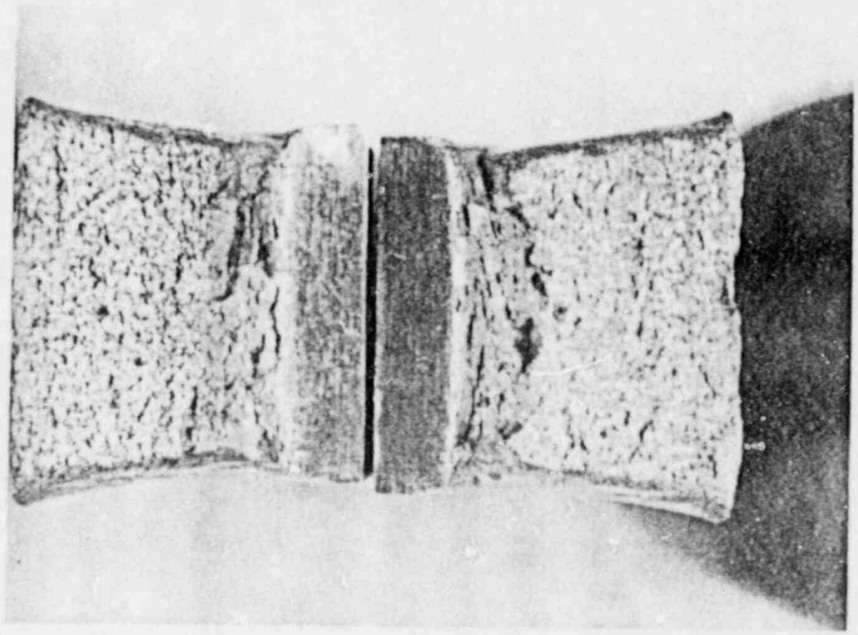

WELD:	7BA	MLE:	58
TEMP:	70°F	% SHEAR:	28
ENERGY:	65.0 ft-lb		

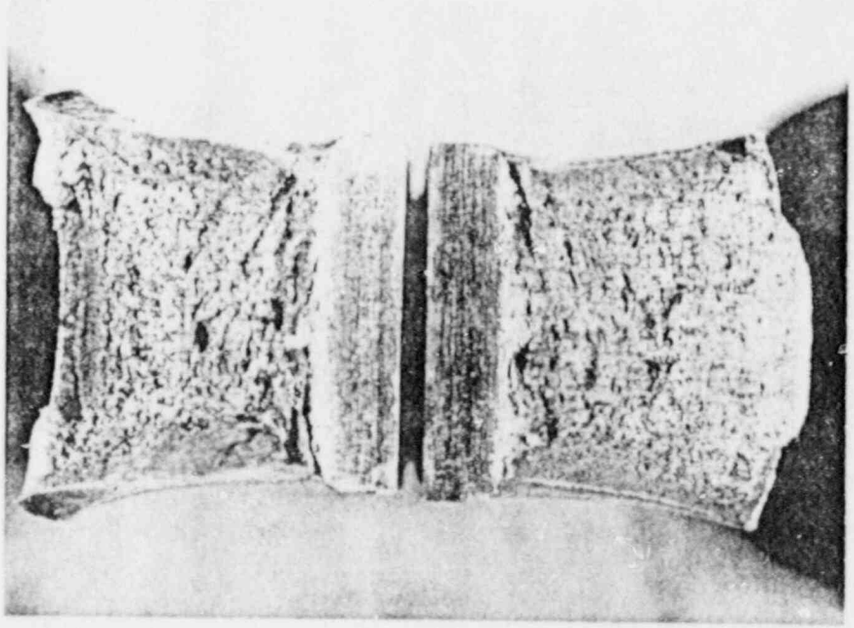

WELD:	7AM	MLE:	79
TEMP:	140°F	% SHEAR:	83
ENERGY:	95.5 ft-lb		

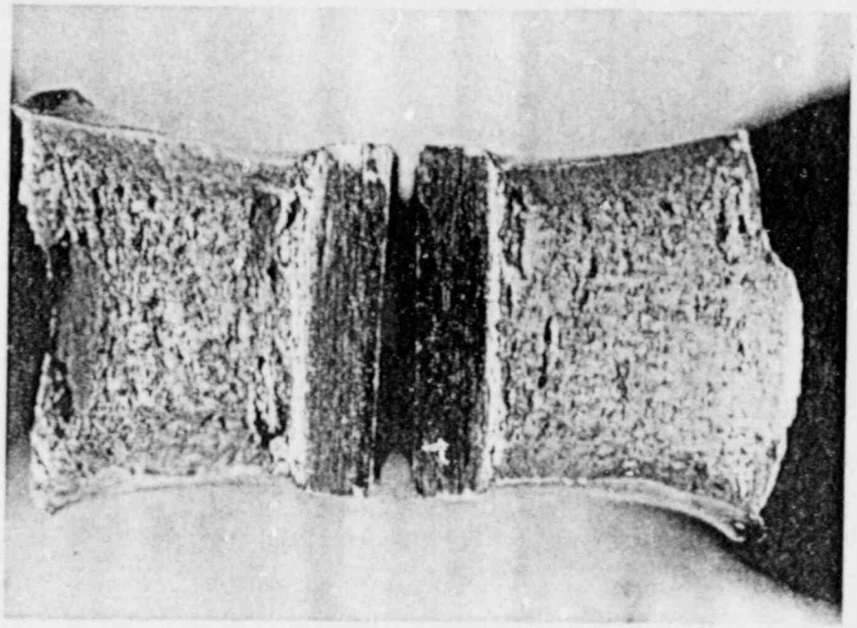

WELD: 7BL
TEMP: 200°F
ENERGY: 108.0 ft-lb

MLE: 86
% SHEAR: 100

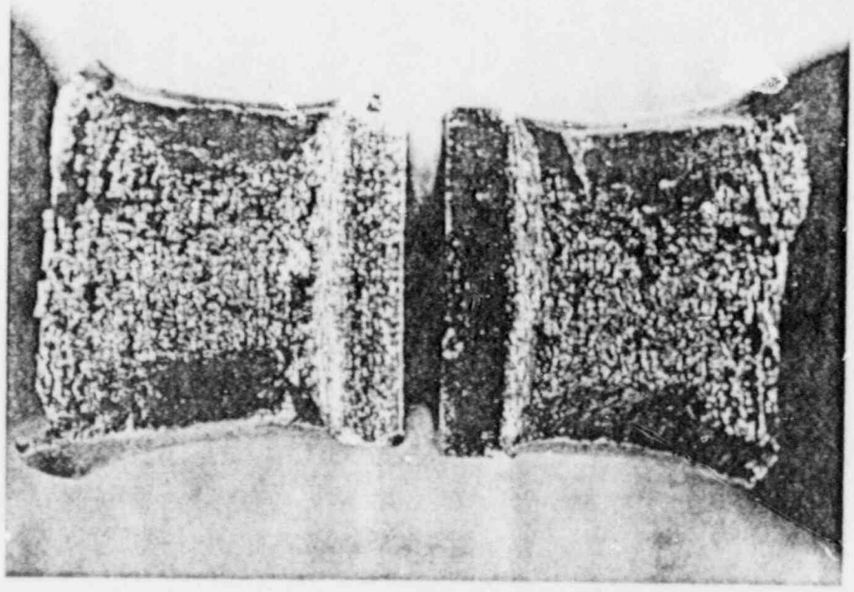

WELD: 7B4
TEMP: 300°F
ENERGY: 114.5 ft-lb

MLE: 88
% SHEAR: 100

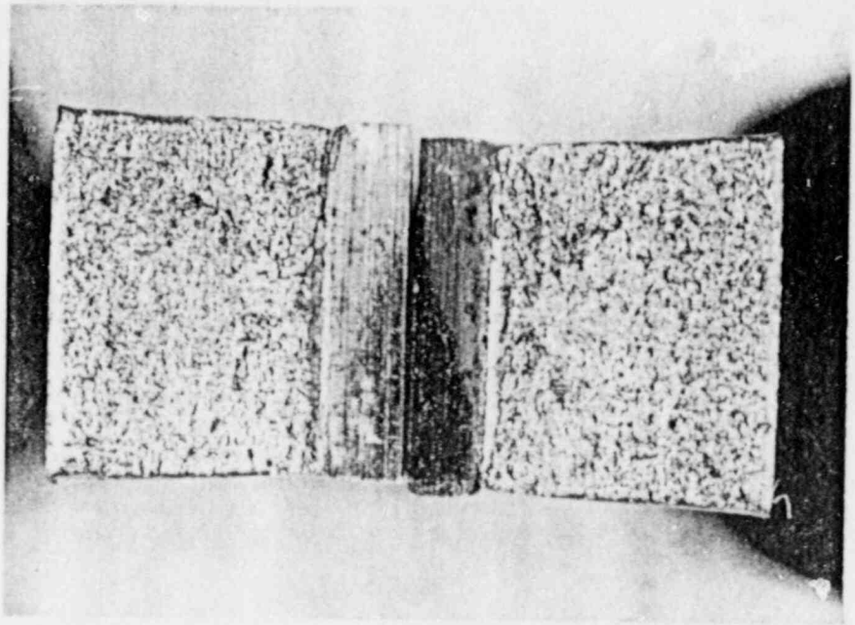

HAZ: 7D1
TEMP: -20°F
ENERGY: 24.0 ft-lb

MLE: 21
% SHEAR: 4

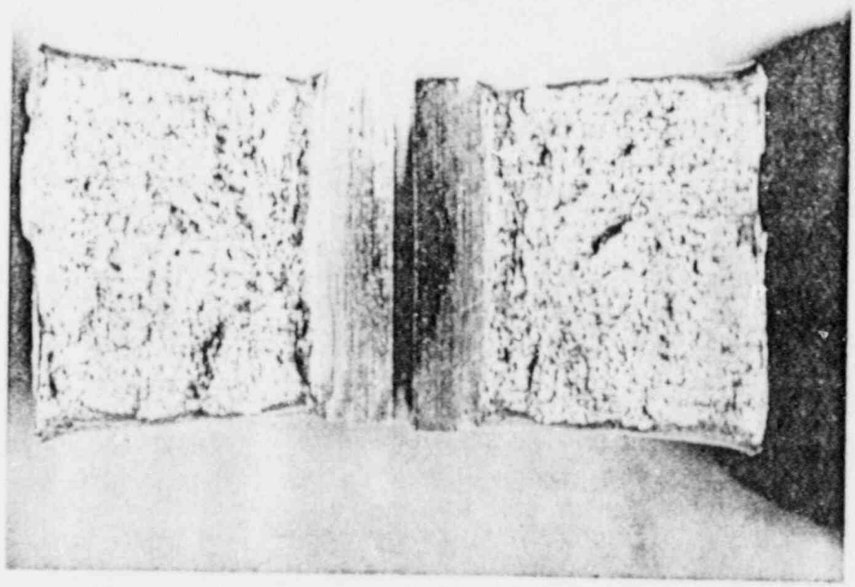

HAZ: 7J3
TEMP: 20°F
ENERGY: 47.0 ft-lb

MLE: 45
% SHEAR: 12

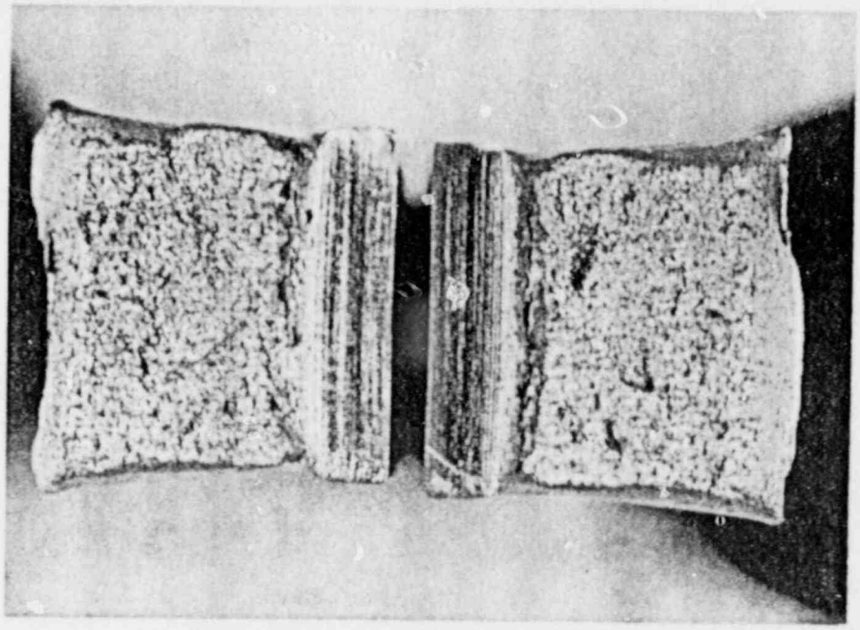

HAZ: 7DK
TEMP: 40°F
ENERGY: 52.C ft-lb

MLE: 44
% SHEAR: 26

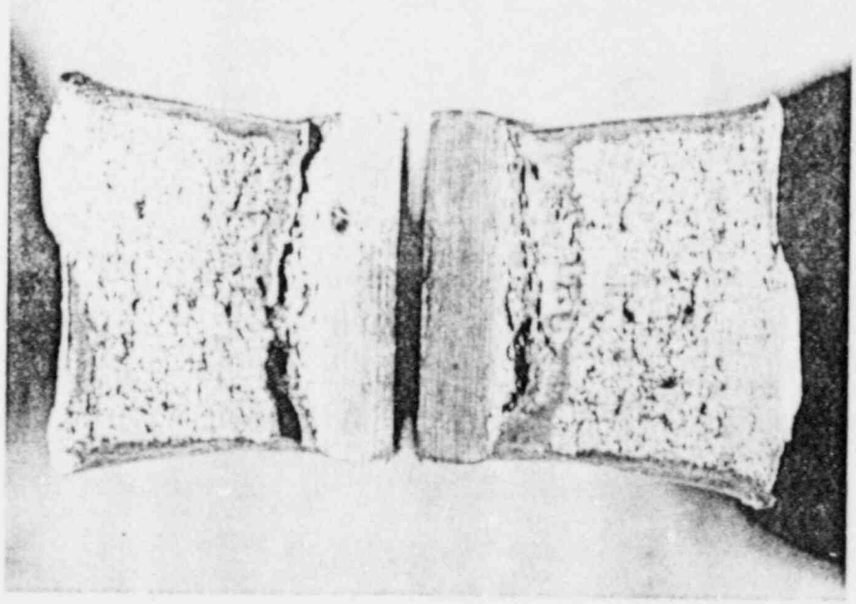

HAZ: 7J1
TEMP: 60°F
ENERGY: 75.0 ft-lb

MLE: 64
% SHEAR: 50

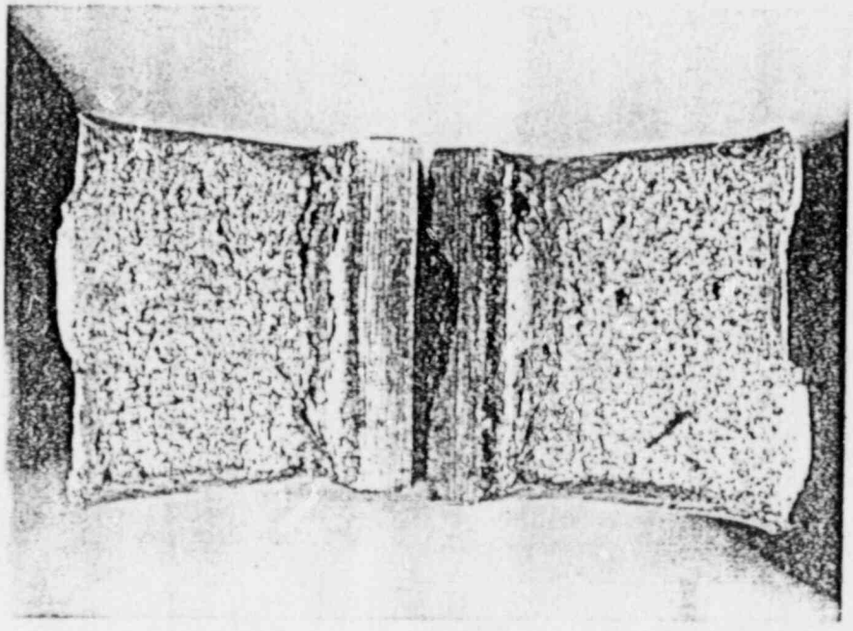

HAZ:	7D3	MLE:	49
TEMP:	70°F	% SHEAR:	25
ENERGY:	55.0 ft-lb		

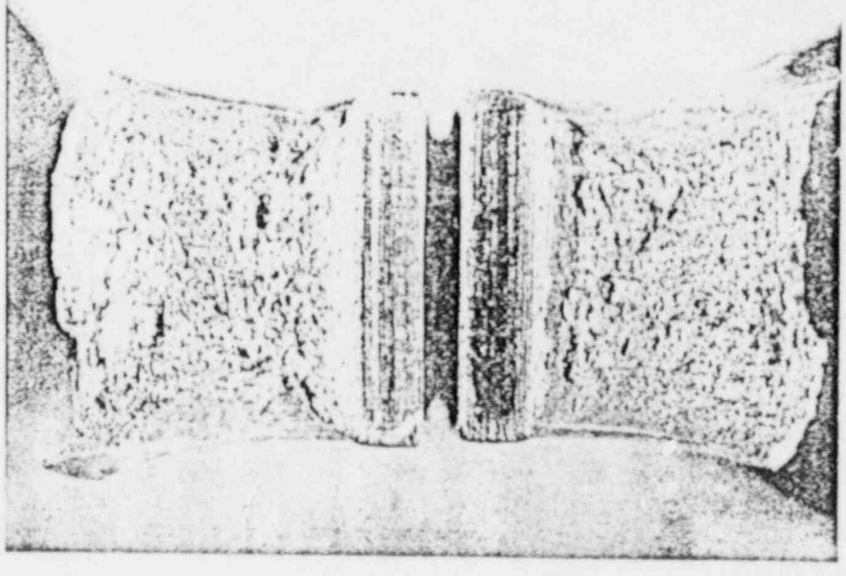

HAZ:	7DU	MLE:	80
TEMP:	140°F	% SHEAR:	83
ENERGY:	102.5 ft-lb		

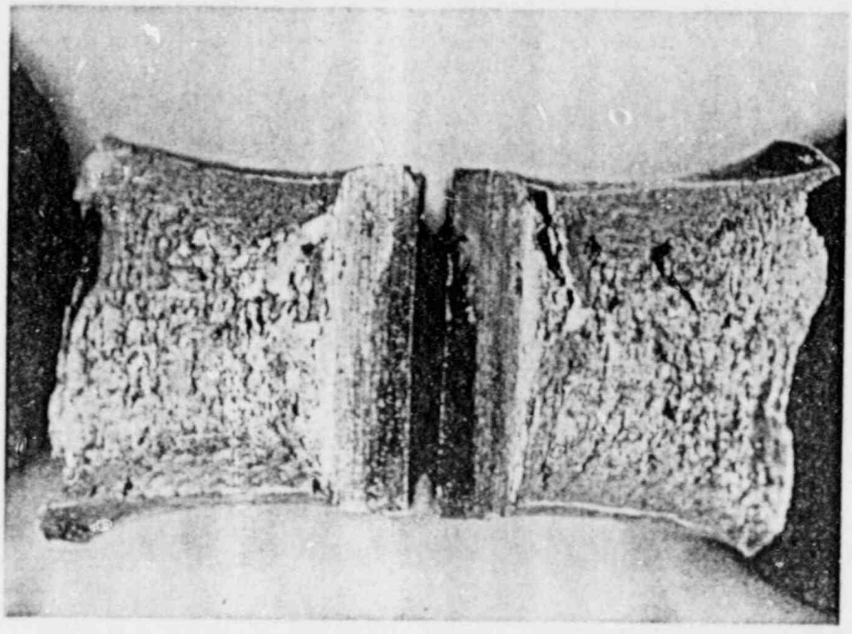

HAZ: 7JA
TEMP: 200°F
ENERGY: 116.0 ft-lb

MLE: 87
% SHEAR: 100

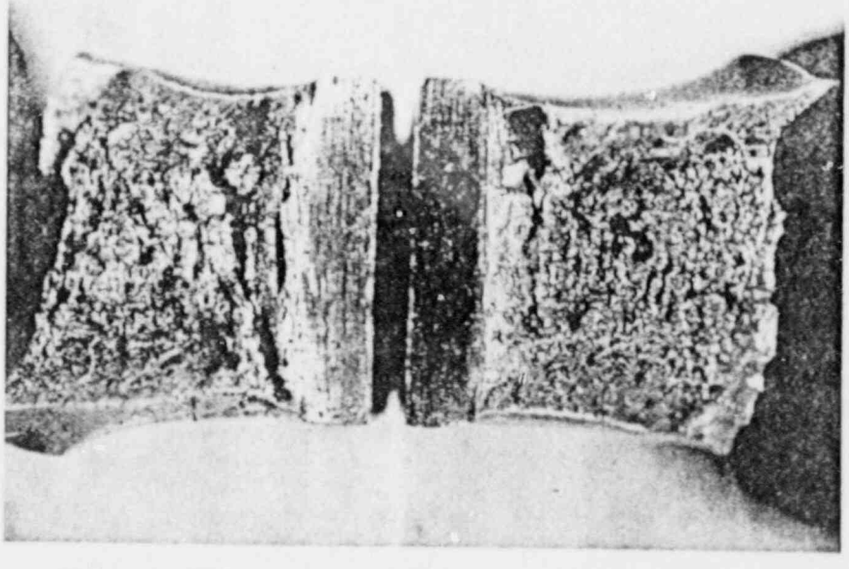

HAZ: 7DL
TEMP: 300°F
ENERGY: 152.0 ft-lb

MLE: 87
% SHEAR: 100